ADAMA SCIENCE AND TECHNOLOGY UNIVERSITY

SCHOOL OF MECHANICAL, CHEMICAL AND MATERIALS ENGINEERING

Aerodynamic Drag Reduction on Locally Built Bus Body Using Computational Fluid Dynamics (CFD): A Case Study at Bishoftu Automotive Industry

A thesis submitted in partial fulfillment of the requirements for the award of the degree of Master of Science in Automotive Engineering

By

Yesfalgn Damissie

MAJOR ADVISOR: - N. RAMESH BABU(Associate Professor)

CO-ADVISOR:- ASMELASH HAFTU(Lecturer)

DEPARTMENT OF MECHANICAL AND VEHICLE ENGINEERING

September, 2015

Adama, Ethiopia

CANDIDATE'S DECLARATION

I hereby declare that the work which is being presented in the thesis entitled “Aerodynamic Drag Reduction on Locally Built Bus Body Using Computational Fluid Dynamics (CFD): A Case Study at Bishoftu Automotive Industry” in partial fulfillment of the requirements for the award of the degree of Master of Science in Automotive Engineering is an authentic record of my own work carried out from <u>February 2015</u> to <u>September 2015</u> under the supervision of <u>N. RAMESH BABU</u> Department of Mechanical and Vehicle Engineering, Adama Science and Technology University, Ethiopia.

The matter embodied in this thesis has not been submitted by me for the award of any other degree or diploma. All relevant resources of information used in this thesis have been duly acknowledged.

Name	Signature	Date
<u>Yesfalgn Damissie</u>	____________	<u>2015-09-16-GC</u>

Student

This is to certify that the above statement made by the candidate is correct to the best of my knowledge and belief. This thesis has been submitted for examination with my approval.

Name	Signature	Date
<u>N. Ramesh Babu</u>	______________	________________

Advisor

ADAMA SCIENCE AND TECHNOLOGY UNIVERSITY

SCHOOL OF MECHANICAL, CHEMICAL AND MATERIAL ENGINEERING

DEPARTMENT OF MECHANICAL AND VEHICLE ENGINEERING

Aerodynamic Drag Reduction on Locally Built Bus Body Using Computational Fluid Dynamics (CFD): A Case Study at Bishoftu Automotive Industry

By

Yesfalgn Damissie

Approved by board of Examiners

____________________________________ _____________

Chairman, Department graduate committee

____________________________________ _____________

Advisor

____________________________________ _____________

Internal Examiner

____________________________________ _____________

External Examiner

DEDICATION

To her who is my source of grace, my source of commitment, and my source of knowledge, and whose love is a source of joy. I love and remember you grand mam forever, even if I lost you a few months ago. May God give you Heaven. This is your son!!!....

ACKNOWLEDGEMENT

All praises to the Almighty Lord and Savior Jesus Christ with his mother Saint's Marry, my shield, my strength, and my present help in time of need, for giving me the strength, patience and guidance throughout the process of completing this thesis. All I do and will continue doing unto him.

I gladly take the opportunity to regard thanks to my advisor Mr. Ramesh Babu, Associate professor, Adama Science Technology University for his valuable suggestion, comments, advice and inspiring me in this thesis. All the discussion made were very important to understand every detailed in this bus aerodynamic analysis.

I would like to thank Mr. Asmelash Haftu, lecturer, Defense Engineering College, for his kind support and guidance.

It is my great pleasure to acknowledge Mr. Kassu, lecturer, Defense Engineering College, for his invaluable guidance, enormous assistance and excelled cooperation which was extended to me for the smooth completion of the thesis. My thesis would have never been completed without his valuable advice at hard times of the process.

Special Thanks should also be forwarded to my beloved family. Last but not least, I would like to thank all my friends and all my classmates who are either directly or indirectly involved during the process of this thesis was conducted.

TABEL OF CONTENTS

LIST OF FIGURES

LIST OF TABLES

ACRONYMS AND ABBREVIATIONS

A_D	Drag Area
A_L	Lift Area
BAI	Bishoftu Automotive Industry
BEM	Boundary Element Method
Cp	Specific Heat Capacity
CAD	Computer Aided Drafting
CFD	Computational Fluid Dynamics
C_L	Lift Coefficient
CPU	Central Processing Unit
Cp	Coefficient of Pressure
C_d	Drag Coefficient
DNS	Direct Numerical Simulation
Dp	Pressure Drag
Df	Friction Drag
F_L	Lift Force
F_d	Drag Force
kmph	kilometer per hour
FVM	Finite Volume Method
FEM	Finite Element Method
g	gravity
GB	Gaga Bite
GHz	Gaga Hertz
K	Coefficient of Thermal Conductivity

LBM	Lattice Boltzmann Method
LES	Large Eddy Simulation
ρ	Density
ω	Omega
ϵ	Epsilon
Φ	Viscous Dissipation Function
Ps	Static Pressure
Pd	Dynamic Pressure
Po	Free Stream Pressure
P	Pressure
RAM	Random Access Memory
RANS	Reynolds-Averaged Navier-Stokes
SST	Shear Transport Stress
SUVs	Sport Utility Vehicles
3D	Three Dimensional
T	Temperature
μ	Viscosity
%	Percentage
V	Speed
V_∞	Free Stream Velocity

ABSTRACT

Buses are preferred as the major mode of mass transportation around the globe. In recent times hike in fuel price is meticulously observed and pertaining to current day's strict government norms, current buses are on track of being much more inefficient in terms of fuel costs. Aerodynamically efficient and accordingly redesigned bus body may improve their fuel economy. Even fuel used being from natural source, saving it will be a boon for mankind. To achieve better economy and good performance, it is necessary to redesign a bus with minimum drag resistance. This study relates three redesigned and retouched model of buses among themselves and their analysis for obtaining better aerodynamic design through ANSYS Fluent 14.5 package. CFD's aerodynamic simulations can give the detailed idea of the various parameters for all models which assist in redesigning the bus. This work depicts how the modifications could reduce the drag and the lift forces acting on the bus. CFD analysis for redesigned models shows remarkable results for the reduction in drag values and lift values. Drastic reduction in the pressure at front and wake region was obtained. Redesigning the overall body shape also improves vehicle stability and handling. This project Modified the outer surface of the bus aerodynamically in order to reduce the effect of drag force of the bus which in turn results in reduction of fuel consumption of the bus. Three Models are used and the models were entirely designed using the software CATIA V5R19 and SOLIDWORK 2014. The models are namely model 1, model 2 and model 3. Model 1 is existing Yutong cross-country bus model and model 2 and model 3 are modifications of existing Yutong bus. A simulation of a bus model dimensions 10771 x 2446 x 2727 mm was conducted using CFD software FLUENT 14.5, in order to investigate the flow around a bus and to reduce the drag force. The study was conducted for three wind speeds. Numerical tests has been conducted in CFD to prove the effectiveness of the new concept design. It is evident from the test result, that there has been a considerable reduction in drag force of about 39.4% from the existing bus to the new concepts and 22.8%(5 to 6 liters) of fuel can be saved for the every 100 Km.

Keywords: Yutong Bus, Drag Force, Pressure coefficient, Fuel consumption, Wind Speeds.

CHAPTER ONE

1. INTRODUCTION

1.1 Background of the Study

In the early 19thcentury mankind started to travel in a modern way. This was due to industrialization, which was in need of mobile labor. The first efficient transport system for long-distance travel was the railway. In the 1830s and 1840s public transport systems were established in major European cities, and the horse-drawn omnibus became a common feature in city traffic. The horse-drawn buses were followed by steam engine buses, although the latter were not always appreciated due to contamination and noise. At the end of the 19th century the steam engine was replaced by electric motors and soon came the internal combustion engine. The first buses were motorized horse carriages and later on trucks became a common base for building buses. The early truck-based buses had the engine located at the front, as shown in Figure 1. In the 1940s the demand for higher passenger capacity and a larger luggage compartment led to alternative engine locations. Since the rear-mounted engine has the advantage of easy adaptation of a truck engine, i.e. cost-efficiency, this type has become the most common engine configuration. The rear-mounted engine configuration also enables an easy entrance, especially for disabled persons, which has a high priority in public transport systems.

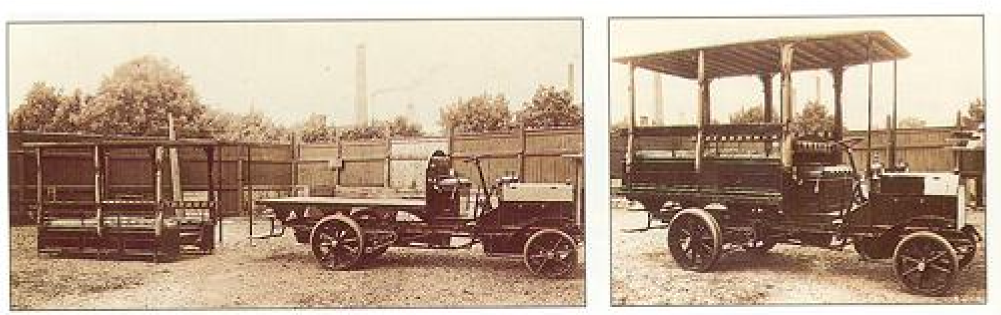

Figure 1. A Scania truck with a detachable passenger body (1909) [80].

In addition to the customer demands, the bus has to fulfill a number of legal requirements, concerning, for example, permissible axle loads, the minimum front axle load, steering effort, turning radiuses and body sweep area. The customer and legal demands have together led to the bus of today; see an example in Figure 2.

Figure 2. Typical tourist coach, Scania-Irizar PB (Coach of the Year 2004) [90].

Aerodynamics of cars became more and more important with the increase of their velocity. In the beginning of the 20th century, the shape of vehicles was adopted from the field of aviation and ships. Cars had an aerodynamic shape but their velocity was very low, mainly due to the quality of the roads. Aerodynamics is the branch of dynamics that deals with the motion of air and other gaseous fluids and with the forces acting on bodies in motion relative to such fluids. Automotive aerodynamics is the study of the aerodynamics of road vehicles. The main concerns of automotive aerodynamics are reducing drag, reducing wind noise, minimizing noise emission and preventing undesired lift forces at high speeds. For some classes of racing vehicles, it may also be important to produce desirable downwards aerodynamic forces to improve traction and thus cornering abilities (D. Gillespie, 2000).

Air is the gas with which the science is most concerned. Although aerodynamics is primarily concerned with flight, its principles are also used in designing automobile and train bodies for minimum drag and in computing wind stresses on bridges, buildings, smokestacks, trees, and other structures. It is also used in charting flows of pollutants in the atmosphere and in determining frictional effects in gas ducts. The wind tunnel is one of the aerodynamicist's basic experimental tools; however in recent years, it has been supplanted by the simulation of aerodynamic forces during the computer-aided design of aircraft and automobiles. Vehicles with an aerodynamic shape use less fuel. Air flows easily over them and less energy is needed to move them forward. At 95 Kmph 60-70% of a vehicle's energy is used to move it through the air, compared with only 40% at 50 Kmph. Installing a sloping front roof on a lorry could save you as much as 7% of your fuel costs. Even small changes to design and shape will make a difference. Vehicles that travel at higher speeds and for longer distances will benefit most from aerodynamic styling, giving you greater savings. Drag is the energy lost pushing through air, and it accounts for most of the fuel used on long-distance journeys, regardless of vehicle type. Overcoming drag uses approx. 60% of fuel used at cruising speeds when loaded, 70% when empty. Sharp corners, racks and parts that stick out will add “parasitic drag”, further reducing fuel efficiency[7].

Buses are the major mode of mass transportation all over the globe, despite of the rail network. Buses are inefficient in term of fuel consumption, thus in order to decrease the fuel consumption of vehicles, improvement in the aerodynamics of bus shapes will add to the value. It becomes essential to thoroughly design a vehicle for its aerodynamics, as it directly relates to the fuel economy and resisting forces, which further this, become a parameter for mankind to purchase the vehicle. More precisely the reduction of their drag coefficient becomes one of the main topics of the automotive research. Decreased resistance to forward motion allows higher speeds for the same power output or lower power output for the same speeds. Aerodynamics being the aid to form a body shape that maximizes the down force, the negative lifts and minimizes the force that opposes the forward movement and the drag forces. The aerodynamically efficient design of the bus reduces the drag force improving the fuel efficiency.

In a moving vehicle, the engine power is used to overcome tractive resistance, which is the combination of rolling and aerodynamic resistance. The rolling resistance will be dominant over the aerodynamic resistance at lower speeds. Aerodynamic resistance (drag) amounts for more than three fourth of total engine power while operating at higher speeds, since the drag increases as the square of the speed [3]. Thus the maximum power generated by the engine is utilized to overcome the aerodynamic resistance. Due to this the engine load increases substantially which further raises the fuel consumption rate.

The external flow analysis of a bus is important as the aerodynamics drag dominate at speed above about 65-80 kmph. Generally speaking, an incremental decrease in drag can translate into significant fuel savings. Furthermore, buses are used mostly for long-distance travel and the fuel consumption is a big deal for the bus operators. As shown in Table 1, the current typical value of drag coefficient for the buses is smaller than Pre-1970 vintage, and it is projected to be smaller in future by more radical or thorough approaches.

Table 1: Approximate ranges of drag coefficient values for various types of vehicle (Source: Barnard, R.H. 2001)

Vehicle type	Pre-1970	Current	Probable near future minimum
Medium-sized cars	0.4-0.55	0.28-0.4	0.25
Light vans	0.4-0.6	0.35-05	0.3
Buses	0.5-0.9	0.4-0.8	0.3
Large articulated trucks	0.7-0.95	0.55-0.8	0.4
Box truck and drawbar trailer	0.75-1.0	0.7-0.9	0.5

Conventional aerodynamic development of bus is carried out by wind tunnel testing of a miniature model with the working floor representing the road. Recognizing the limitations of the wind tunnel boundary conditions, considerable efforts were made to study aerodynamics computationally. In this study, a computational Fluid Dynamics (CFD) tool, called ANSY Workbench 14.5 and Fluent 14.5 were used to predict the physical parameters on the external surface of a bus, drag and lift force analysis, pressure and velocity distribution of the bus. The flow distribution was calculated by solving the Reynolds-averaged Navier-Stokes equations with a realizable K-E turbulence model.

Bishoftu Automotive Industry (BAI) was established in 1999 and placed under the management of the ministry of Defense. It was incorporated into the Metals and Engineering corporation in 2010. It is located 45 km outside of Addis Ababa in the town of Bishoftu. BAI assembles city buses, tractors, dump trucks, low-bed trucks and high-bed trucks, pick-ups, cross country buses, mid-size buses, and sport utility vehicles (SUVs). Its Products used for Public transport, construction, transportation of materials and goods, and military purposes. But the research focused on cross country(highway use) buses facing aerodynamic drag problem.

The main objective of this study is to simulate the physics of the flow field around a bus and to modify the outer surface of the bus aerodynamically in order to reduce the effect of drag force of the vehicle which in turn results in reduction of fuel consumption of the vehicle by using CFD software (Fluent). It will be evaluated based on the comparisons of predicted drag coefficient, surface pressure, and flow visualization to the experimental data.

1.2 Statement of the Problem

Crude oil prices have gone down in the past year, however the world proven crude oil reserves are depleting, from 1985 world oil reserve additions have been less than consumption for the year [106]. World crude oil demand grew an average of 1.76% per year from 1994 to 2006, with a high of3.4% in 2003-2004. World demand for oil is projected to increase 37% over 2006 levels by 2030 (118 million barrels per day from 86 million barrels) [106]. Since there has not been an effective alternative source of energy to replace crude oil there is a need to improve the fuel consumption of the bus. Also about 45% of the fuel consumption is caused by rolling resistance, 25% by aerodynamic drag and 30% by acceleration and climbing resistance [16].

Reducing fuel consumption, and therefore reducing the carbon dioxide emissions, is one of the most important goals in today's car industry. A need for a more efficient less fuel consuming bus is needed and that can be achieved by designing the bus in a more aerodynamic shape and also by introducing proper drag reduction systems on buses.

According to Hucho, the aerodynamic drag of a bus is responsible for a large part of the vehicle's fuel consumption and contributes up to 50% of the total vehicle fuel consumption at highway speeds[17]. Reducing the aerodynamic drag offers an inexpensive solution to improve fuel efficiency and thus shape optimization for low drag become an essential part of the overall vehicle design process[72].

One way this can be achieved is by reducing the aerodynamic drag of the bus. It is a great importance when it comes to velocities over 60km/h. Above this velocity, the aerodynamic resistance is higher than the rolling resistance. Streamlined body design in a passenger car helps reducing the aerodynamic drag and eventually improves the engine mileage. (H.K. Versteeg, 2007). On the contrary, accessories attached to the body skin of a bus cause the unfavorable aerodynamic examples.

1.3 Objectives of the Study

1.3.1 General Objective of the Study

- ❖ This research aims to modify the outer shape of the existing bus(Yutong bus) aerodynamically in order to reduce the effect of drag force which in turn results in reduction of fuel consumption of the bus using CFD tool fluent software.

1.3.2 Specific Objectives of the Study

- ❖ To model an existing Yutong bus(baseline model) and the two new models using CATIA and SOLIDWORK(CAD modeling software).
- ❖ To mesh the models using ANSYS workbench**.**
- ❖ To perform the flow analysis on the baseline model and the two new design models using CFD tool fluent.
- ❖ To compare the pressure force, viscous force, total drag force, lift force, drag coefficient, lift coefficient and pressure coefficient of the three models in three different high speeds.
- ❖ Drawing out the outcomes of rolling resistance, power required and fuel consumption comparing the three models in three different high speeds.
- ❖ Analyze the results and draw the conclusion between the cases on the aerodynamics performance and drag.

1.4 Scope of the Study

This project requires extensive knowledge about fluid flow, and understanding the nature of the flow. Knowledge on drag and the effects of drag on a body moving in a fluid is required, also research on the different types of active drag reduction system utilized today needs to be acquired. The bus models have been designed in CATIA, and SOLIDWORK and then transferred to ANSYS workbench for defining boundaries and meshing before exporting it to the simulation program. Simulation around the bus has been done by computational fluid program FLUENT. From the simulation the effects of drag on the different models used has been recorded.

1.5 Limitations of the Study

The main limitation of this project was computer power. The simulations have been run on a laptop with a 2.10GHz CPU formed by seven cores with 8 GB of RAM memory. Because of this limitation, the simulations needed at least 24 hours for 1000 iterations before achieving reasonable levels of residuals. This limitation also forced the meshes to be as optimized as possible which is to be compatible to fluent software and the geometry had to be simplified in order to reduce the cell number not more than 2 million.

Apart from the simplifications undertaken on the geometry to reduce cell number, other important simplifications were done to the model. The model is missing any internal flow, so the down force generated by the bonnet vents flow, together with the drag generated by the cooling systems is missing from the simulations. Both simplifications can potentially change the flow over the vehicle and the results from the simulations significantly.

CFD tool (ANSYS Fluent) software available at the hands of me is not functioning properly. Because it is not genuine(cracked one). That made me to spend a long time in understanding and resolving the problems.

In addition to that, due to lack of experience and training with the software, I spent the first two months of the project process in designing, creating geometry and meshing the models which are compatible to the software. But, I endeavored to resolve the problems facing in accordance with the nature of the software and finally I came up with results.

Other major dependencies were the designs were generated on CATIA V5R19. The researcher has previous knowledge of using CATIA instead of designing the geometry in ANSYS Fluent. This consumed a major time as modifications and iterations based on the basic model, the researcher had to refer back to the initial models in the CAD format.

Although the project started with a delay in analysis, much of the major time loss was a result of the initial geometry design and using ANSYS Fluent.

1.6 Significance of the Study

Hugely expensive wind tunnels are now supplemented by computational Fluid Dynamics (CFD) software, which enables 'virtual' wind-tunnel testing using computers. Therefore, the outcome of this study would give a contribution for bus manufacturers especially during styling process. It would provide some guideline on how to perform the external flow analysis using a CFD tool, especially in terms of the applying a turbulence model. It is also expected to give better understanding about the flow field over the bus and emphasizes more on how to implement an aerodynamic experiment and gathered qualitative and quantitative values.

Apart from that, it can offer the optimization on the bus aerodynamics for the sake of performance and fuel economy. It is true that aerodynamics can be improved by properly designing various component profiles. Hence, it can ensure that the aerodynamic drag can be kept within the limits during the styling process.

Computational Fluid Dynamics (CFD) is done to save cost and time of running high cost experiments using experimental wind tunnel. The research reduced the consumption of fuel and produce less harmful emissions to the atmosphere during the usage of automotives. From this research, it will help to increase the importance of usage of computational results to analysis a certain experiment with high cost and long duration.

Where as the result of this paper can be useful as one of the reference for any individual, researcher or manufacturer who are engaged in bus body design.

1.7 Structure of the Report

This report is consists of six chapters. The first chapter is introduction about the research study. It includes the background of study, problem statement, objectives, scopes, limitations, significant of the study and the structure of report. Next chapter focuses on the literature review based on the previous aerodynamic experiments done. Chapter three includes the fundamental of aerodynamic and CFD, the factors that influence aerodynamic and parameters associated with the aerodynamic effect assessment. So, this chapter has major influences to increase better understanding on this research study and is very helpful to design the methodology of study. Chapter four describes the methodology of the procedures of this research which was done. The methods and procedures are described in general. Besides that, the details of used simulation settings and boundary conditions are briefly described. Other than that, the data analysis method is also explained at the end of this chapter. The results and discussions are presented in next chapter. The generated data of pressure force, viscous force, total drag force, lift force, pressure coefficient, drag coefficient and lift coefficient are presented in form of tables and graphics for quantitative and qualitative discussion respectively. The contours of flow are also discussed to understand the best design characteristics. The correlation between the experiment result and simulation result is also discussed. The final chapter of this thesis consists of conclusion and recommendation of this research study. The overall conclusion with finalized details is discussed with some recommendation for improvements proposed.

CHAPTER TWO

2. LITERATURE REVIEW

2.1 Aerodynamic Forces

The natural environment for a ground vehicle takes place in the atmospheric region, where the interaction with the atmosphere creates forces. The relative motion to the atmosphere generates aerodynamic forces on the vehicle's surfaces. In order to model the fluid motion properly it is essential to understand and apply the fluid dynamic and thermodynamic principles. In automotive aerodynamics the analysis is divided into external and internal flow categories [11]. Current thesis is concentrating on the external flows, thus this topic will be presented along the chapter.

Generally the external flows characteristics are governed by the geometrical configuration and Reynolds number of the flow. External flows are differentiated into three major term called the drag, lift and stability [60]. A moving vehicle relative to the atmosphere, with a velocity vector is effected with two type of aerodynamic forces. On the opposite direction of the motion the force is called drag, while the perpendicular component is defined as lift. The shape of the vehicle and atmospheric conditions have a key role to determine the aerodynamic loads. It is a sensitive balance of the lift (pitching moment) and side forces (yawing moment), while the rotating moment has a role only in extreme cases [117].

2.1.1 Drag

Drag is a sum of mechanical forces generated on the surface of an object due to the interaction with the fluid. In automotive aerodynamics drag is a major concern of investigation, since the magnitude of it is largely affect the vehicle characteristics such as fuel consumption. Acting drag force can be divided into two source, but the physical origin makes them dependent to each other. In case of viscous flow the boundary layer has a strong influence on the external flow development, like separation where the adverse pressure gradient causes the detachment. So the viscosity and the pressure distribution is related. The drag consist a pressure source term normal to the surface (pressure drag), and a viscosity originated shear stress term parallel to the surface (friction drag). In other approach the aerodynamic drag is an integral of static pressure, friction and turbulence stresses over the surface of the vehicle [48].

The friction drag Df in a viscous flow is present all over the wall. Due to the molecular friction, shear stress is acting on the surface. The integration of this force component along the wall in the free stream direction is called the friction drag. For streamlined bodies like airfoils or flat elongated bodies, where separation does not occur, this component is the dominant term of the drag [116]. The pressure drag is the dominant source for automotive flows, compared to the friction drag from the shear stresses. Generally the pressure distribution along a bluff body or a vehicle consist a high pressure area in front (stagnation), and a low pressure area at the rear in the separation zone (wake). The flow separation is highly determines the pressure drag, thus it is important to understand the detachment of the flow.

Flow separation which governs the pressure drag component can be divided into two types. The first type is where the separation line is perpendicular to the flow direction. The separation zone is unsteady and vortices are generated with a rotational axis perpendicular to the flow and parallel to the separation line. A significant pressure loss behind the body is occurring due to the vortex field kinetic energy dissipation in the wake region (separation zone), where depression and low velocities are characterizing the flow. The other type is when the separation line is closing an angle with the flow direction. It leads to a three dimensional separation, which induce suction (pressure drag) behind the body. These two separation are in relationship and have a very complex three dimensional, unsteady phenomenon. Different angle of attacks leads to vortex breakdowns and vortex burst which is a highly important area to understand the physics behind it. It is a major research area in the topic of drag reduction.

The previous paragraphs are introducing the drag and the fluid mechanical background to understand this force component. As a measure of the drag, it can be expressed as a dimensionless coefficient, so it is easier to compare different vehicles. The expression Equation (2.1) contains the ratio of drag force D, where, D = Df + Dp, sum of friction and pressure drag over the multiplication of dynamic pressure and the largest area from the free stream direction A_D.

$$C_D = \frac{D}{\frac{1}{2} \cdot \rho \cdot v_\infty^2 \cdot A_D}$$

Equation 2.1

Traditionally this drag representation is used, but there exists advanced approaches, where not only the surface integrals are in the formula, but it takes into account the vortex evolution in the rear wake of the flow in order to understand the relationship between components. Onorato et al [65] is introducing a simplified model based on the momentum equation. Assume the flow incompressible, steady and the effect of turbulence and gravity are negligible compared to pressure effects.

2.1.2 Drag Reduction

In the previous sections the origin and physical phenomena is introduced to define drag. For vehicle aerodynamicist primary issue is to decrease drag. Companies objective is that is possible to reduce the drag with control solution by 30% without confront the constrains [84]. Drag can be reduced by controlling the separations location with flow intervention near the wall region with or without additional external energy using devices [104]. Controlling can be used as acoustic or noise regulation as well, not just drag reduction [104]. Methods can be categorized into active and passive control systems. Passive approach applies shape modification on the vehicle body, while the active techniques are introducing a directly controlled external device.

The main objectives are to relocate the separation point to decrease the separation effect and size of it or increase the base pressure. Keep the flow attached to the wall as further possible or help to reattach (for trucks). If these conditions are fulfilled the drag coefficient will be smaller, and the aerodynamic performance become more effective.

2.1.2.1 Passive Control

Passive techniques have been applied on a wide range, since the modification of the geometry is simpler to change. These methods are very effective for general passenger cars, but plays an important role in heavy duty vehicles too. The most elementary step is to avoid the sharp edges if it's possible and apply rounding or tapering.

In case of a square back geometry the boat tailing is one of the most common technique what can be done in two ways limited by the constrains. It is a gradual reduction of the cross section through the length till the base [87]. Tailing with curvature for passenger cars or apply parallel elements for trucks or generic car models. For buses it is a well approved technique to round a certain part of the end vertical edges. It helps to reduce the base area on the rear end and uses the underbody flow which comes up. As the separation zone gets smaller, de acting pressure also increases so the total drag is considerably lower.

Another method is to apply cavities near the rear roof edges [85] or cylindrical element along it for a slant Ahmed body as Pujals [83] with a smaller drag reduction results. Similarly a base cavity with variable depth, which can be ventilated by slots [82]. These approaches does not have a that significant change as boat tailing but still achieve drag reduction. The study at Durham [82] show that overall drag is decreased but a minimum drag is reached at a certain depth. With ventilation slots a greater reduction can be obtained with a bigger depth cavities. Add on devices or elements called splitters can be used both at the rear or front end, so the flow can be controlled.

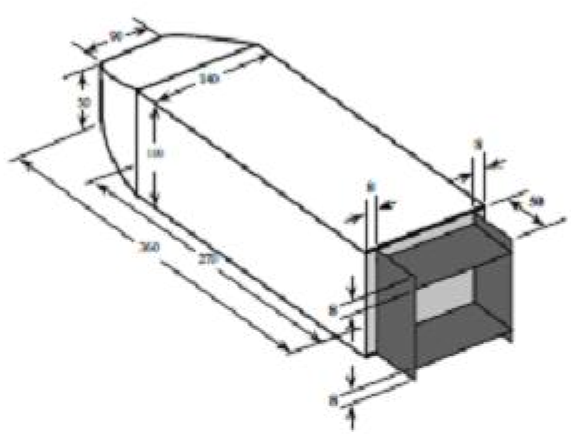

Figure 3: Ahmed body with added elements

These modifications are affect the detachment or reattachment depending on the position. The acting forces are different because of the area of the added splitters and it can change the wake structure in the back.

A very promising new technique which is using a porous layer on the surface. For a square back Ahmed body with almost a full cover it resulted a 40% drag reduction by simulation. This approach very dependent on the boundary conditions so the proper assumptions has to be made. [47].

Different passive techniques affect the total flow in different parts and each method has a ”minimum” value where it is most effective, but it is possible that the other applied device has an optimal value on another condition. If more device is applied it has to be optimized together in order the reduce drag in the most efficient way Figure 4.

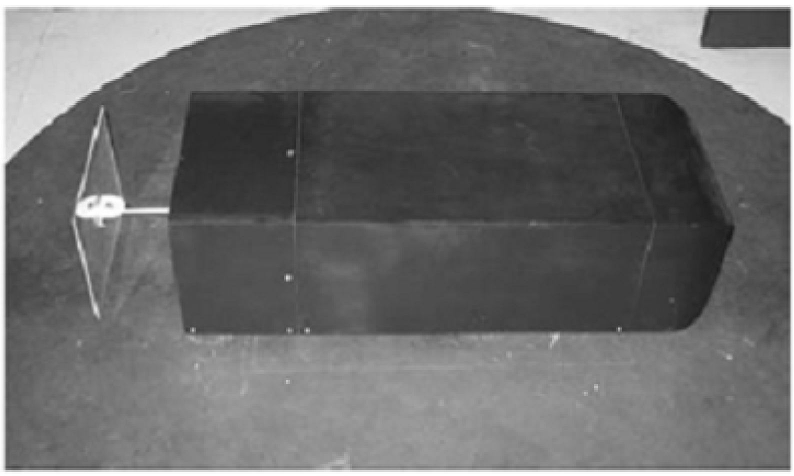

Figure 4: Ahmed body with drag reduction element

2.1.2.2 Active Control

Compared to passive methods active techniques are more fresh and has more potential as the technology improves and more radical solutions take place [47]. For example in the case of the Volkswagen XL1 prototype automobile, a big fan is applied in the back of the car to suck the air from the wake region. These techniques are using external energy source and control the flow. The great advantage compared to passive techniques is that it can be optimized depending on the flow conditions, it has a feedback, so it’s kind of an interactive control solution for drag regulation.

A popular approach is the application of boundary layer suction or blowing so the separation zone and pressure distribution can be controlled. It is possible to combine these two. The approach induce energy into the system so it can counteract to the dissipation in the wake region.

Numerical simulations and experiments show that span wise vortex weakening is coupled with the stream wise vortices along the backlight edges in the separated flow for an Ahmed body [47].

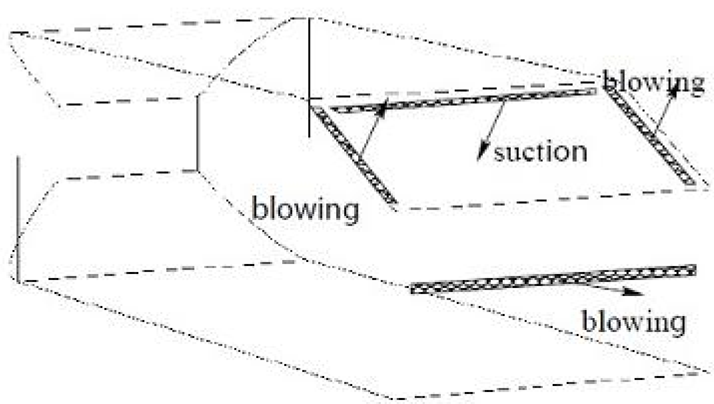

Figure 5: Ahmed body with applied Active Control

In [23] a 2D and 3D Ahmed body have been tested and investigated to find the best position in terms of suction and blowing on Figure 5. The main vortex structure were captured which determine the generated drag. The final conclusion have three option. One of them is propose a transverse suction of the top of slant edge or a transverse blowing in the bottom edge of slant, while the last option is to apply blowing on both sides of the slant to weaken the longitudinal vortices.

2.1.3 Lift

The perpendicular component of the acting load is the lift, which is basically generated by the pressure difference between the upper and lower surface of the body involved in the flow. Similarly to the drag, the lift can be expressed by a dimensionless coefficient as well, depending on the free stream velocity v1 and initial conditions. Lift force in Equation (2.3) is denoted with L, the characteristic horizontal area A_L, and the density of fluid.

$$C_D = \frac{L}{\frac{1}{2} \cdot \rho \cdot v_\infty^2 \cdot A_L}$$

Equation 2.2

In a general passenger car case, the created lift force is significantly smaller than the gravity force, thus the effect on the road characteristic is negligible. The lift force is coming in the front for stability and tyre performance reason in the field of race car aerodynamics. The down force is an essential property in the high performance race cars. Greater down force increases the turning speed, acceleration and stability conditions, improve braking performance.

2.2 Bluff and Streamlined Bodies

In aerodynamics the ground vehicles can be classified in the category of bluff bodies. Beside vehicles another class the buildings can be placed in this group, for external flow point of view. Both vehicles and buildings are influenced by the ambient conditions and natural wind. Major contribution for bluff bodies are that the significant drag component originated to the generated pressure drag compared to the friction type. In general if the streamlines are following the body's surface (streamlined body) due to the D'Alambert paradox the pressure forces are small, while the friction forces are dominating.

D'Alambert paradox states that in inviscuid fluid flow, if the streamlines are follow the surface, applying the Bernoulli equation to determine the flow properties, from the momentum equation we get the final result that the forces acting on the body is zero [107]. In viscous case both pressure and rampant friction forces plays a role.

Streamlined bodies such as aero foils can behave as bluff bodies as the angle of attack reaches a certain value [34]. For streamlined bodies to reduce drag advanced flow control methods are available to decrease skin friction. For bluff bodies to reach our goal it needs to be considered that pressure drag has to be minimized. Avoid separation of the boundary layer, keep flow attached to the surface as much as possible.

Bluff body flows are characterized by separation of the boundary layer, thus an unsteady velocity field and a low pressure zone evolves in the rear body called wake. In 2D bluff body cases these wake regions are generally characterized by periodic vortex shedding. A common example for this phenomenon is the K ´ arm ´ an vortex for lower Reynolds number flows. Due to these conditions the wake has a large energy dissipation rate, thus a high drag arise behind the geometry.

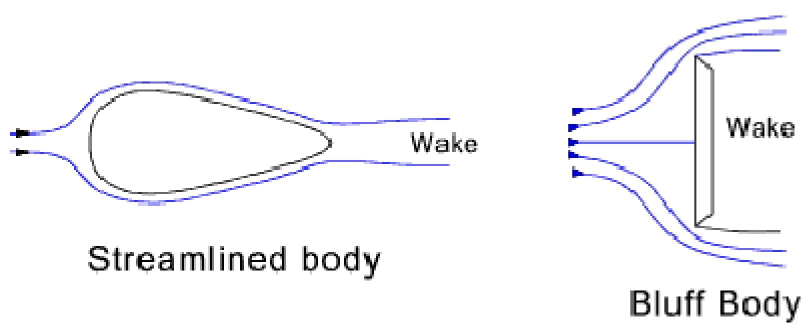

Figure 6: Streamlined and Bluff body

In order to reduce the drag it is essential to understand the physics behind it. So the main problem, the boundary layer separation must be investigated. Boundary layer remains thin and does not separate in accelerating flow, that's why in the fore body region near the stagnation point there is no separation. The pressure forces can be related to the boundary layer.

Two basic condition for boundary layer separations is the vicinity of the wall, where the effect of the wall shear stresses arise (viscosity) and the adverse pressure gradient related to stream wise velocity decreasing too. Separation takes place if the deceleration effect of the wall shear stresses and the adverse pressure gradient tops the sum of momentum of velocity distribution.

There exist conditions what are influencing the separation, help it to happen or avoid, decrease the possibility. Those conditions which accelerate the process are the following. An obvious case is when the wall shear stress are larger in the turbulent layer when the roughness of the wall is bigger. Larger pressure gradient also affect the separation, it takes place where the flow direction is changing such as cases in front of a concave or behind a convex edge, small rounding up radius. Low kinetic energy (slow velocity) near wall and sudden change in radius also helps the separation. The techniques and methods to prevent or relocate separation are trying to reduce the previous listed cases. Increase the kinetic energy by higher velocity near the wall or blowing in or suction of the boundary layer. For replacing the separation the easiest way is to interfere the laminar-turbulent transition with turbulence generators

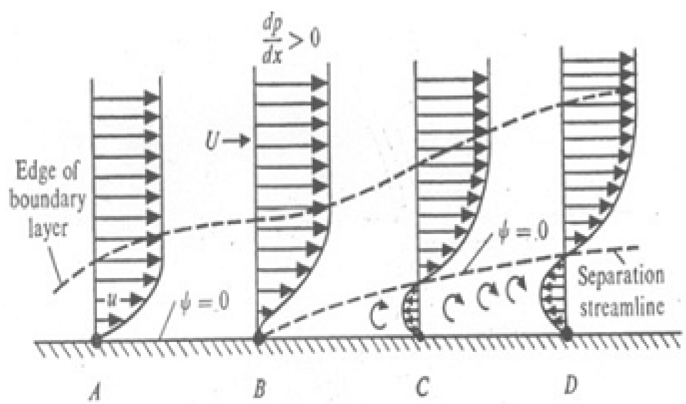

Figure 7: Boundary layer separation

Boundary layer separation is a mode of vorticity transport in potential flows by convection. As a result of boundary layer separation, the shear layer enters the flow by creating a closed separation bubble or an open vortex tube. Both cases the characteristic pressure are smaller than the ambient. Separation bubbles and vortex tubes are the typical vehicle aerodynamic flow features in the wake region.

A closed separation bubble development process are containing the following steps. First the boundary layer separation, the formation of shear layer, large velocity gradient across the shear layer and an intense turbulent mixing takes place. Next section is the entrainment, which needs a reverse flow, which has pressure below ambient. It affects the curvature of the streamlines, reattachment or separation bubble closing and the final structure develops[34].

Main features of the closed separation bubble are important to know if the task is to reduce the size effectively. In the bubble compared to the undisturbed motion a relatively slow (20-30% of velocity) reverse flow takes place. The bubble is surrounded by walls and the closed shear layer. An approximately constant lower pressure compared to the ambient, which is affected by the angle of the undisturbed flow and the tangent of the shear layer at the separation point. An intense turbulent mixing and high turbulence intensity region with a fairly definable passive flow structure[34].

The other structure the open vortex tube is generated when an edge and the flow close a relatively small angle, eg. delta wings. The tube's diameter is increasing downwards with length. The pressure and velocity is decreasing as the tube axis is approached. Open vortex tubes are active flow structures, with lower pressure then the ambient. This phenomenon arises at buildings top edges and as well in hatchback cars[86].

Generally the separation's place is fixed in case of sharp edges of the bodies. For rounded, curved shapes where is no sharp edge, the separation depends on the pressure distribution and the position is moving until it reaches the equilibrium. The place of separation can move periodically in time[101].

To sum it up the forces acting on a bluff body is mainly caused by the unbalanced pressure distribution along the geometry. The wall shear stress is playing only a small role compared to streamlined bodies where this force is the dominant, but essential for the boundary layer separation. Bluff body flow are characterized by separation of closed bubbles or open vortex tube depending on the geometry and flow conditions. This low pressure near wake region contains the vortex structure which leads to the high drag [59]. Ground vehicles are categorized as bluff body because of the geometry and aerodynamics flow features. In automotive aerodynamics streamlining is not a straightforward tool to reduce drag, since the shape of the body is determined by other designing constraints and different purposes (heavy vehicles) [79]. Drag reduction can be reached by base flow modifications by active and passive techniques.

2.3 Simplified Models

Automotive industry has to face a lot of challenges these days. Companies have to satisfy the customers, fulfill the international standard and maintain the future development. As the vehicles are getting more sophisticated and become the one of the state of the art technology in engineering. The fossil energy resources are finite and one of the main cause of global warming is the high amount of CO_2 produced by the industry and transportation, so the clever fuel consumption is essential. In case of vehicles one of the solution to the problem is the aerodynamic optimization. The first fossil fuel crisis in the 70's affect largely this sector of the industry. Drag reduction came in to the front that time and since then this aspect is still and getting more important as hybrid technology and solar power driven green vehicles are the options for the prospective future. Important consideration to the road vehicles [86]:

- Separation leads to high drag
- Ground effect influences both lift and drag

- Presence of wheels
- Wind is introducing yawed flow and turbulence
- Interference due to other vehicles

In the 20th century different tools were applied to reach aerodynamic performance optimization goals. From wind tunnel measurements to nowadays CAE techniques the motorsport, passenger and heavy duty vehicles can be managed. There are two ways to done the development process. The first and more applied method is to start aerodynamic concerns in a later phase of design development, the shape and detail optimization. Other approach is to start the full design process with a genuine streamlined body and develop the whole vehicle on that configuration. To test and create such models, simplified or streamlined bodies are used. This is a well approved methodology to investigate the aerodynamic characteristics. From the results of these reduced detailed models relations and conclusion can be drawn to the original vehicles. Studies on these cases show that these simplified bodies can perform realistic flow features as actual cars such as of on Figure 8

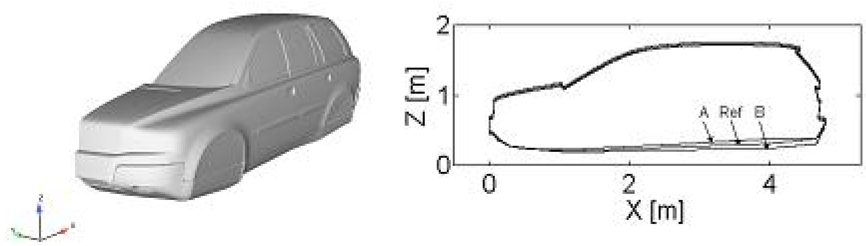

Figure 8: Simplified Model Geometry[68]

Due to the reduced complexity these models allow to prepare experiments and CAE simulations. The simple geometry has a great potential to equip the measurements cheaper, in simulation point of view the CAD model and CFD mesh are significantly easier to generate. The advantage of this approach appears in the reproducing process, to measure and redo a simulation in order to validation or checking the case. For common models there exist a large range of available data both experimental and numerical, which is a good comparison possibility and a good basis for investigation. Drawback of this approach is that an artificial case is generated and some major details can be different to the actual vehicle concepts, such as the underbody or the flow conditions. Furthermore this chapter covers one of the most commonly applied simplified bluff body car model the Ahmed body and the actually investigated shape the Windsor model.

2.3.1 Ahmed Body

Ahmed Body is a well know study, what becomes a standard benchmark problem formulation in ground vehicle flows, in order to investigate new turbulence solvers, CFD codes Figure 2.5. Researchers have been made several measurements[50] and numerical simulations in different configurations to analyze the backlight angle effect in the wake structure Figure 2.6. These cases are well documented and published. Their original study [118] focused on the backlight angle variation and its effect to the wake structure and base drag. This base model is able to reproduce the general vehicle aerodynamic.

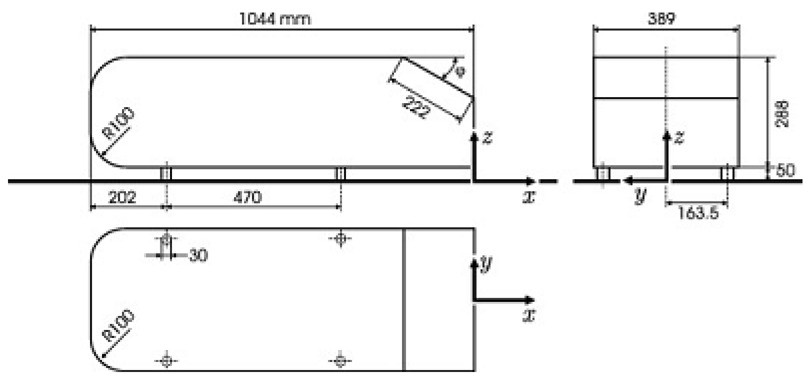

Figure 9: Ahmed body baseline configuration

This base model is able to reproduce the general vehicle aerodynamic features in the wake structure as a real vehicle configuration. Experiments have been carried out on different boundary conditions (moving ground) wide range of velocity and techniques from simple pressure, velocity measurements to PIV, LDA [22]. Main CFD techniques were used to deal with the problem from RANS, URANS, LES to hybrid techniques. It is popular that added elements are tested on the original layout. Deflectors, splitters or induced cavities to investigate the effects on the flow wake structure and drag coefficient.

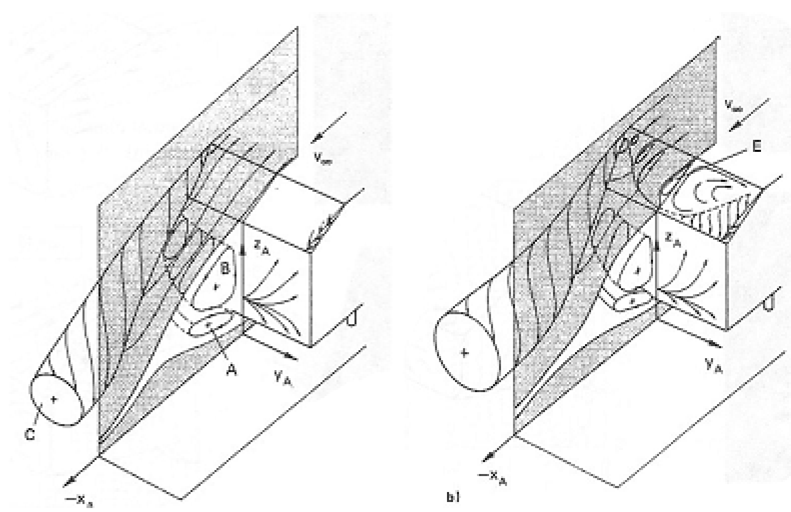

Figure 10: Ahmed body flow structure [77]

Significant differences arise in terms of modeling to real cases for wheels and underbody. The wheel-house and wheel effect is neglected in most of the configuration, but there exist studies in this field too [5]. It can be further extended with rotating wheels and proper ground conditions, which is necessary for the diffuser studies. Usually the underbody is smooth for all type of simplified models, for actual cars it is very rare to have a covered smooth layout. It could be a possible future focusing area, since the combination of ground effect and diffuser can reduce the drag and affect the whole wake structure

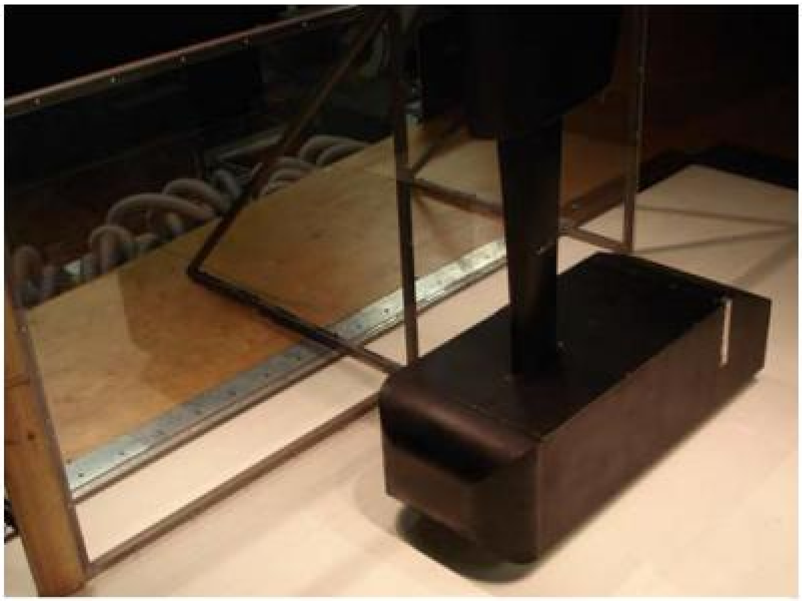

Figure 11: Ahmed body LDA measurement layout[76]

Conclusions from the model can be utilized in the hatchback cars, since the geometry has a similar backlight angle configuration and the wake structure is also very similar. For further studies the full model is a square back case what can be applied for vans and heavy duty vehicle [75]. This case has the most similarity to the thesis Windsor model, due to the end, the difference is in the forebody which is more ”hood” like for Windsor. The detailed and well documented Ahmed body is a good basis to understand what is happening in the wake behind a car.

2.3.2 Heavy Vehicles

Heavy vehicles are obviously aerodynamically inefficient constructions since the main purpose is to specialize in a certain type of job eg. construction site (excavator), agricultural (harvester) and transportation. In vehicle aerodynamics point of view the long distance transportation consume a significant proportion of fuel consumption, thus the regulation and trends lead to the necessity of reducing aerodynamic resistance [71].

The basic idea of trucks and buses is to transport as many goods, passengers as possible in one way, thus the primary importance is to extend the useful space as big as possible. It leads to a sharp edged box shape configuration, with a big length over height/width ratio, which is a specific bluff body situation. It describes a flow field, with separations and reattachments, unsteady wake and the interaction between the truck-trailers also makes it more complex, while the overall lift is totally negligible. Because of the large side areas, the crosswind stability and handling is a big issue. Since the basic design is not dealing with aerodynamics, manufacturers must modify the basic shape. Studies says that at highway conditions the 50% of the energy consumption is due the drag, thus it is essential to reduce the resistance as much as possible[100].

Main areas of the generated drag can be divided into four section. The frontal area, interaction between truck elements, underbody and the rear wake. The proportion of these parts depends on the initial flow conditions (cross wind) [57].For buses this distribution suites as well except the interaction part.

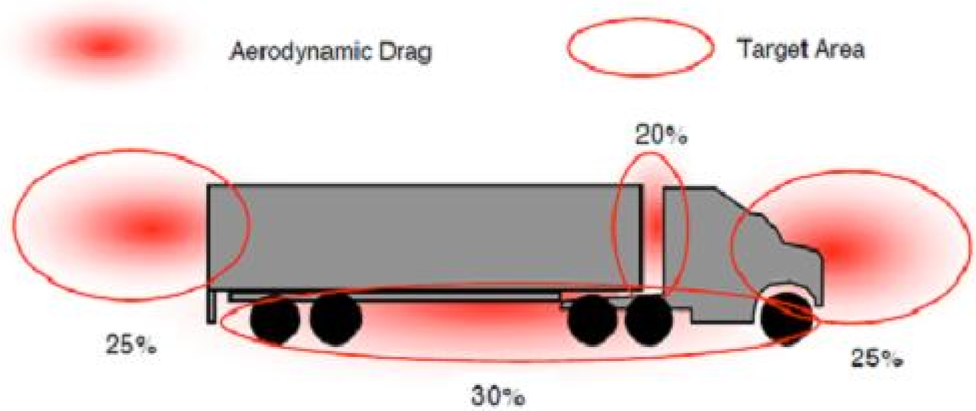

Figure 12: Heavy Vehicle Drag Distribution[67]

Despite the bus-truck flow similarities the drag reduction methodology needs a different approach. For buses it's more likely to apply the general passenger car techniques. Rounding the sharp edges, simple boat tailing, add-on devices, frontal inclination angle, underbody smoothening etc.

Figure 13: Truck Boat Tailing Examples[67]

Truck aerodynamic should handle the interaction-interference between body parts with active and passive flow control devices [100]. Some passive methods as the upper surface curvature shape optimization (depends on the country, UK) [64], different cab configurations, add-on devices, applied boat tailing flaps like on Figure 2.17, cover the gap between the trailer and truck, smoothened underbody [67]. The active control devices are somehow affect the flow characteristic by inducing disturbance. Rotating elements on the roof top (moving surfaces) Figure 14, autonomous self-adjustable add-on on devices (boundary layer manipulation), pressure rising at the base region by bleeding etc

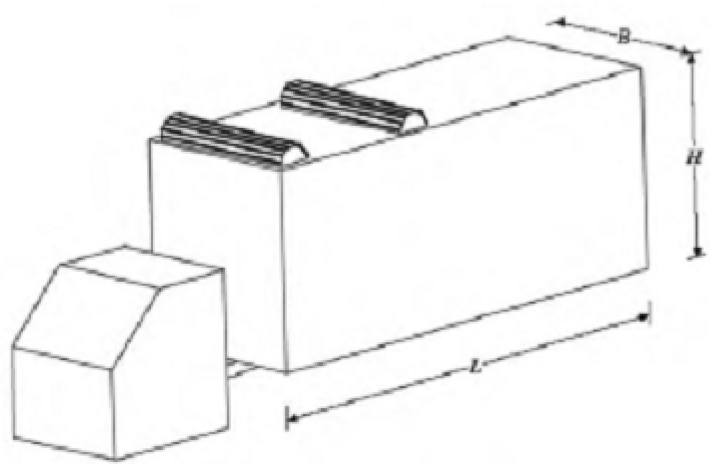

Figure 14: Truck Rotating Element Design,[67]

2.4 Flow Separation

At sufficiently high velocities, the fluid stream detaches itself from the surface of the body, that effect is called flow separation. The location of the separation point depends on several factors such as Reynolds number, the surface roughness and level of fluctuations in free stream and it is usually difficult to predict exactly where separation will occur unless there are sharp comers or abrupt changes in the surface of the solid surface [63]. When a fluid separates from a body, it forms a separation region between the body and the fluid stream. The low pressure region behind the body where recirculation and backflows occur is called the separated region, the larger the separated region the larger the pressure drag. The region of flow trailing the body where the effects of the body on velocity are felt is called the wake. The separated region comes to an end when the two flow stream reattach.

A paper on bus drag reduction by trapped vortex concept for a single bus and two buses in tandem talk about vehicle design paying a great deal of attention in fuel economy, which is achieved by stream lining a vehicle so that the flow can move with less unsteadiness (aerodynamic drag reduction), other benefits that come out of this is better handling.

Fletcher and Stewart [61], where able to achieve 17% reduction in drag of a MC-7 intercity bus and a corresponding 11.7% reduction in fuel consumed at a steady speed of 88 Kmph by adding aerodynamics in existing shapes of buses.

Gotz says for a typical bus 45% of fuel consumption is caused by rolling resistance, 25% by aerodynamic drag, and 30% by acceleration and climbing resistance. Fletcher and Stewart [220], where able to reduce the drag coefficient Co by 0.29 by using optimal radii on the forebody/roof junction, 8 o tapers behind the forebody and in front of the tail (see figure 15).

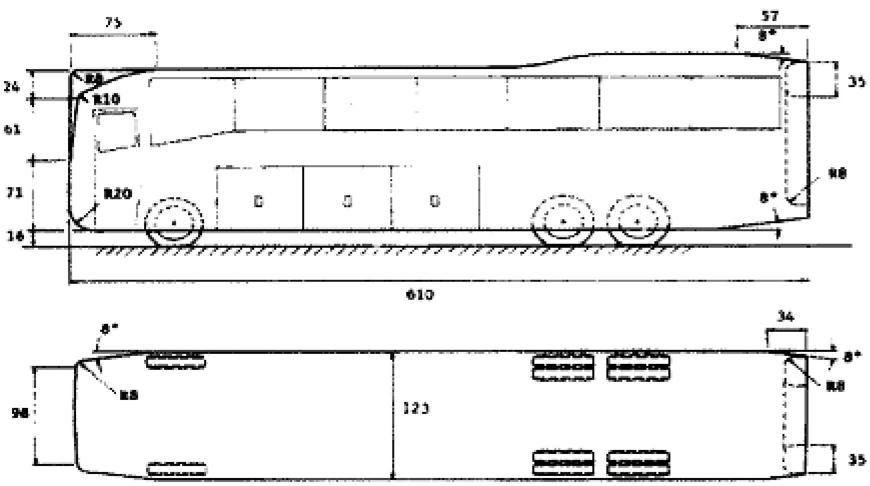

Figure 15: Bus with drag reduction modification [61].

Bus drag reduction has focused on mainly introducing a sufficient larger radius at the forebody/roof and forebody/side junctions of the buses to prevent flow separation and on reducing small scale obstruction into the flow (e.g. mirrors and window frames).

Less attention has been paid to the rear of the bus to produce a higher pressure recovery and reducing the drag coefficient. A cavity in the rear ward of the buses was introduced to encourage a standing vortex to be produced so that the flow past the bus will be assisted in turning towards the bus wake center line (see figure 16). By smoothing the edges and the inclusion of the vortex trapping system they managed to improve the flow separation and where able to streamline the flow at the rear of the bus that way they recovered some pressure at the rear of the bus.

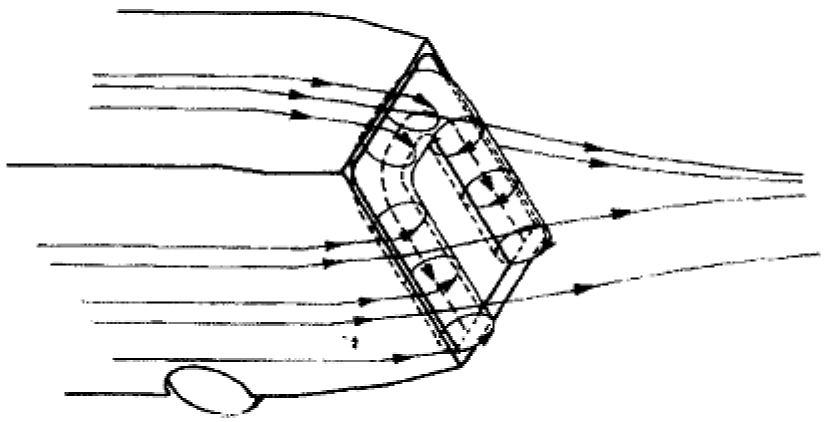

Figure 16: Conceptual flow field associated with a trapped horseshoe vortex [61].

From all this it can be seen that the main issue when dealing with reducing drag is to make sure that the object is streamlined in hopes to reduce flow separation to prevent unsteady state in the fluid flow.

A paper on drag reduction of an Ahmed car model (Ahmed model is a reference car model with a variable slant angle a controlling the near wake flow structure and the aerodynamic drag) by means of active separation control at the rear vehicle slant talks about the experimental investigations which deal with the reduction of the total aerodynamic drag of a generic car model (Ahmed-Body) by means of periodic forcing. The experiments carried out in this study focus on a unique approach to separation control using fundamental frequencies for local forcing of the shear layer separated from the rear end of the car model. The excitation of large scale vortex structures by periodic forcing intensifies the primary momentum transfer between the separation region and the outer flow, resulting in a substantial reduction of the separation length. A total drag reduction of27% was achieved using the flow control method described in this study [30].

2.5 Pressure drag

Drag force is the net force exerted by a fluid on a body in the direction of flow due to the combined effects of wall shear and pressure force. The part of drag due directly to pressure is called pressure drag, also called form drag because if it's strong dependence on the form or shape of the body. When the friction and pressure drag coefficients or forces available, the total drag force can be determined by simply adding them, the pressure drag is proportional to the frontal area and to the difference between the pressures acting on the front and back of the immersed body [63]. The vortex trapping system is one of those systems designed to remove or minimize the effect of pressure drag by recovering pressure at the rear end of the bus.

Another system is found in a paper on the effect of vehicle spacing on the aerodynamics of a representative car shape by Simon Watkins [55] talks about Inter vehicle spacing on highways which is considered and an analysis of spacing is presented, deduced from data from an instrumented highway. There are many variables in a study of this kind; these include vehicle geometric configuration (e.g. truck or car, including fastback, notchback, etc.), the lateral and longitudinal positioning of vehicles relative to each other and the nature and relative direction of the atmospheric wind. In order to restrict the number of variables, the investigation is limited to a wind-tunnel simulation of representative car geometry in calm conditions (i.e. no yaw angle) and vehicles that are directly aligned (i.e. co-linear) [55].

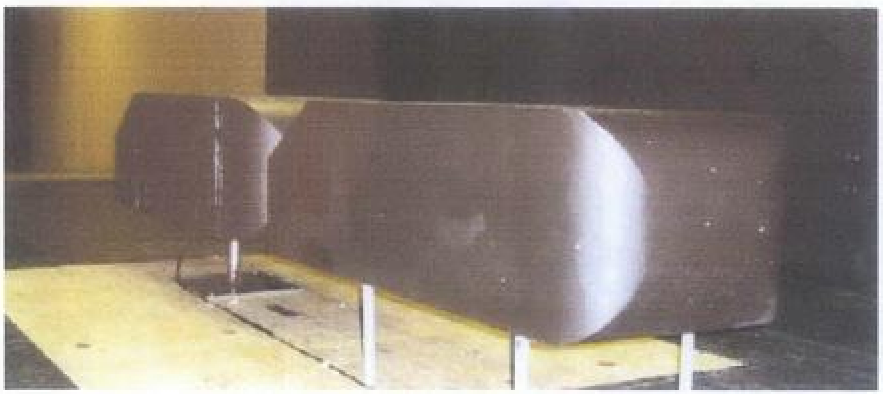

Figure 17: Sample drafting arrangement [55]

Roy and Srinivasan [1] concerned the aerodynamics of trucks and other high sided vehicles that are of significant interest in reducing road accidents due to wind loading and in improving fuel economy. They performed, a three-dimensional near field flow analysis for axial and cross wind loading to understand the airflow characteristics surrounding a truck. Their results provide associated drag for the truck geometry including the exterior rear view mirror. They stated that modifying truck geometry can reduce drag and improve fuel economy.

Wood [93] considered the assessment of the role of fluid-dynamic resistance and/or aerodynamic drag and their relationship to energy consumption in the United States. His data indicates that 16% of the total energy consumed in the United States is used to overcome aerodynamic drag in transportation systems. He suggested that application of existing pressure drag reduction technologies to all ground vehicles within the United States will reduce yearly energy costs by 20 billion dollars.

Abdel Aziz and Abdel Gawad [53] investigated experimentally and numerically the effect of air-stream velocity, gap ratio, and front shape of buses on the flow filed characteristics and heat transfer from the rear of bus to surrounding air flow. They designed three bus models (with flat-, inclined- and curved-front shapes) and constructed them from Plexiglas. They tested the model by using a suction-type wind tunnel. They provided a heating panel with copper constantan thermocouples for measuring the temperature and heat transfer coefficient on the rear surface of the models. Their numerical was carried out using the commercial CFD code „"Fluent"". Also, they used visualization technique to give an overall view of flow pattern around the bus models. They found that for both the flat- and inclined front vehicles, the front of the vehicle is pushed to turn towards the adjacent side wall of the tunnel. For the curved-front vehicle, the front of the vehicle is generally pushed away from the adjacent side wall of the tunnel. Also, the cooling of the inclined- and curved-front vehicles is better than the cooling of the flat-front vehicle by about 20%.

François et al. [52] studied the aerodynamics characteristics and response of a double deck bus, which is used in the Argentinean routes, submitted mainly to cross-wind. They carried out wind tunnel experiments for a 1:20 scale bus model, for different wind directions related to the vehicle axis, and at different free stream mean velocities, corresponding to a Reynolds number range from 53000 to 200000. They measured pressure distributions over the frontal and lateral part of the bus and also drag and lateral forces related to the center of gravity position. They recorded pressure coefficients distributions and the drag and lateral forces coefficients for different incident wind directions related to the bus axis.

Yelmuleet et al. [76] studied the aerodynamics of bus trips in open window buses where airflow due to motion provides comfort. There experiments by flow visualizations in a water channel using a redesigned exterior body showed a reduction of from 0581 to 0.41 at a speed of 100 km/hr overall aerodynamic drag reduction by about 30% due to combined effect of reduced and frontal area.

Alam et al. [36] stated that over 80% of the required total vehicle power is essential to overcome the aerodynamic resistance (and the remaining power is used for rolling resistance), they mentioned that add-ons causes extra drag to the total system hence extra fuel cost. Their primary objectives of this study were to experimentally measure the aerodynamic drag generated by various vehicle add-ons under a range of vehicle operating speeds. Their study was conducted using a reduced scale (25%) detailed model of a production large family size passenger car manufactured in Australia. They related the aerodynamic drag coefficient to fuel consumption and performed a detailed analysis of fuel savings.

Thorat and Rao [103] redesigned fuel saving an intercity bus with enhanced exterior styling that reduces aerodynamic drag and increases comfort for the passengers. They carried out extensive product study and market study they used Fluent, a CFD code to evaluate the aerodynamic performance. The benchmarked high- floor bus was redesigned with low floor for reduced aerodynamic drag. The exterior of the chosen bus was redesigned with emphasis on improving aerodynamic performance and appealing looks. The interior was modified to meet aspirations of the commuters. They found that for the best configuration, the drag was reduced by 29% and the comfort zone increased from 11% to 52% of the passenger volume.

Gopal and Senthilkumar [88] studied the variation of pressure coefficient, dynamic pressure, coefficient of lift and drag with and without vortex generators (VG) on the roof of a utility vehicle at varying yaw angles of VG. The yaw angles used are 10°, 15° and 20°.They performed testing wind tunnel with 1:15 scaled model of the utility vehicle with velocities of 2.42, 3.7, 5.42 and 7.14m/s. Their experiments showed that a great reduction of the aerodynamic drag can be achieved with vortex generators.

Muthuve et al. [8] aimed to modify the outer surface and structure of the bus aerodynamically in order to reduce the effect of drag force of the vehicle which in turn results in reduction of fuel consumption of the vehicle. They conducted experimental and numerical tests in Wind Tunnel to prove the effectiveness of their new concept design. Their results revealed that there is a considerable reduction in drag force of about 30%-34% from the existing bus to their new design and 6 to 7 liters of fuel is consumed for the every 100 Km.

Most of the researches were focused only on the race car, sedan aerodynamics rather than the heavy vehicles. This is mainly due to market forces at work and consumer preferences. However there were few researches, (Sachin Thorat and G Amba Prasad Rao, 1999) [96] conducted an research on “Computational Analysis of Intercity Bus With Improved Aesthetics And Aerodynamic Performance On Indian Roads” and reduced the drag force by 30%. (Edwin j Saltzman and Robert R Meyer, 2007) [81] carried out studies on reducing the drag of trucks and buses. The final model equipped with rounded horizontal and vertical corners ,smoothed under body and a boat tail achieved Cd value of 0.242. (Peter bilt Motors Company, 2009) [51] presents a white paper on Heavy vehicle aerodynamics and fuel efficiency. This paper reviews the aerodynamics drag losses which make the vehicles to utilize large capacity engines. (G Buresti, 2007) [81] carried out a research on Methods for the drag reduction of bluff bodies and their application to heavy road- vehicles in which they stated that in order to reduce the bluff body drag, boat- tailing has been applied & this reduced the base drag to about5% to 10% respectively. Further to reduce the drag force Tractor – Trailer gap has been occupied by a device so that both drag reduction and also the trailer can turn easily around the turns without any clashing. Also fairings and flow-deflection devices have been provided in the pressure drag not only of the axle but also of the trailer base. This paper also points out the wheels of the road vehicles are, in general, a source of considerable aerodynamic drag, therefore in order to reduce such drag wheel housings have been provided. It has also been said clearly that optimization.

Mc Callen (2004) [73] in their experiments found out removal of rear view mirror alone will bring down the drag of the vehicle by4.5%. Any gap in the vehicle body will result in flow separation and flow circulation. This investigation revealed a reduction in drag value until the front leading edge radii value reaches 150mm.

Panu Sainio (2007) [81] from a alt University conducted a research on aerodynamics possibilities for heavy vehicles and they came out with a conclusion that boat tail approach is known to be a good solution in terms of aerodynamics. The classical boat tail may increase the length of the vehicle significantly, but by using trailing edge blowing there might be possibilities to shorten the solution and still to have the full aerodynamically performance of the long boat tail.

E Selvakumar (2013) [35] conducted research on "Aerodynamic exterior body design of bus "experimental numerical tests have been conducted in wind tunnel to prove the effectiveness of the new concept design. It is evident from the test result, that there has been a considerable reduction in drag force of about 30 – 40% from the existing bus to the new concept and 6 to 7 liters of fuel is consumed for the every 100 km

Lietz conducted a CFD validation study on nine car-like benchmark models which are identical from the B-pillar forward but have different back configurations. The purpose of the study is to evaluate the effect of back end geometry variations on aerodynamic lift an drag. Predicted surface pressure coefficients on the front, under body and rear surfaces were correlated well with the experimental data. However, the over-predicted of separation bubble size occurring at the bottom of the front bumper and more up wash from the A-pillar rearward resulting in a higher drag coefficient. Unfortunately, they did not mention what kind of turbulence model used in their simulations[49].

Roy and Srinivasan performed a fully three-dimensional near field flow analysis to understand the airflow characteristics surrounding the truck-like bluff body. The unsteady flow distribution is calculated by solving the Navier-Stokes equation with a two-equation (k-ε) turbulence closure model. They found that modifying the truck geometry could significantly reduce the drag coefficient, hence improving fuel efficiency[94].

Basara conducted a numerical simulation of the flow around vehicles by examining a number of various industrial benchmarks. The computations showed a substantial difference in the flow patterns predicted by standard k-ε model and by the full Reynolds-stress model. Compared to the standard k-ε model, the Reynolds-stress model predictions of the pressure distribution on the car body agree extremely well with the measurements[87].

Patel and vijayakumar carried out an external flow analysis over 3 types of vehicles, namely sedan, wagon and coupe using a standard k-ε turbulence model. Based on the CFD study, the predictions were made on the drag coefficients, velocity fields and pressure distributions over the vehicles. Their study gives a better understanding of the flow characteristics near the vehicle body surfaces. Several suggestions were provided in order to improve the aerodynamic coefficients, such as the rake angle at the rear of the vehicle roof[87].

Murad conducted a simulation study of vehicle A-pillar aerodynamics using various turbulence models. Although the research was focused on a vehicle region, they managed to show that the k-ε turbulence model using second order upwind differencing scheme gave the best correlation against the experimental data[48].

Yang and Khalaghi conducted a CFD investigation to analyses flow around a pickup truck using realization k-ε two-equation eddy viscosity transport model. In their study, the comparisons between steady state CFD, transient CFD and test data were made. It is found that the steady state CFD gives the same quality of data as the transient CFD. This finding is very useful to the development in vehicle aerodynamics because the steady state calculations require much less computational resources and lead to faster turnaround time, hence more economical[121].

Reviews from past literatures suggest that the predictions can be made on the drag coefficients, velocity fields and pressure distributions over the vehicles based on the Car body agree extremely well with the measurements compared to the standard k-ε model. However, the k-ε turbulence model using second order upwind differencing scheme could give the best correlation against the experimental data. Besides, the over-predicated of the CFD calculation such as separation bubble size would result a higher drag coefficient. The most interesting finding from the literature review is that the steady state CFD did give the same quality of data as the transient CFD. This finding is very useful to the development in vehicle aerodynamics because the steady state calculations require much less computational resources and lead to faster turnaround time, hence more economical.

Advanced Aerodynamics Devices to Improve the Performance, Economics, Handling and Safety of Heavy Vehicles by Robert, J. E [2001] [44], The Research is being conducted at the Georgia Tech Research Institute (GTRI) to develop advanced aerodynamic devices to improve the performance, economics, stability, handling and safety of operation of Heavy Vehicles by using previously developed and flight-tested pneumatic (blown) aircraft technology. Recent wind-tunnel investigations of a generic Heavy Vehicle model with blowing slots on both the leading and trailing edges of the trailer have been conducted under contract to the DOE Office of Heavy Vehicle Technologies. These experimental results show overall aerodynamic drag reductions on the Pneumatic Heavy Vehicle of 50% using only 1 psig blowing pressure in the plenums, and over 80% drag reductions if additional blowing air were available. Additionally, an increase in drag force for braking was confirmed by blowing different slots.

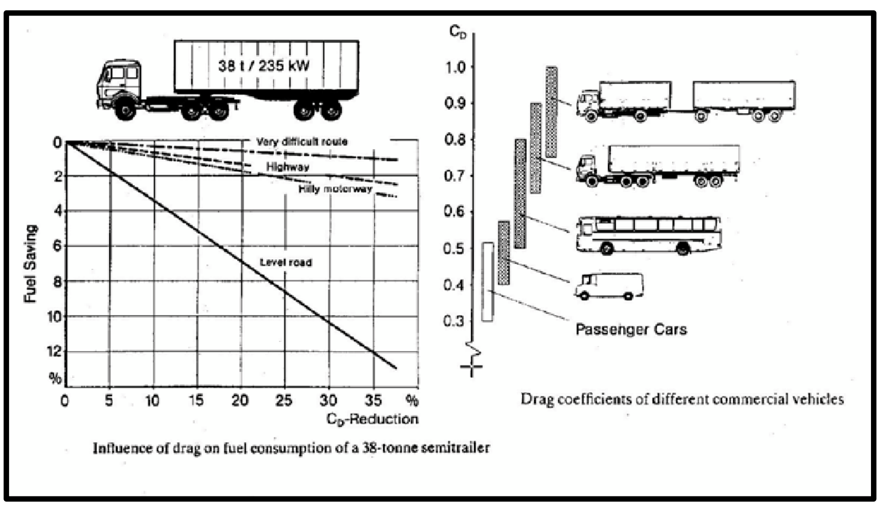

Figure 18: Effect Of Drag Coefficient Reduction on Fuel Consumption.
Source: Huncho, W.H. [1990] [742]

Lift coefficient was increased for rolling resistance reduction by blowing only the top slot, while down force was produced for traction increase by blowing only the bottom. Also, side force and yawing moment were generated on either side of the vehicle, and directional stability was restored by blowing the appropriate side slot. These experimental results and the predicted full-scale payoffs are presented in this paper, as is a discussion of additional applications to conventional commercial autos, buses, motor homes, and Sport Utility Vehicles.

In another research, the title Aerodynamic Drag of Heavy Vehicles (Class 7-8): Simulation and Benchmarking by McCallen, R. et al. [2001] [41] describes research and development for reducing the aerodynamic drag of heavy vehicles by demonstrating new approaches for the numerical simulation and analysis of aerodynamic flow. Experimental validation of new computational fluid dynamics methods are also an important part of this approach. Experiments on a model of an integrated tractor-trailer are underway at NASA Ames Research Center and the University of Southern California (USC). Companion computer simulations are being performed by Sandia National Laboratories (SNL), Lawrence Livermore National Laboratory (LLNL), and California Institute of Technology (Caltech) using state-of-the-art techniques.

The research title Vehicle Dynamics Model For Predicting Maximum Truck Acceleration Levels done by Rakha, H. et al. [1999] [40] presents a simple vehicle dynamics model for estimating maximum vehicle acceleration levels based on a vehicle's tractive effort and aerodynamic, rolling, and grade resistance forces. In addition, typical model input parameters for different vehicle, pavement, and tire characteristics are presented. The model parameters are calibrated/validated against field data that were collected along the Smart Road test facility at Virginia Tech utilizing a truck and trailer for 10 weight-to-power configurations, ranging from 85 kg/kW to 169 kg/kW (140 lb/hp to 280 lb/hp). The model was found to predict vehicle speeds at the conclusion of the travel along the section to within 5 km/h (3.1 mi/h) of field measurements, thus demonstrating the validity and applicability of the model.

Most of the researches were focused only on the race car, sedan aerodynamics rather than the heavy vehicles. This is mainly due to market forces at work and consumer preferences. However there were few researches, (Sachin Thorat and G Amba Prasad Rao, 1999) [40] conducted an research on "Computational Analysis of Intercity Bus With Improved Aesthetics And Aerodynamic Performance On Indian Roads" and reduced the drag force by 30%. (Edwin j Saltzman and Robert R Meyer, 2007) [39] carried out studies on reducing the drag of trucks and buses. The final model equipped with rounded horizontal and vertical corners, smoothed under body and a boat tail achieved Cd value of 0.242. (Peterbilt Motors Company, 2009) presents a white paper on Heavy vehicle aerodynamics and fuel efficiency.

This paper reviews the aerodynamics drag losses which make the vehicles to utilize large capacity engines. (G Buresti, 2007) [39] carried out a research on Methods for the drag reduction of bluff bodies and their application to heavy road- vehicles in which they stated that in order to reduce the bluff body drag, boat- tailing has been applied & this reduced the base drag to about 5% to 10% respectively. Further to reduce the drag force Tractor - Trailer gap has been occupied by a device so that both drag reduction and also the trailer can turn easily around the turns without any clashing. Also fairings and flow-deflection devices have been provided in the pressure drag not only of the axle but also of the trailer base. This paper also points out the wheels of the road vehicles are, in general, a source of considerable aerodynamic drag, therefore in order to reduce such drag wheel housings have been provided. It has also been said clearly that optimization.

Mc Callen (2004) [38] in their experiments found out removal of rear view mirror alone will bring down the drag of the vehicle by 4.5%. Any gap in the vehicle body will result in flow separation and flow circulation. This investigation revealed a reduction in drag value until the front leading edge radii value reaches 150mm.

Panu Sainio (2007) [39] from aalto University conducted a research on aerodynamics possibilities for heavy vehicles and they came out with a conclusion that boat tail approach is known to be a good solution in terms of aerodynamics. The classical boat tail may increase the length of the vehicle significantly, but by using trailing edge blowing there might be possibilities to shorten the solution and still to have the full aerodynamically performance of the long boat tail.

E Selvakumar (2013) [15] conducted research on "Aerodynamic exterior body design of bus" experimental numerical tests have been conducted in wind tunnel to prove the effectiveness of the new concept design. It is evident from the test result, that there has been a considerable reduction in drag force of about 30 - 40% from the existing bus to the new concept and 6 to 7 liters of fuel is consumed for the every 100 km.

Edwin J Saltzman and Robert R Meyer [31] carried out studies on reducing the drag of trucks and buses. The final model equipped with rounded horizontal and vertical corners, smoothed under body and a boat tail achieved C_d value of 0.242. Ludovico Consano and Davide Lucarelli [78] at IVECO truck building company came up with an aerodynamically efficient truck. They paid particular attention on the corner surfaces of the vehicle. Moreover the lateral lowered side skirts have been added to mask the tanks, rear wheels and axles. To prevent flow detachment, many rounded surfaces have been added to the exposed surfaces, such as the roof window, side mirrors, sun visor, etc. The test results revealed a fuel reduction of 8%.

R. Mc Callen, et al [91] in their experiments found out removal of rear view mirror alone will bring down the drag of the vehicle by 4.5%. Any gap in the vehicle body will result in flow separation and flow circulation. A Gilhaus [46] Investigation revealed a reduction in drag value until the front leading edge radii value reaches 150 mm. Further increase in the radius did not affect the drag value of the bus. G W Carr [18] investigated the effects of streamlining the front end of the rectangular bodies in ground proximity. Experiments shown a stream lined front end with low leading edge resulted in a drag coefficient of 0.21. W H hucko and H J Emmelmann [54] found that detailed shape optimization of parts such as roof radii, rain channels, headlights will result in reduction of drag force.

The Drag co-efficient of the Vehicle's body is evaluated by numerical computations performed with commercial CFD software, Finite Volume based solver, using the Navier-Stokes Equation.

Indeed, it is worth noticing that the changes on the drag when changing the shape deal with pressure force. Moreover as only 30% of the Drag Co-efficient depends on the front of the shape, the slanted surfaces and vertical base surface of the rear end will contribute strongly to pressure drag.

A way to have a good working definition of what CFD is to break down the word. "CFD is the acronym of Computational Fluid Dynamics. Computational means having to do with mathematics, computation and Fluid Dynamics refers to the dynamics of things that flow."

So, CFD is a computational technology that enables us to study things that flow. CFD not only predicts fluid flow behavior, but also the transfer of heat, mass, phase change, chemical reaction, mechanical movement and stress or deformation of related solid structures.

"The Drag busters" by R. Hendrickson, Grumman, with Dino Roman and Dario Rajkovic, has given the importance of drag. Drag is the heart of aerodynamic design. The subject is fascinatingly complex. All aerodynamicists secretly hope for negative drag. New design that employ advanced computational aerodynamics methods are needed to achieve vehicles with less drag than current vehicles.

"Aerodynamic shape optimization in automotive Industry" by **Fredrique Muyl, Laurent Dumas and Vincent Herbert(2001)** [7] has given the important aspects of the aerodynamic shape optimization tool for complex industrial flow. For each evaluation required by the optimizer, The Navier-Strokes equations are solved with a commercial CFD code on an unstructured mesh surrounding the shape to optimize.

"Reducing drag forces in future vehicles", project in the course road vehicle and aerodynamic design, MTF 235, AUTUMN (2002) [13] by **Alexander Diehl, Jose nuno Lopes, Rui Miranda**, Chalmers university of technology, has explained the relationship between drag force and speed of the car, drag force and change in drag coefficient and several ways to reduce the drag co-efficient of a vehicle.

Numerous research works have been reported in the literature on the aerodynamics of road vehicles. However, limited work is published with respect to the aerodynamics of heavy vehicles when compared to those related to study of aerodynamics of passenger cars. Saltzman and Meyer [33] in their experimental studies on reduction of drag of trucks and busses showed that by tuning the exterior with rounded horizontal and vertical corners, smoothed under body and a boat tail, the coefficient of drag could be reduced to 0.242. Ludovico Consano and Davide Lucarelli [69] at IVECO truck building company came up with an aerodynamically efficient truck. A higher and smoother roof was designed with DAM fully integrated into the frontal bumper. The lateral lowered side skirts were added to mask the tanks, rear wheels and axles. To prevent flow detachment, many rounded surfaces were added to the exposed surfaces, such as the roof window, side mirrors, sun visor, etc. The test results revealed a fuel reduction of 8%. Callen et al [90] in their experiments found out removal of rear view mirror alone would bring down the drag of the vehicle by 4.5%. This study reiterated that gap in the vehicle body would result in flow separation and flow circulation. Studies by Gilhaus [19] concentrated on fine tuning the front leading edge radii. An optimum front edge radius of 150 mm was reported in this study, and a further increase in the radius was found to have the least influence on the coefficient of drag of the bus. Carr [18] investigated the effects of streamlining the front end of the rectangular bodies in ground proximity. Experiments shown a stream lined front end with low leading edge resulted in a drag coefficient of 0.21. Huco and Emmelmann [45] found that detailed shape optimization of parts such as roof radii, rain channels, headlights also would result in considerable reduction of drag force. Mason and Beebe [70] carried out experiments on the use of add-on devices on trucks and busses. These investigators investigated the effect of use of horizontal and vertical splitter panels extending from vehicle body at the rear end, vanes and non ventilated cavities close to vehicle bodies. Splitter panels were shown to have no affect on the drag value whereas the vane arrangement increased the drag. The addition of non ventilated cavities reduced the drag coefficient by 5%. The studies on aerodynamic tuning of the exterior of bus and truck bodies [98] and the numerical studies reported in the literature on the aerodynamic studies [122] were found to be useful in deriving useful tips for the present investigation. The report on urban transport crisis in India [62] motivated this study and the new design of the bus was based on AIS-052 code for bus body design and approval [6].

CHAPTER THREE

3. THEORY OF AERODYNAMICS AND CFD

In this chapter the general basics of aerodynamics around a bus are explained together with some of the existing drag reducing devices. Furthermore, a brief introduction is given to fluid dynamics and the tool in this project, Computational Fluid Dynamics (CFD).

3.1 Bus Aerodynamics

Aerodynamic drag consists of two components, pressure drag (force acting normal to surface) and friction drag (force acting tangential to surface). Friction drag is due to shear stress between the fluid and the surface, whereas pressure drag is due to a pressure difference between the front and the rear of the body. For a bus, and other blunt bodies, the pressure drag is the most dominating one and contributes to more than 90 percent of the total drag [107]. In addition to the bus front, the regions that represent the main drag contributing areas around a bus are: the roof, side and the base wake behind the bus and the undercarriage [24].

3.1.1 Rear of The Bus

At the rear of the bus a dominant base wake is created, containing unsteady turbulent flow. This is a result of a low-momentum flow along the top and the sides of the bus that separates at the trailing edge of the bus. The low-momentum flow from the undercarriage interacts with the base wake, resulting in an even greater turbulent base flow. A consequence of this is a low-pressure region that is created behind the trailer that contributes to drag. There exist different types of aerodynamic devices to decrease and stabilize the base wake by guiding the flow at the rear of the bus. By extending the rear with different types of angled plates, the flow attachment is maintained and the air can be guided into the center of the base wake. Other devices are added to the sides and the roof of the bus to generate energized vortices to delay the separation and thereby decrease the base wake[22].

Decreasing the fuel consumption of road vehicles, due to environmental and selling arguments reasons, concerns bus manufacturers. Consequently the improvement of the aerodynamics of bus shapes, more precisely the reduction of their drag coefficient, becomes one of the main topics of the automotive research sectors. Designing a vehicle with a minimized Drag resistance provides economical and performance advantages. Decreased resistance to forward motion allows higher speeds for the same power output, or lower power output for the same speeds.

The main motivation for reducing drag resistance is:

Ø. Fuel consumption reduction and

Ø. Performance increasing.

3.1.2 Regimes of External Flow

Consider the external flow of real fluids. The potential flow and boundary layer theory makes it possible to treat on external flow problem as consisting broadly of two distinct regimes, that immediately adjacent to the body's surface, where viscosity is predominant and where frictional forces are generated, and that outside the boundary layer, where viscosity is neglected but velocities and pressure are affected by the physical presence of the body together with its associated boundary layer. In addition, there is the stagnation point at the front of the body and there is the flow region behind the body (known as the wake). These flow regimes are shown in Figure 19.

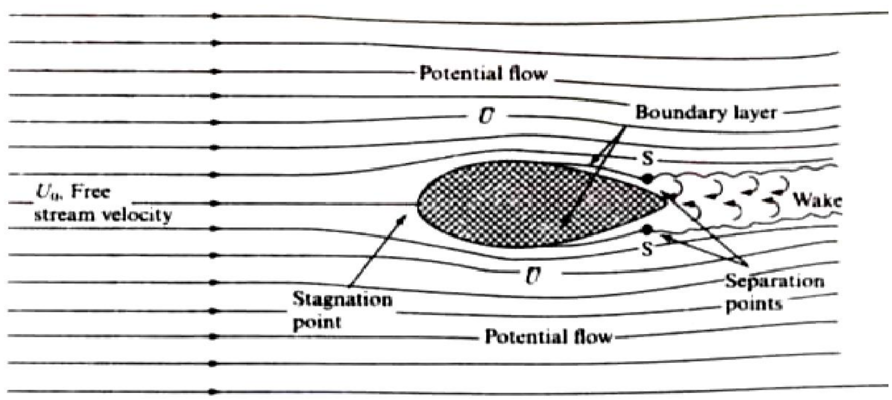

Figure 19: Flow Regimes around an immersed body

The wake starts from the points "S" at which the boundary layer separation occurs. Separation occurs due to adverse pressure gradient, which combined with the viscous forces on the surface produces flow reversal, thus causes the stream to detach itself from the surface. The same situation exists at the rear edge of a body as it represents a physical discontinuity of the solid surface.

The flow in the wake is thus highly turbulent and consist of large scale eddies. High rate energy dissipation takes place there, with the result that the pressure in the wake is reduced. A situation is created whereby the pressure acting on the body (stagnation pressure) is in excess of that acting on the rear of the body so that resultant force acting on the body in the direction of relative fluid motion exerts. The force acting on the body due to the pressure difference is called pressure drag.

3.1.3 Total Drag

Any object that moves through a fluid (water/air) can get a decrease in form drag by streamlining. Automobiles are streamlined, which translates (allows) better gas mileage; there is less drag so less fuel is required to "push" the car forward. Buses, vans, and large trucks are less streamlined, and this is the reason why they use more fuel than smaller, streamlined cars (weight is another reason).

The drag is a resistance force. This force works to slow the forward motion of an object, including planes. There are four types of drag: friction drag, form drag, induced drag and wave drag. These drag types develop around the shape of the body, the smoothness of the surfaces, and the velocity of the plane. All four sum together for the Total drag force. The total drag on the body, often called profile drag is therefore, made up of two contributors namely the pressure drag and the friction drag. The drag forces are the opposite of thrust. If the thrust force is greater than the drag force, the vehicle goes forward, but if the drag force exceeds the thrust, the vehicle will slow down and stop.

The friction drag is sometimes also called the skin friction drag. The force on the body acting in the direction of relative motion due to fluid shear stress is known as Frictional drag. Thus in external flow the immersed body is subjected to functional drag over its entire surface. Figure 20 shows the situation where air flowing along a surface will create lot of friction drag. There is a large fast-moving air next to the non-moving surface. In contrast, there will be little pressure drag because there is very little frontal area for anything to push against.

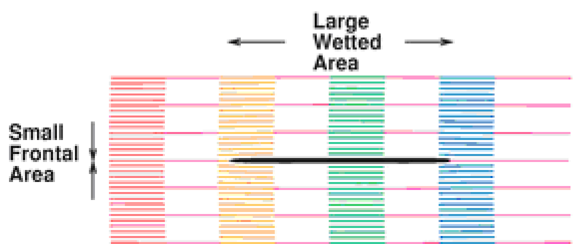

Figure 20: Friction Drag Airflow Orientation

The form drag, or pressure drag as it is sometimes called, is directly related to the shape of the body of the vehicle. Figure 21 shows the situation where air flowing along a surface will create lots of friction drag.

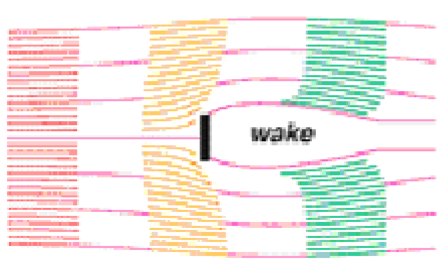

Figure 21: Pressure Drag Airflow orientation

Thus,

Total drag = Pressure drag + Friction drag

The relative combination of pressure drag and friction drag to the profile drag depends upon the shape of the body and its orientation with respect to the flow.

3.1.4 Minimizing Drag on a Medium Mass Vehicle (Bus)

There are several ways to reduce the C_d of a vehicle. The vehicle's global shape has the most direct influence in the final value of C_d . Still, improvement in details like the rearview mirrors, underbody, or the use of some particular devices may contribute to a lower final C_d.

3.1.5 Expression of Drag Force

Drag in general physics is referred or defined as the resistive force experienced by an object/ body

when it is in motion with respect to the fluid surrounding it. Drag forces are dependent on the velocity of the object and is shown by a formula defined as:

The Drag force(F_d) value for a moving vehicle is given by the following expression:

$$F_d = 1/2\ A\ \rho\ C_d\ V^2 \qquad \text{Equation 3.1}$$

Where

- C_d is the drag coefficient
- A is the projected frontal area of the vehicle
- ρ is the density of air
- V is the speed of the vehicle relative to the air

This equation shows that to calculate drag we need to know three things: C_D, the drag coefficient; A, the frontal area of vehicle/bus, and V, the speed of air past the vehicle. This equation shows important point aerodynamic forces are proportional to the square of the speed. That means you quadruple the drag or lift when you double the speed. Since speed is never the item that is pretended to be decreased and the density of air is not even possible to change, the aerodynamic resistance can only be reduced or minimized by manipulating the vehicle's design characteristics, obtaining lower C_d, or even reducing the vehicle's frontal area.

3.1.6 Expression of Lift Force

In aerodynamics lift is a force that holds an object in the air. In automobiles the pressure difference of the high pressured frontal end to the low pressure rear end generates the lift.

But how actually it is generated with velocity?

The answer lies in simple physics. Whenever air flows over an object or vice versa, the molecules of the gas move freely. According to David Bernoulli (Bernoulli's concept explained: 2.1.*)

the pressure is directly proportional and relates to the local velocity of the air (NASA, 2013). This explains why velocity varies and pressure too. Lift is always perpendicular to the flow of the air on the automobiles.

It is explained by the following equation in aerodynamics:

$$F_L = \mathbf{1/2}\boldsymbol{\rho} V^{2} \boldsymbol{C_l A} \qquad \text{Equation 3.2}$$

Where, F_L is the lift force

$\boldsymbol{\rho}$ is the density of the fluid.

V speed of the object

C_L is the lift coffieicient

A is the cross sectional area.

This equation will be used further in the chapter of results and discussion a to find the lift force obtained in the car body. Generally the lift force will be the total force of the forces in y direction in addition to the viscous forces in the y direction.

3.1.7 Aerodynamic Pressure Distribution

As the car moves through an ambient mass of air, the body of the car displaces bundle of imaginary streamline filaments that constituent of the airflow field. Now as the stream line is displaced these streamlines are made to accelerate from rest up to a velocity. This creates a pressure distribution across the air field and the boundary of the body of the car (figure 22). The high static pressure also referred as zero velocity. Generally the stagnation point in the front of the car while the low static pressure area is the wind screen header and the top roof peak of the car. (John D. Smidth, 2014)

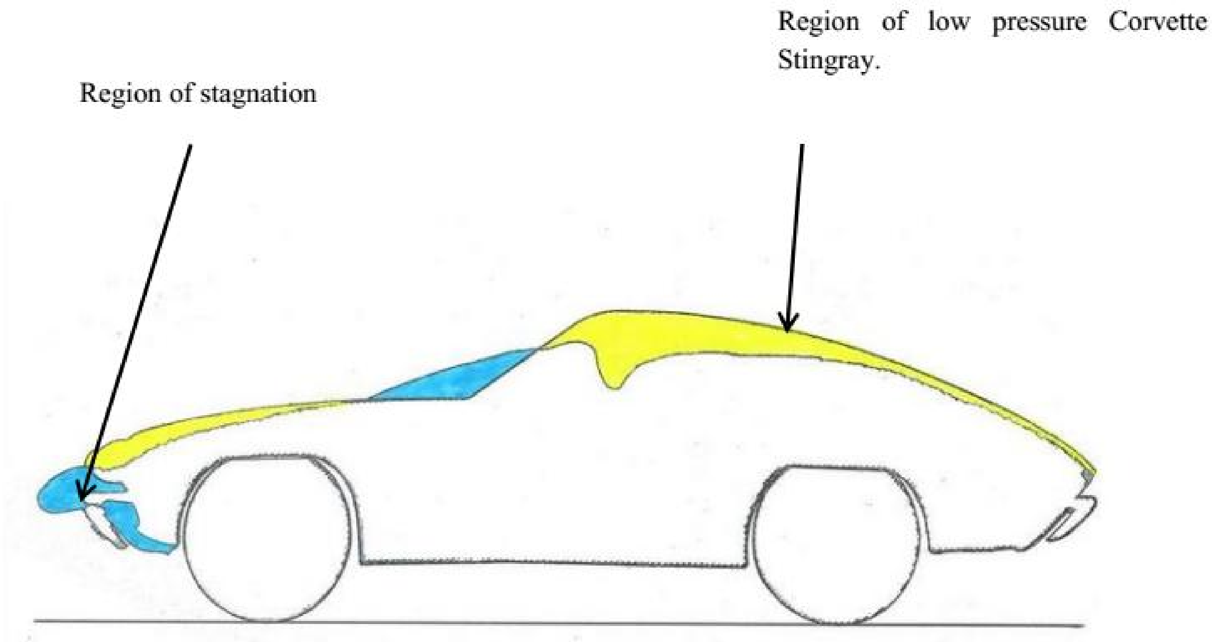

Figure 22: Region of high (blue) & low (yellow) pressure of a corvette Stingray

P static + P dynamic = P total

$$Ps + 1/2\rho V^2 = Pt \qquad \text{Equation 3.3}$$

The coefficient of pressure at any point on the surface of the car is characterized by the following equation given by: $C_p = \frac{(p - p_0)}{(\frac{1}{2}\rho v^2)}$ where Cp is the coefficient of pressure, p is the static pressure at the vehicle surface, p_0 is the free stream static pressure and rest of the variables are defined earlier.

Usually the value of Cp at the stagnation point is 1 & zero when the local as well as free static pressure is same all over the flat section of the car body. The negative pressure coefficients can be obtained in certain cases when the local velocities are greater than the free stream velocities.

The coefficient of the pressure depends upon the geometry of the car, hence is a function of the shape. The distribution of pressure on most of the surface of the car is done by using Bernoulli's equation [Eq. 33]. The net upward force is calculated by the integration of the total pressure distribution. The force obtained (Which is usually negative) means that there is no requirement to enhance the stability of the car. The exact opposite reactive force is the down force(Duysinx, 2014-2015).

Certain experiments on the pressure distribution calculated by different car manufactures and individual research analyses are shown below. This will help to generate a clear concept of the pressure distribution around a car.

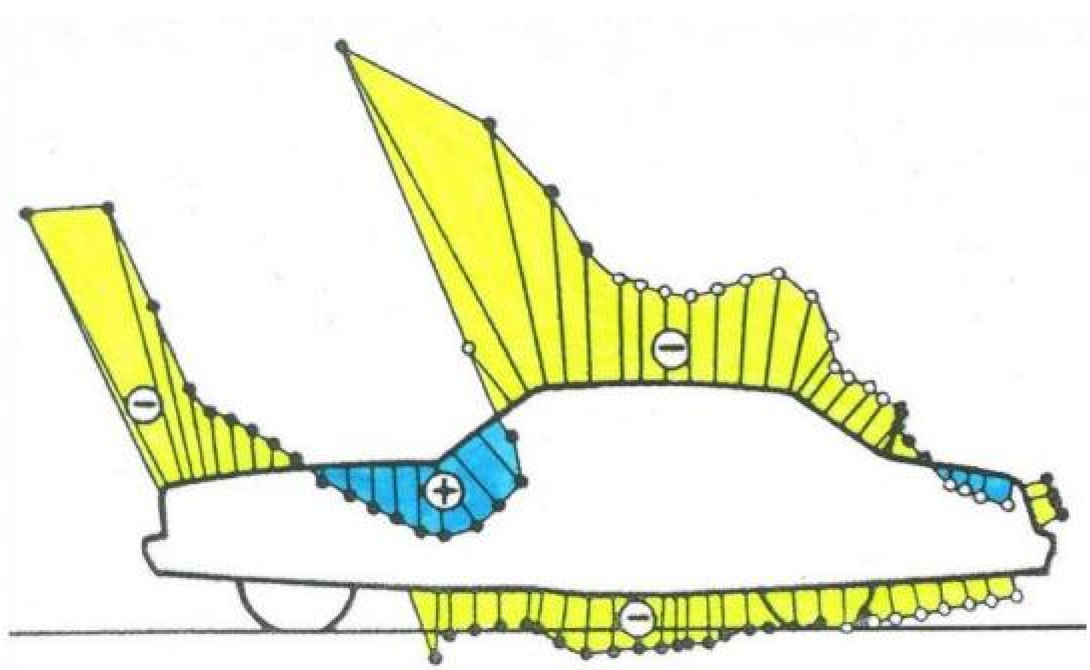

Figure 23: Region of high & low pressure around a car

3.1.8 Styling and Aerodynamics

Drag force acting on the vehicle depends on frontal projected area and the coefficient of drag value of the vehicle. Any reduction in these values will directly reduce drag force experienced by the vehicle. Frontal projected area of the highway bus is decided by the interior packaging of the bus. Coefficient of drag value is determined by the shape of the vehicle. These two factors influence the exterior styling of the vehicle. Exterior styling of the vehicle is important due to the fact that the vehicle has to attract customers. The vehicle should project its performance and comfort capabilities through its exterior design. Finding harmony with the aerodynamic requirements will lead to a successful vehicle with low fuel consumption. Yutong ZK6116D bus was evaluated for its aerodynamic performance and guidelines for better aerodynamics were collected from literature survey. Based on these guidelines and user study concepts were generated. The model was analyzed using CFD and improvements in drag values were predicted.

3.1.8.1 Shape of The Vehicle's Body

The vehicle's global body shape states the average aerodynamic performance, so it is the most important design feature. The main requirement is that the shape should maintain attached flow over most of the surface. This is accomplished by having a streamlined shape. The most efficient shapes are the simple 'teardrop' or the airfoil based one.

- Turbulent Flow

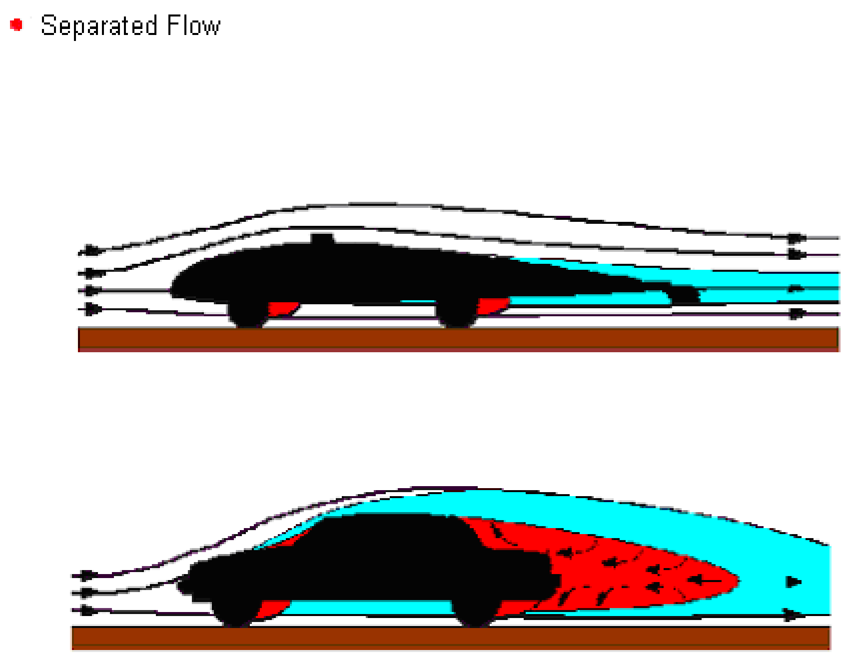

Figure 24: Shape of Vehicle's Body

Unfortunately, these two body shapes are very hard to put in practice because they have very little or sometimes non acceptance by the customers. Furthermore, these shapes tend to cause obstacles to some functional aspects of the vehicles, like storing space, and dynamic stability.

3.1.8.2 Drag

For bluff bodies where the drag is mainly due to direct stresses, the drag coefficient is defined in terms of a dimension normal to the flow. This is in contrast to streamlined bodies where the drag is mainly due to shear stress, where a dimension parallel to the flow is used. The drag is sometimes divided into fore body drag, due to the pressure distribution around the front, and base drag, due to that round the back. This is useful because, by and large what goes on in the wake does not depend to any extent on the fore body, provided separation occurs at the same place, and similarly the flow over the fore body is not influenced much by changes in the base region.

Typical values for drag coefficient are:

Table 2: C_d for various objects

PARTICULARS	**VALUES OF C_d**
Circular cylinder normal to stream	0.35 to 1.2, depending on aspect ratio
Flat plate normal to stream	2.0
Rectangular section	0.9 to 3, depending on aspect ratio
Sphere	0.1 to 0.4, depending on aspect ratio
Disk normal to stream	1.2

Cube, face on to stream	1.1
Saloon car	0.22-0.4
Sports car	0.28-0.4
Light van	0.35-0.5
Buses and Coaches	0.4-0.8
Articulated container truck	0.55-0.8
Ridged truck & draw bar trailer	0.7-0.9

3.1.8.3 Components of Drag

There are mainly four components of drag. These are:

1. Driving Force
2. Resistance Force
3. Weight
4. Lift/Reaction Force.

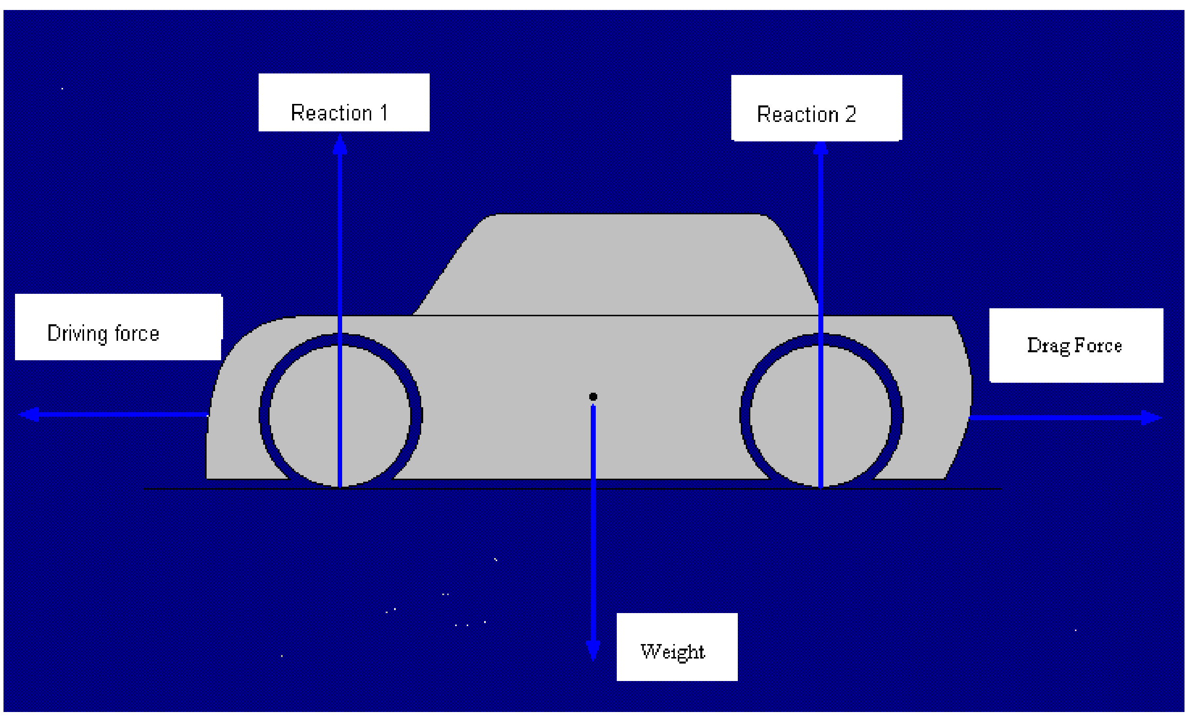

Figure 25 : Components of Drag

1. Thrust/Driving Force: - Driving Force is the Force Developed by the motion of the vehicle in forward Direction.

2. Drag/Resistance Force: - Resistance Force is the resistance developed by the motion of the air in the opposite direction of the motion of the vehicle.

3. Weight: - Weight is nothing but the weight of the vehicle itself, acting in the downward direction.

4. Lift/Reaction Force: - Lift is upward force acting on the vehicle. It acts on both the front and rear wheels of the vehicle. It is induced due to the vortices created on the back of the vehicle and it is the reason that the lift on the rear wheel is more than the lift on the front wheel.

3.1.8.4 Thrust vs. Speed of Bus

When we start moving in a car the resulting force is forward. In the following figure we assume that the car's engine will produce constant thrust, no matter what its speed.

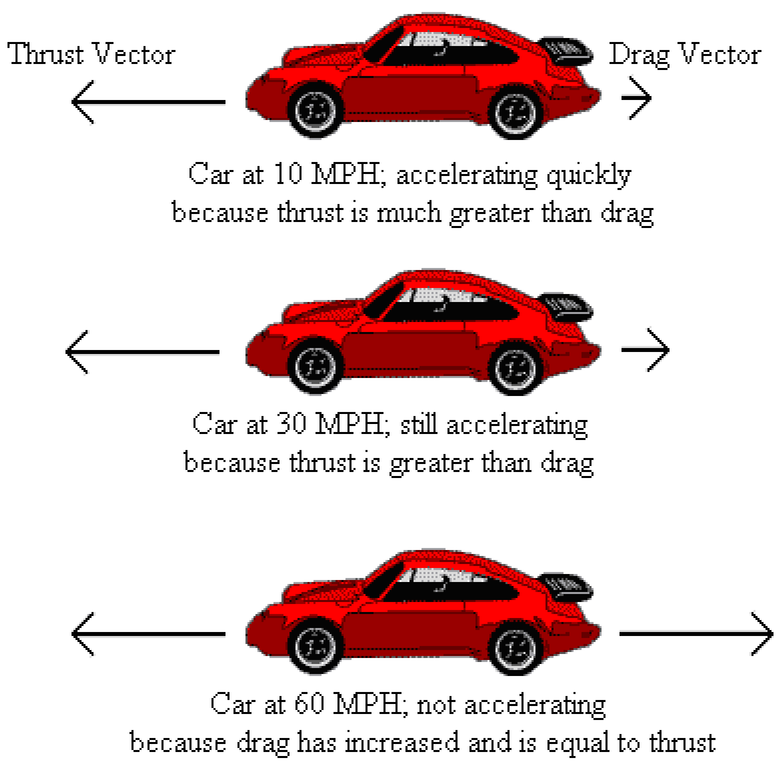

Figure 26: Cars at Different Speeds

Once the drag vector length equals the thrust vector line length, there is no more acceleration. The car has reached "equilibrium" speed. We've just learned a new term, equilibrium. Equilibrium exists when all force vectors are balanced. They cancel each other out.

Note that at 30 MPH the drag vector is only 1/4 the length of the drag vector at 60 MPH. We just want to reinforce the facts that drag increases as the square of the velocity.

3.2 Computational Fluid Dynamics(CFD)

3.2.1 Introduction

A way to have a good working definition of what CFD is to break down the word. "CFD is the acronym of Computational Fluid Dynamics. Computational means having to do with mathematics, computation and Fluid Dynamics refers to the dynamics of things that flow."

So, CFD is a computational technology that enables you to study things that flow. CFD not only predicts fluid flow behavior, but also the transfer of heat, mass, phase change, chemical reaction, mechanical movement and stress or deformation of related solid structures.

Computational Fluid Dynamics or simply CFD is concerned with obtaining numerical solution to fluid flow problems by using computers. The advent of high-speed and large-memory computers has enabled CFD to obtain solutions to many flow problems including those that are compressible or incompressible, laminar or turbulent, chemically reacting or non-reacting. Computational Fluid Dynamics (CFD) is the science of predicting fluid flow, heat transfer, mass transfer, chemical reactions, and related phenomena by solving the mathematical equations which govern these processes using computational methods.

CFD is the art of replacing the differential equation governing the Fluid Flow, with a set of algebraic equations (the process is called discretization), which in turn can be solved with the aid of a digital computer to get an approximate solution. The well known discretization methods used in CFD are, Finite Volume Method (FVM), Finite Element Method (FEM), and Boundary Element Method (BEM).

In brief, it is implemented by dividing a computational domain into small cells where the flow is modeled and flow equations are solved. Since almost all fluid flows are turbulent, different CFD methods are used in order to simulate turbulence. These can be divided in different categories where some of them are; Turbulence models for Reynolds-Averaged Navier-Stokes (RANS) equations, Large Eddy Simulation (LES), Direct Numerical Simulation (DNS) and Lattice Boltzmann method (LBM). The LBM differs from the other methods by simulating the movements of particles and aims at recover the hydrodynamics of the Navier-Stokes equation. RANS on the other hand, uses the Navier Stokes equations as a starting point and aims at solving them [28]. DNS does not use a turbulence model; it computes all the turbulent velocity fluctuations and therefore demands both small time steps and cells that require substantial computer resources. LES focus on the large eddies in the flow and requires quite large computer resources. However, the most common way to simulate turbulence is to calculate the time averaged properties of the flow, such as mean pressure, mean velocity and so on, which in most cases give sufficient information about the flow. This method has a modest computer demand and is conducted with RANS-models [49].

3.2.2 Computational Domain

The computational domain and its cells, the so-called volume mesh, can be generated and designed indifferent ways. The cells can be constructed in shapes of tetrahedral, hexahedral and polyhedral. The different cell types have different advantages and disadvantages that depend on the geometry and flow characteristics. For this project the hexahedral mesh with prism layers has been chosen since it is faster to generate and requires less memory, compared to the polyhedral mesh for example. For external aerodynamic flow simulations that have a predominately streamlined flow, the hexahedral mesh also gives a faster convergence. These are the reasons why this mesh type is recommended by CD. This method divides the computational domain into small cubes, which are subdivided until they reach a desired resolution. Each subdivision dimidiates the size of the cube and provides a smooth variation in cell size [4000].results seems to depend on this value.

3.2.3 The Benefits of CFD

Insight: There are many devices and systems that are very difficult to prototype. Often, CFD analysis shows parts of the system or phenomena happening within the system that would not otherwise be visible through any other means. CFD gives a means of visualizing and an enhanced understanding of the various designs.

Foresight: Because CFD is a tool for predicting what will happen under a given set of circumstances, it can answer many 'what if?' questions very quickly. We give it variables. It gives us outcomes. In a short time, we can predict how the design will perform, and many variations may be tested until you arrive at an optimal result. All of this is done before physical prototyping and testing. The foresight we gain from CFD helps us to design better and faster.

Efficiency: Better and faster design or analysis leads to shorter design cycles. Time and money are saved. Products get to market faster. Equipment improvements are built and installed with minimal downtime. CFD is a tool for compressing the design and development cycle.

3.2.4 Fluid Dynamics

Fluid dynamics is the study of fluids in motion and the physics can be described by three conservation laws [37]:

•Conservation of mass - the continuity equation states that the amount of mass flow that enters a control volume must be equal to the amount leaving it.

•Conservation of Linear momentum (Newton's Second Law of Motion) - given a Newtonian fluid, these equations are used to obtain a relation between pressure, momentum and viscous forces, the equations are called Navier-Stokes equations.

•Conservation of energy (First Law of Thermodynamics) - the energy equation is the law saying that the total amount of energy is conserved within the system, however, it can change between the different states.

Due to the mathematical complexity of the equations it is almost impossible to solve them analytically, except for some simplified cases. However, when working with air at room temperature and a Mach number below 0.3, the fluid can be assumed to have constant density, a so-called incompressible flow. This together with the assumption that the viscosity of the fluid is constant, makes it possible to write the conservation laws as following [37]:

$$\nabla V = 0 \qquad \text{Continuity equation} \qquad \text{Equation 3.4}$$

$$\rho\, \partial V/\partial t = -\nabla p + \mu \nabla^2 V + \rho g \qquad \text{Momentum equation} \qquad \text{Equation 3.5}$$

$$\rho c_p dT/dt = k\nabla^2 T + \Phi \qquad \text{Energy equation} \qquad \text{Equation 3.6}$$

where V=velocity field, ρ=density, t =time, p=pressure, μ=viscosity, g=gravity field cp=specific heat capacity, T=temperature, k=coefficient of thermal conductivity, Φ=viscous−dissipation function.

The continuity and momentum equations can be solved independently of the energy equation and when temperature is constant, as assumed in this project, the energy equation is neglected. The continuity and momentum equations describe the motion of the fluid and are solved for velocity and pressure. Almost all fluid flows are turbulent, that is: stochastic, three-dimensional and time dependent [5]. Due to this chaotic behavior the flow will experience fluctuations, which means that pressure and velocity will be defined as the mean value plus a fluctuation term; $u = \bar{u} + u'$ and $p = \bar{p} + p'$ respectively. To handle this, the equations (continuity and momentum), with additional terms due to fluctuations, are time averaged. The new equations are called Reynolds Averaged Navier-Stokes equations, abbreviated as RANS [37]

3.2.5 Turbulence models for Reynolds-Averaged Navier-Stokes equations

There are several different turbulence models within the RANS method that in different ways models the extra terms that forms when the Navier-Stokes equations are time-averaged. Some models worth mentioning are mixing length model, k−ε model, k−ω model and Reynolds stress model, which have none, two, two and seven additional transport equations respectively, which needs to be solved in addition to the RANS equations [49]. Naturally, all models have their advantages and disadvantages; the mixing length model is not suitable for flows with separation and circulations, and the Reynolds stress model is the most complex one of these four and needs fairly large computer capability. Left are the two two-equation models k−ε and k−ω. Both k−ε and k−ω are so-called Eddy viscosity models, which means that they are based on turbulent viscosity. In the k−ε model the two transports equation are solved for the turbulent kinetic energy k and its dissipation ε. ω is the dissipation rate per unit turbulence kinetic energy, in other word the specific dissipation rate ω! ε/k. One of the major differences between these two models is that the standard k−ε model needs wall functions to resolve the boundary layer, whereas the k−ω model is feasible to use all the way into the wall [20]. The k−ω model on the other hand, deals with problems when it comes to the initial value of ω in the free stream. In order to obtain the best features of the two models, Menter developed a modified k−ω model 1992 called Shear Stress Transport (SST) k−ω turbulence model. This model is a mix between k−ε and k−ω,and uses the near-wall features from the k−ω model close to the wall and then applies the k−ε model in the free-stream regions away from the wall. SST k−ε turbulence model is chosen for this project since it is widely used in vehicle aerodynamics and is efficient and accurate [115].

3.2.6 Bernoulli's Equation

$$\mathbf{P} + \mathbf{1/2\rho v^2} + \mathbf{\rho g h} = \mathbf{Constant} \qquad \text{Equation 3.7}$$

The Swiss mathematician & physicist (1700 – 1782) put forward a principle called Bernoulli’s equation (Eqn 3) which held for fluids in ideal state; pressure and density are inversely related: in other terms slowing moving fluids exert more pressure than fast moving fluids. This equation is the fundamentals of the study of the airflow around vehicles. Bernoulli’s equation obtained by integrating Newton’s law F = ma (Munson, Young, and Okishi. 2006) is supported with the following assumptions:

- Air density does not change with the pressure.
- Viscous flow of the fluid is neglected.
- Steady state flow is assumed and always maintained.
- The fluid flow is compressible.
- The formula can be applied at any point in the streamline flow.

This resulted in the formula being derived to

$$\mathbf{P} + \mathbf{12\rho v2} + \gamma z = \text{Constant} \qquad \text{Equation 3.8(Munson 2006)}$$

Or can be written as $\mathbf{P/\rho} + \mathbf{1/2v2} = \boldsymbol{k}$ Equation 3.9(Katz 1995)

The above equation is valid when height is not accountable.

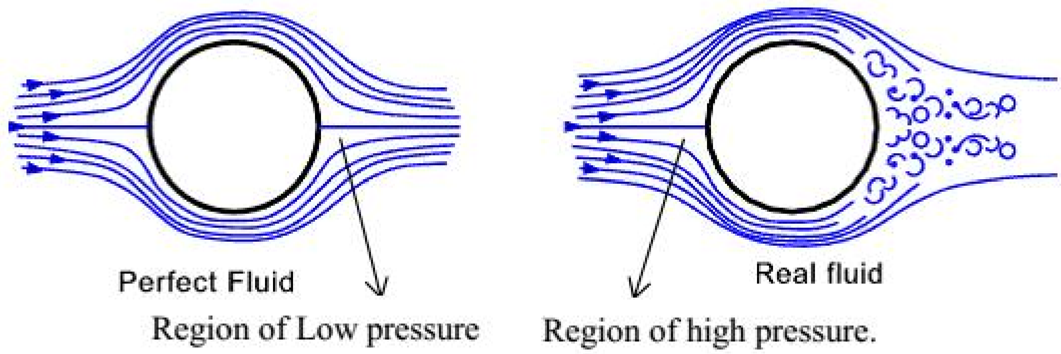

Figure 27: Flow of air/ fluid around a spherical body to demonstrate low and high pressure regions

Whenever the air flows over the body, it generates a velocity distribution resulting in the aerodynamic loads acting on the body of the vehicle. The first is the shear force acting tangentially on the surface of the vehicle body generating the drag force which is because of the viscous boundary layer. The second force is the pressure force. The pressure force acts perpendicular to the surface of the body and has a contribution to both drag and lift. Technically the vehicle's down force is the added effect of the pressure distribution (Katz, 1995)

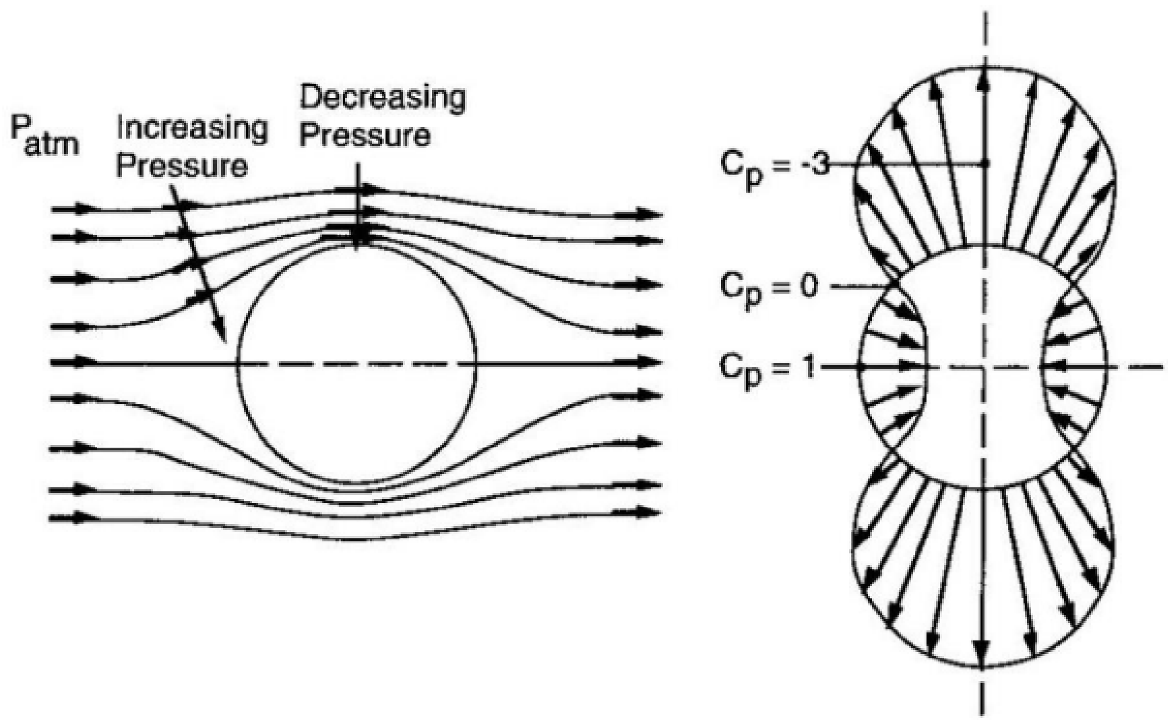

Figure 28 a.) Left shows the low pressure. b) Values of coefficient of pressure around the geometry

CHAPTER FOUR

4. METHODOLOGY

4.1 Bench Marking the Baseline Model

In this study setting the baseline model is the first task. This baseline model is one of the models of Yutong cross-country bus shape. The body of bus was designed to actual Yutong bus dimensions which are almost common to the actual design. The overall body shape is considered for aerodynamic analysis.

Yutong bus was bench marked for the study. It is the latest model in the China market and is popular in Ethiopia nowadays. Engineering parameters of this model was kept as same for the new bus design and was selected as the baseline for studying the aerodynamic performances. This bus model was used to carry out CFD and aerodynamic parameters such as, flow separation and stagnation areas, pressure and velocity distribution around the body, C_d, and contribution of various exterior parts on the overall drag coefficient of the vehicle.

Figure 29: Existing Yutong Bus(Baseline)

Criteria for selecting Yutong bus(baseline model)

- ✓ The bus is currently popular in Ethiopia. Many government and private organizations are using the bus as a service and public transport.
- ✓ Even if the design and the model of the bus are imported from China, it is assembled here in Ethiopia in Bishoftu Automotive Industry.
- ✓ It is the only long and cross-country bus assembled in Bishoftu Automotive Industry(in Ethiopia). It has 60 seats.

- ✓ The bus has no good aerodynamic shape.
- ✓ It consumes 23 liters per 100 km. This needs to be improved in total resistance of the bus. Due to these, I have selected the aerodynamic resistance. Which is serious in cross-country bus while the speed is above 60 kmph and has a significant role in increasing fuel consumption.

4.2 Geometry Generation

Three dimensional model of the baseline model(10771 mm, 2446 mm, 2727 mm), model 2, and model 3 were created using CATIA V5R19 and SOLIDWORK 2014 as shown in (Figure 30, 31, 32 & 33) below. The original(existing) dimension(10771 mm, 2446 mm, 2727 mm) of the baseline model was used for all the models. Fluid domain of 50 m x 30 m x 30 m was created around the bus model which was 3 to 5 times the length of vehicle to X, Y and Z-direction. Bus model was placed inside this domain in such a way that 1/3 length was kept in front of the vehicle. The larger domain was kept at the rear to capture the essential flow features (Figure 5). A smaller domain was created inside this domain to generate fine mesh in and around the bus body. ANSYS WORKBENCH 14.5 pre processor and FLUENT 14.5 post processor were the software tools used to generate the mesh and to solve fluid dynamics problems respectively. Outer volume was meshed with coarse elements. Unstructured tetrahedral hybrid elements of 1,342,263 for model 1, 1,391,681 for model 2, and 1,380,386 for model 3 were used to mesh the entire fluid domain.

A. Model 1

This model is the baseline model that means the actual existing Yutong cross-country bus model design.

B. Model 2 and Model 3

These models are the modified models of baseline model. The models are designed under the consideration of aerodynamic aspects and parameters. Modified aspects are Frontal area, Roof, Rear shape & Side panel shape.

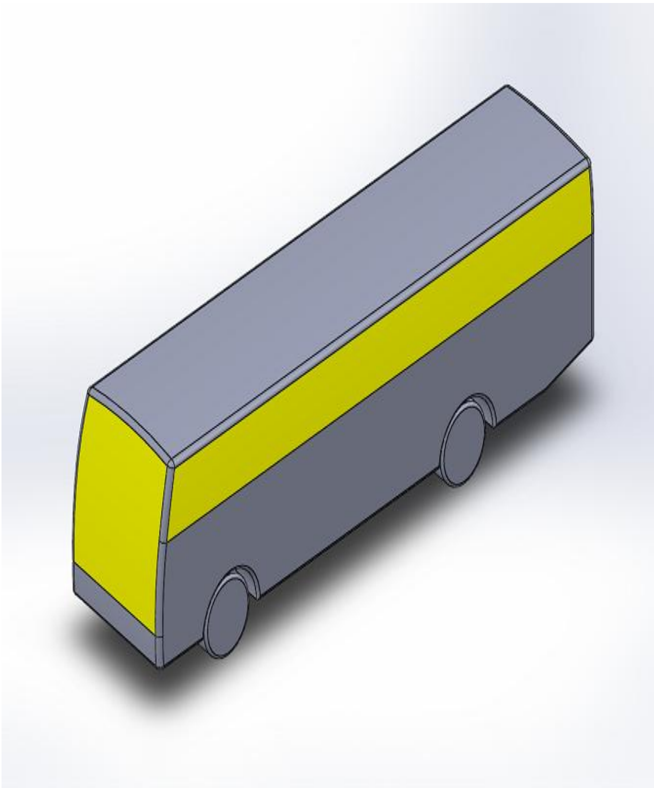

Model 1

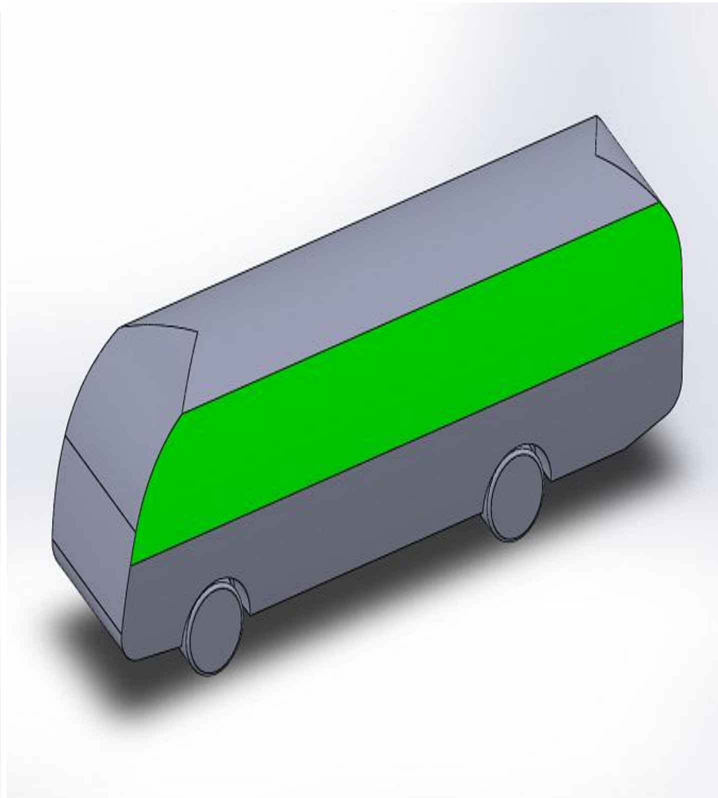

Model 2

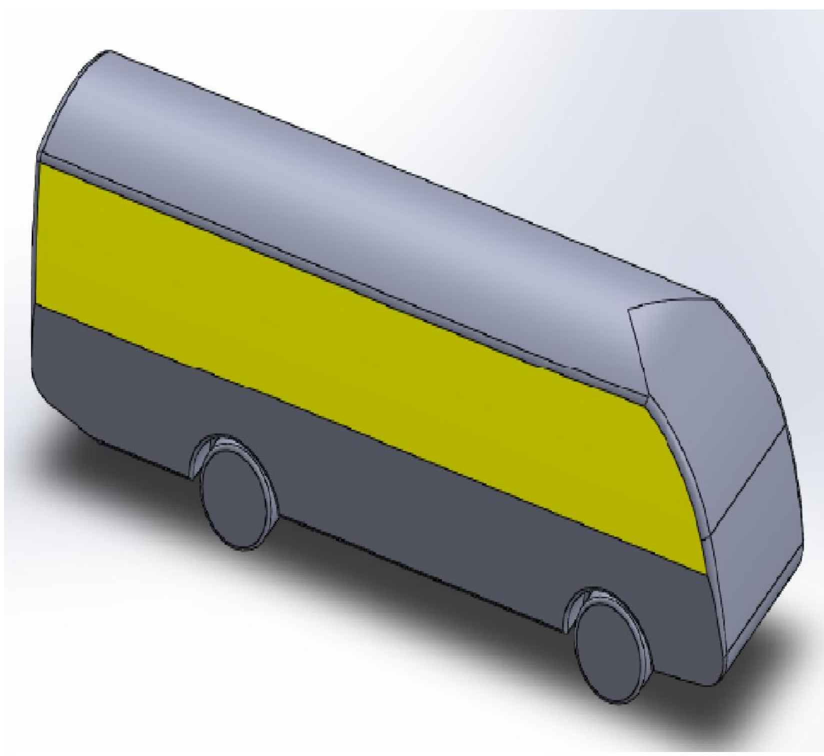

Model 3

Figure 30: Solid Models of Baseline and Two Modified Models(Asymmetric view)

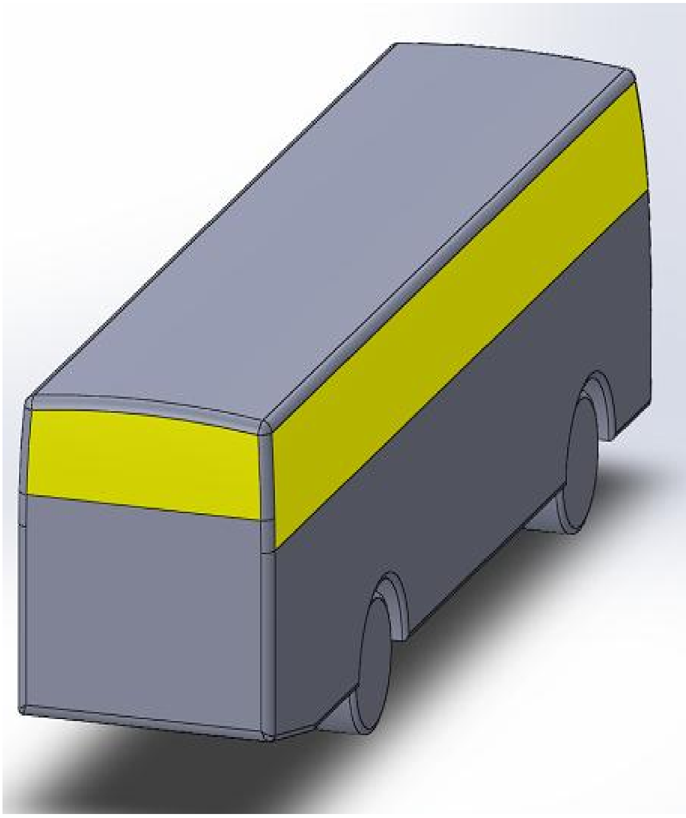

Model 1

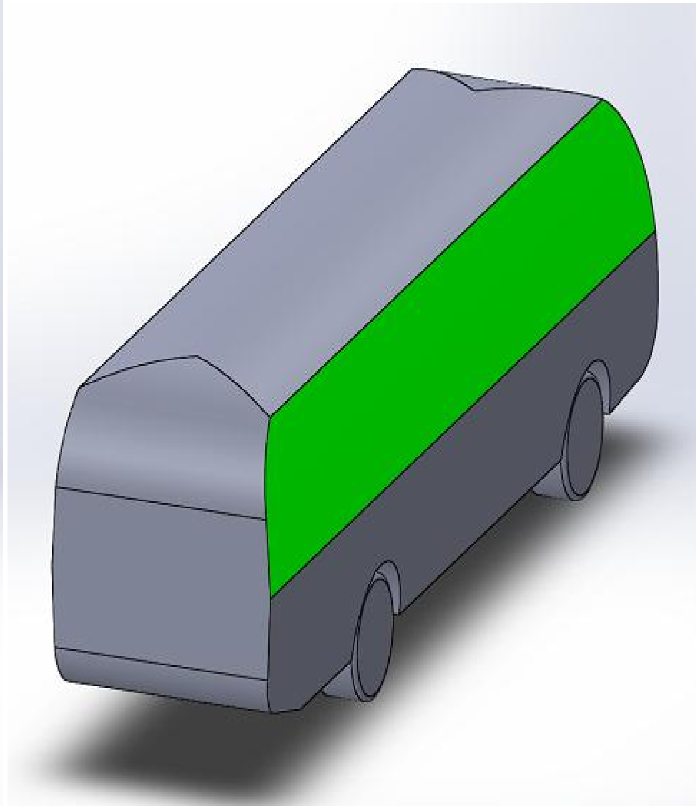

Model 2

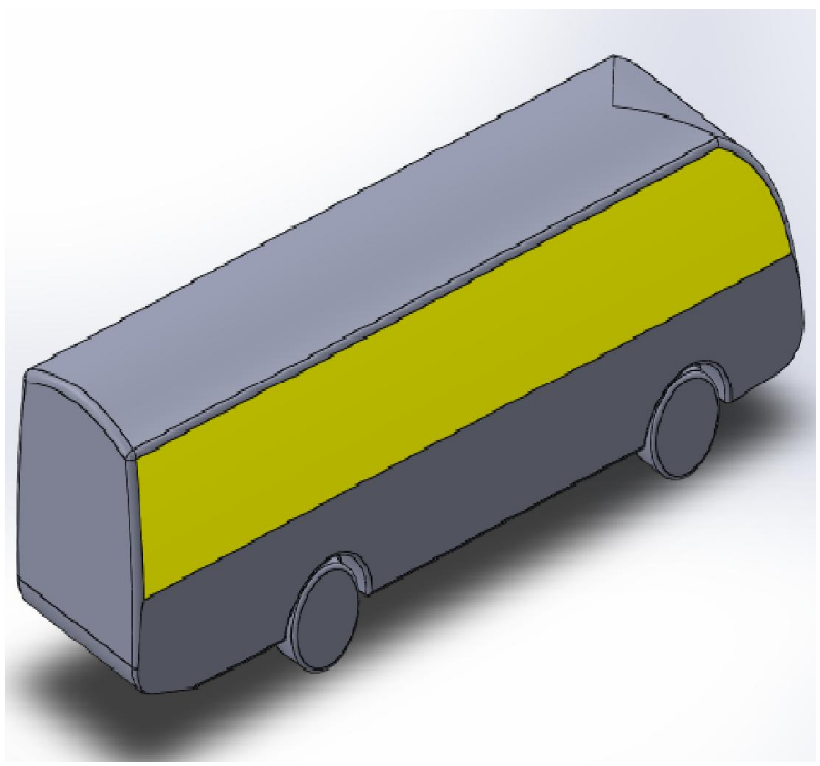

Model 3

Figure 31: Solid Models of Baseline and Two Modified Models(Asymmetric view)

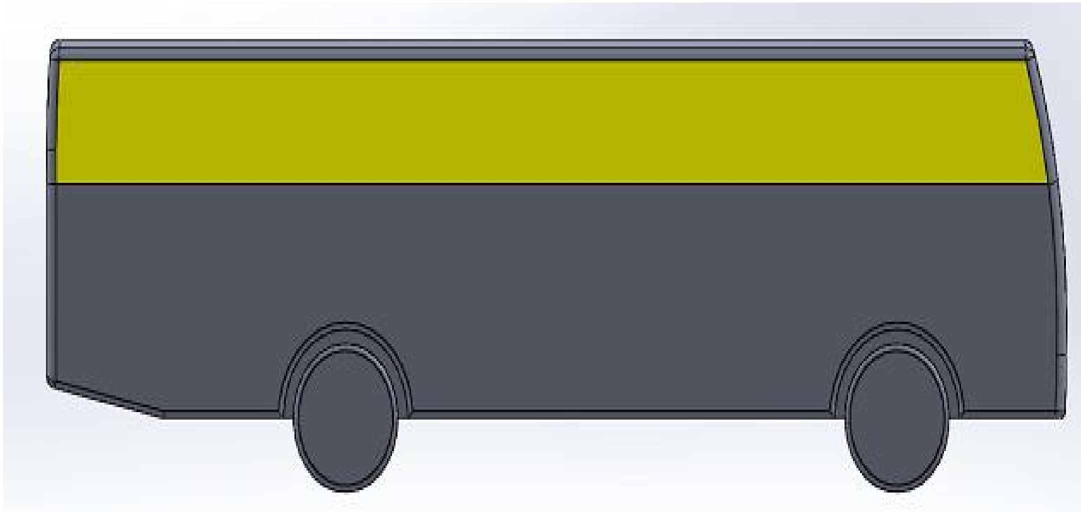

Model 1

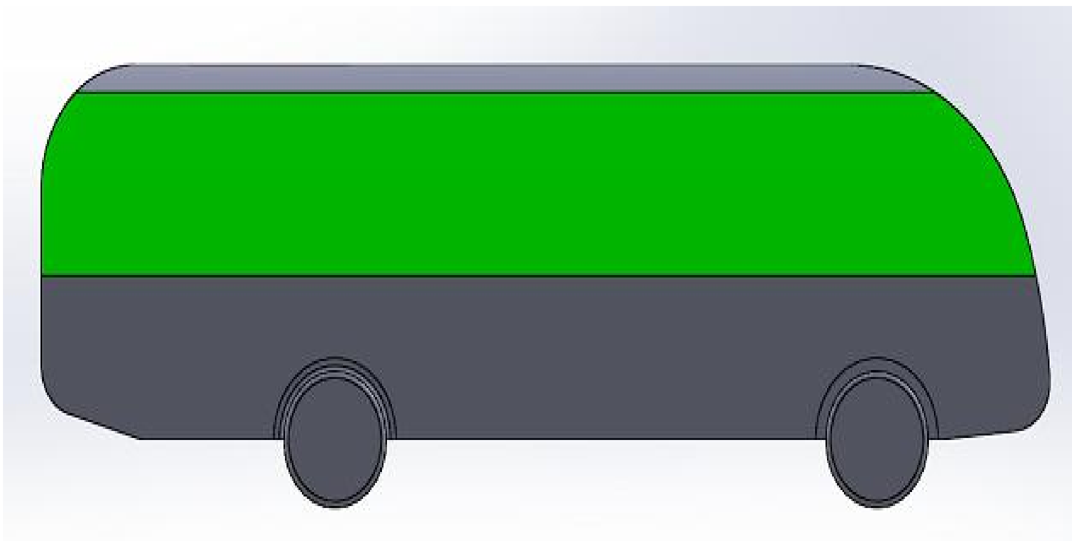

Model 2

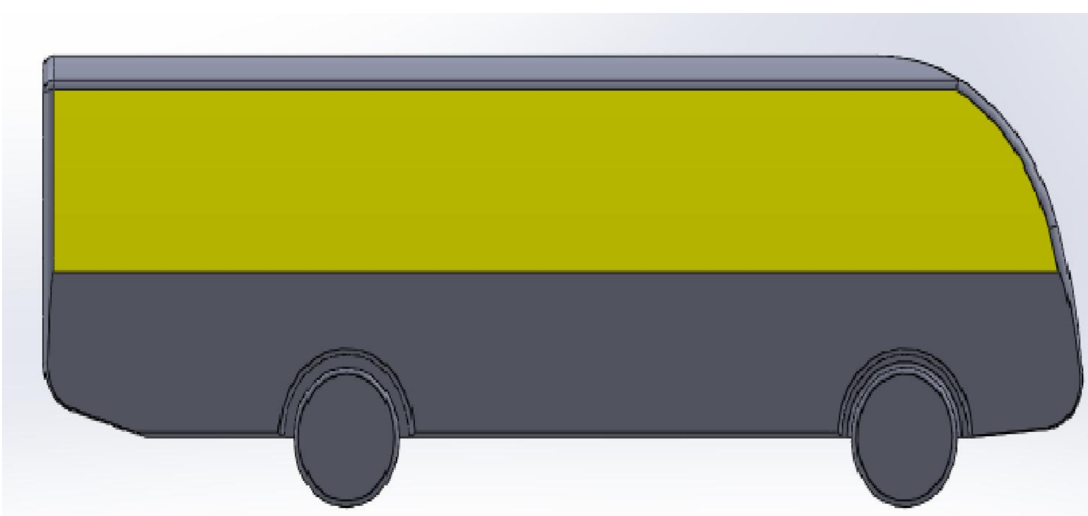

Model 3

Figure 32: Solid Models of Baseline and Two Modified Models(Side View)

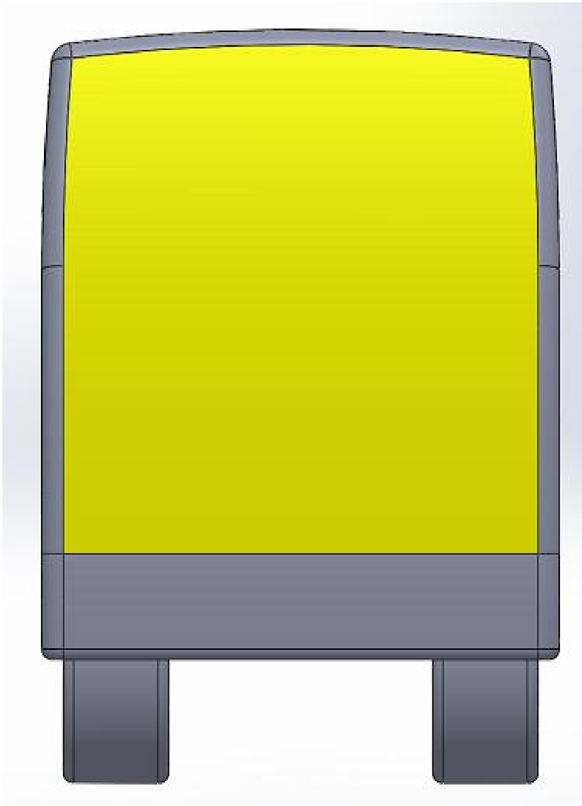

Model 1

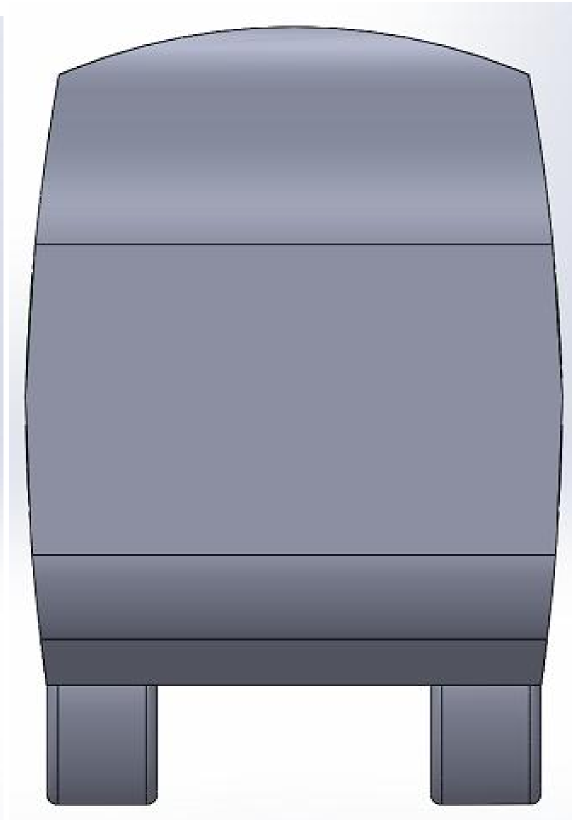

Model 2

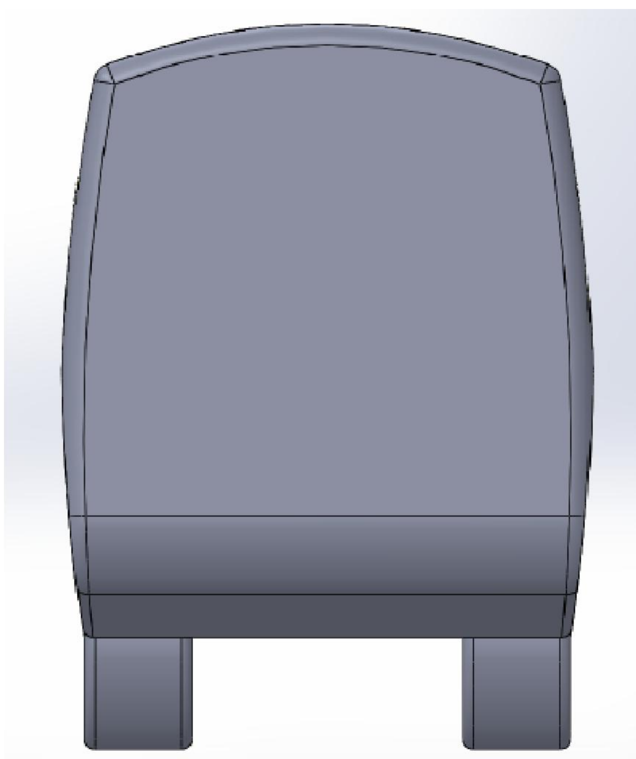

Model 3

Figure 33: Solid Models of Baseline and Two Modified Models(Rear View)

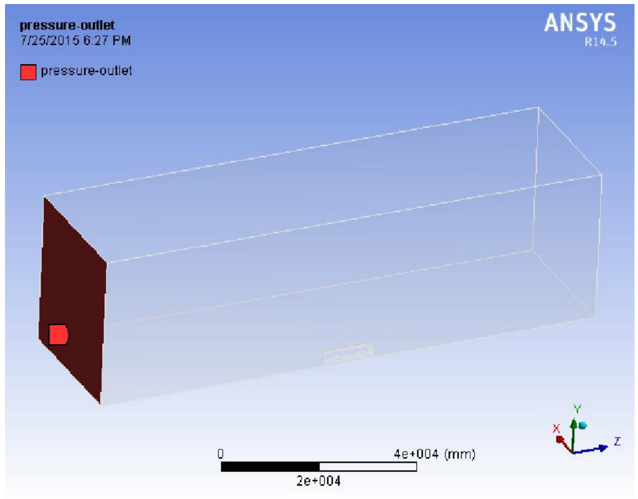

Figure 34: Boundary Conditions

4.3 Boundary Conditions

Boundary conditions(Figure 34) were applied on the meshed model using the ANSYS Workbench 14.5 preprocessor. The analysis was carried out in moving road and rotating wheel condition. In the simulation only straight wind condition was considered at 3 different vehicle speed of 85, 100, 115 kmph. Constant velocity inlet condition was applied at the inlet to replicate the constant wind velocity conditions. Zero gauge pressure was applied at the outlet with operating pressure as atmospheric pressure. All the boundary conditions used in the analysis are listed in table 3.

Table 3: Boundary Conditions

BOUNDARY	BOUNDARY CONDITIONS	VALUES
Inlet	Constant velocity Turbulent Intensity Length scale	V=23.1 m/s V=27.78 m/s V=31.94m/s
Outlet	Pressure outlet	Constant pressure= 0 N/m^2
Road	Moving wall No slip	V=23.1 m/s V=27.78 m/s V=31.94m/s
Bus body	No slip – stationary wall	-
Domain top and side	Stationary wall Specified shear	Shear stress = 0

4.4 Turbulent Model

The solver used for the analysis was FLUENT 14.5 and it uses a control-volume-method to solve the governing equations that can be solved numerically. The solver selected was the pressure based implicit solver. In this type the equations of continuity and momentum are solved sequentially. The flow is considered to be incompressible and steady in nature and the equations are solved using second order upwind method.

4.5 Model Design Specifications and Considerations

4.5.1 Model Design Specifications

It scaled 3-D model of bus with its actual dimensions in table 2, by using the CAD software. We know the outer dimensions of the bus then the model is modeled. It found out the external shape of the bus. After, for the analysis the 2D format is a compatible one to view the result. After the bus model is converted in to IGES (igs) format, this file can be used in the CFD software to analyze the external shape of the vehicle for the analysis. The specifications of aerodynamic bus is in table 4.

Table4: Bus Specifications

Overall Dimensions	
Length (mm)	10771
Width (mm)	2446
Height (mm)	2727
Interior height (mm)	1925
Wheel base (mm)	5800
Tread Front/Rear (mm)	2080/1860
Front/Rear Overhang (mm)	2265/3480
Min. Ground clearance(mm)	380
Approach/Departure Angle(º)	12/10
Brake distance (v=30km/h) in mm	≤10
Fuel consumption (L/100km)	23
Front/Rear Axle (kg)	6500/9500
Kerb weight (kg)	11500
Max. Total Mass(kg)	16000
Max. Speed (km/h)	110
Max. Grade ability (%)	38
Min. turning diameter (m)	24
Fuel Tank Capacity (L)	400
Manufacturer	Zhengzhou Yutong Bus Co., Ltd
Model ZK6116D	

Table 5: Aerodynamic Specifications

S.NO	AERODYNAMIC SPECIFICATIONS
1	Minimum front corner radius of 100 mm
2	Smooth and covered under body from 11.5 º to 15 º
3	Minimum trailing edge radius of 100 mm
4	Side panel tapering of 100 mm
5	Rear roof tapering of 1000 mm
6	Curved front end
7	Roof end lowering
8	Increasing Rake Angle from 30º to 45º

4.5.2 Model Design Considerations

According to the research by (Arun Raveendran, D. Rakesh, S. N. Sridhara) "Using the data collected from the user study the target customer selected were students and working professionals at the age of 18 to 35. To understand the different activities in their day to day life a lifestyle board was prepared. This age group people have lots of energy in them and are at the peaks of their life. It was observed that they lead an energetic, fast and fun loving life in this age period. They never want to waste any time in their life and were constantly on the move between college, office, friends and family.

Most of them were obsessed with travelling, adventure trips, fast bike and cars. After completing the journey in the bus most of them go to office or to their planned work just after a quick fresh up.

From the life style board a mood board was prepared which shows the different emotions and situation this age group goes through in their life. From the mood board the most suitable theme for the bus design was found to be adventure, fast and speed. This theme was also selected because it directly related with the aerodynamics. A theme board was prepared which was related to the adventure theme. The theme board includes objects and things directly related to speed and adventure. Aquatics in the nature exhibit dynamism and have good aerodynamic shape. Killer whales are big in size and are known for their dynamism in the water.

They have a good aerodynamic body as well. These show similarity to the proposed new design of the bus. Hence, the exterior of the bus was designed with the concept of robust appearance of a killer whale." [100]. Similarly my new Yutong bus design is the same as to the design displayed below(Figure 35).

Figure 35: New Bus Concept Design

A. Side View of the Models

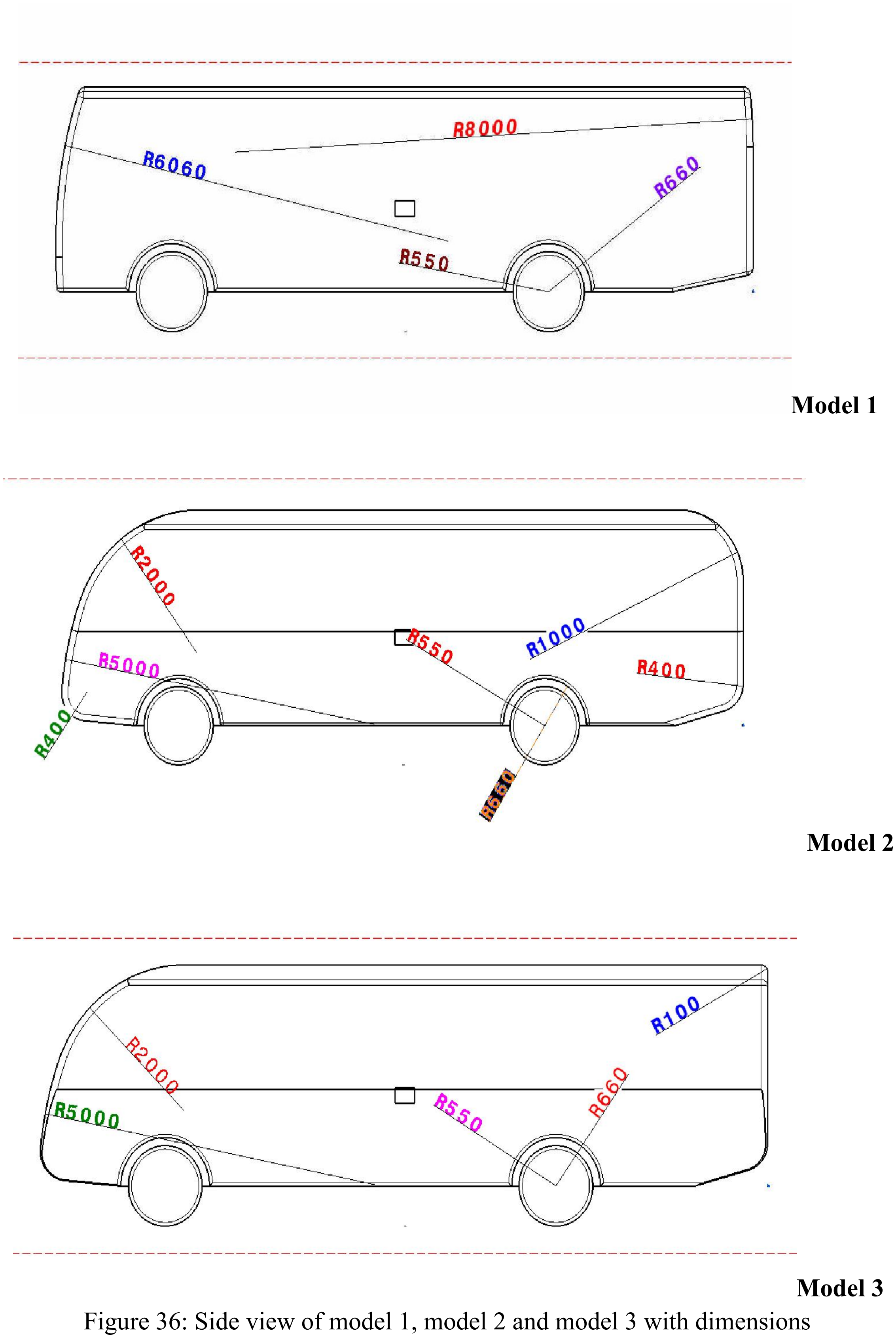

Figure 36: Side view of model 1, model 2 and model 3 with dimensions

B. Front View of the Models

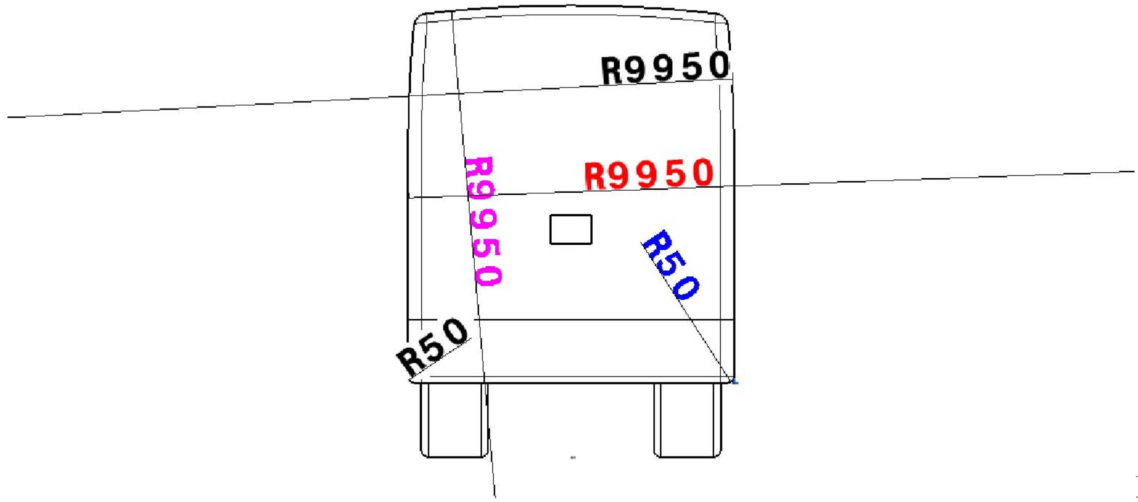

Model 1

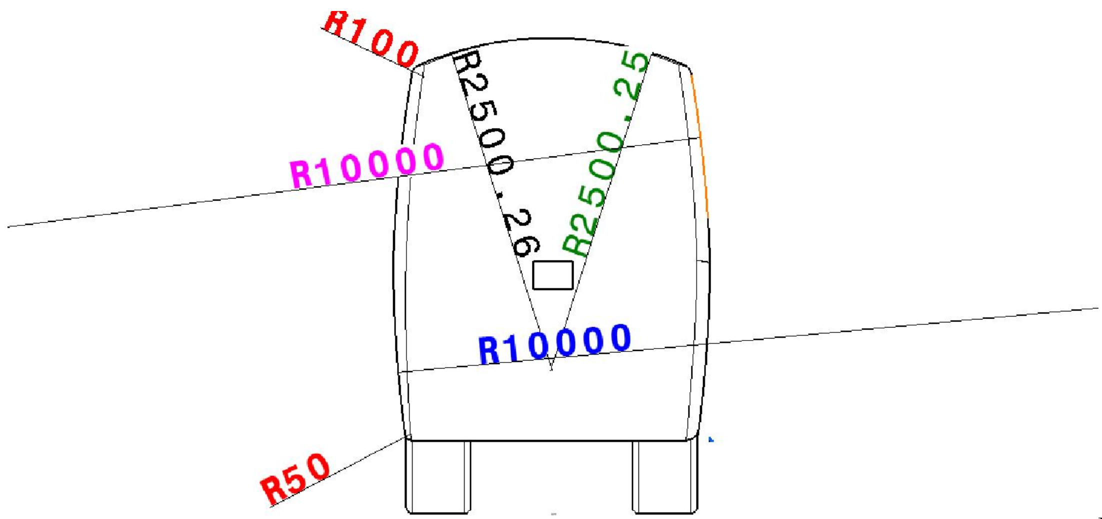

Model 2

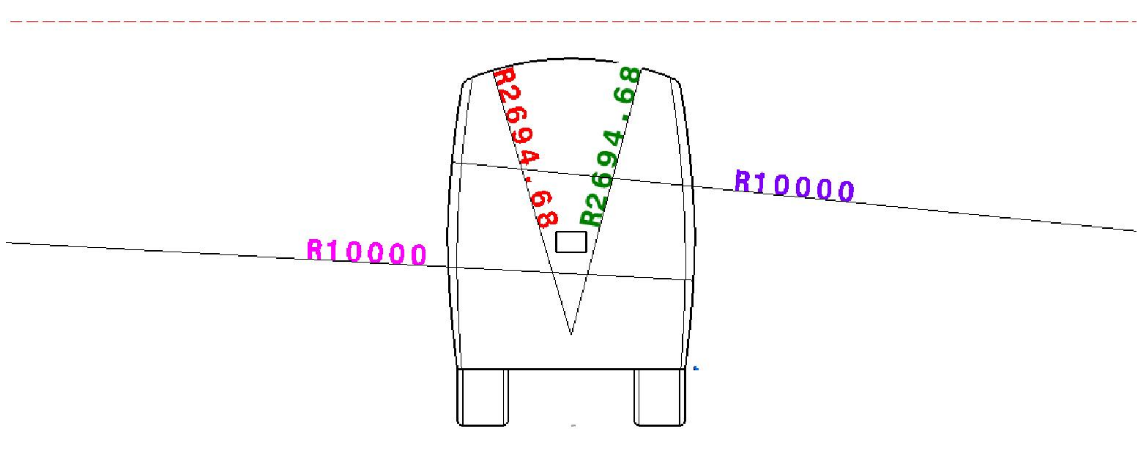

Model 3

Figure 37: Front view of model 1, model 2 and model 3 with dimensions

C. Rear View of the Models

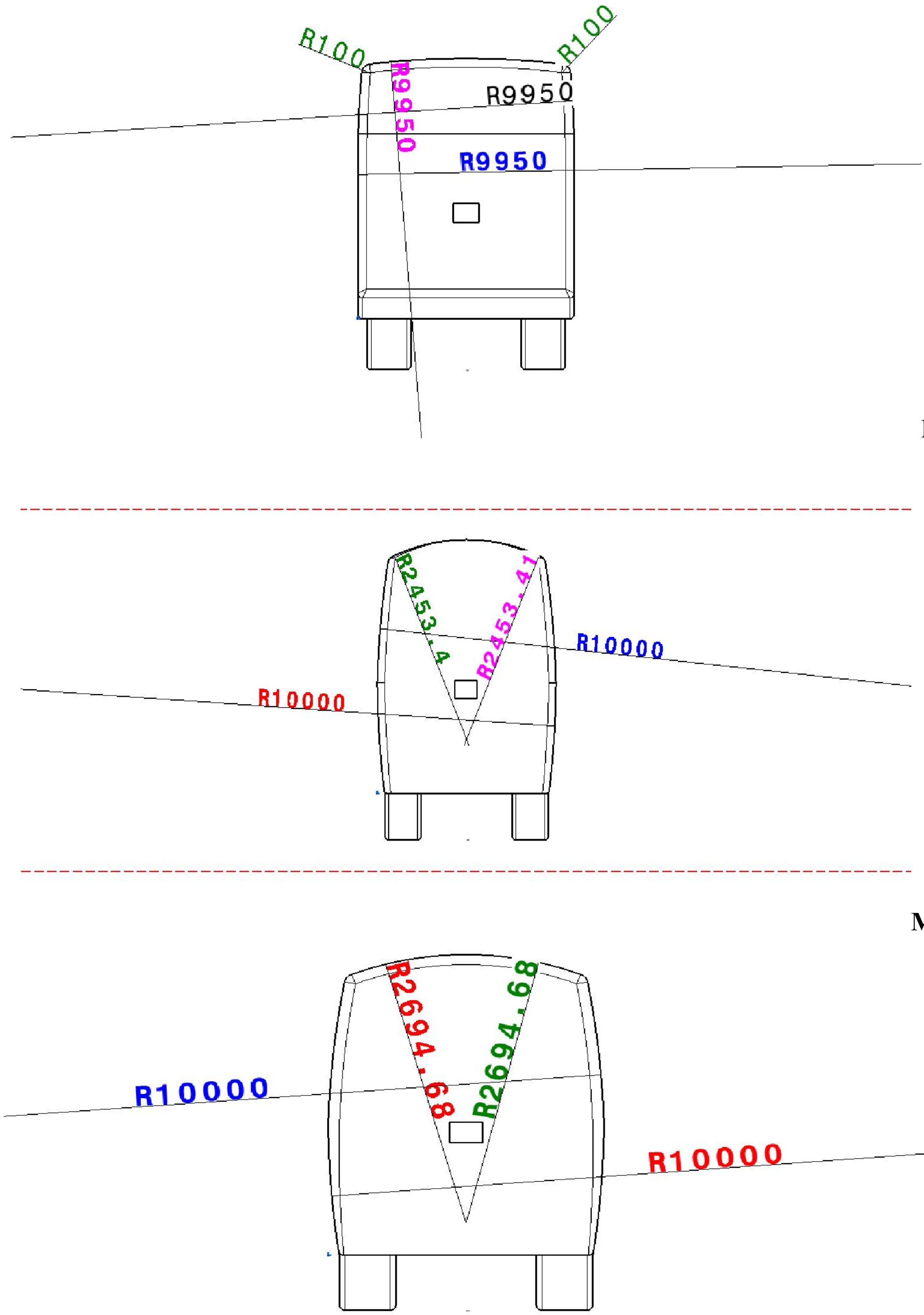

Model 1

Model 2

Model 3

Figure 38: Rear view of model 1, model 2 and model 3 with dimensions

4.6 Mesh Generation

The computational domain is designed to lead to a free with neglectable blockage, which essentially means a box that consists of an inlet, an outlet, two sides, a roof and a ground Surface(road). The size of the domain is taken based on the dimension of the bus such that the real-time road conditions were satisfied.

The surface mesh was created on the geometry of the bus as well as on the surface of the domain. Between the surface of the bus and the domain the computational grid was generated. To capture certain areas of interest (where separation might occur and where the degree if turbulence is high) the cells have to small enough to solve all irregularities and achieve a robust solution. The grid has been redefined around the bus, at the rear and especially at front the bus since this study is focusing on the overbodies influence on the flow field.

A. Model 1

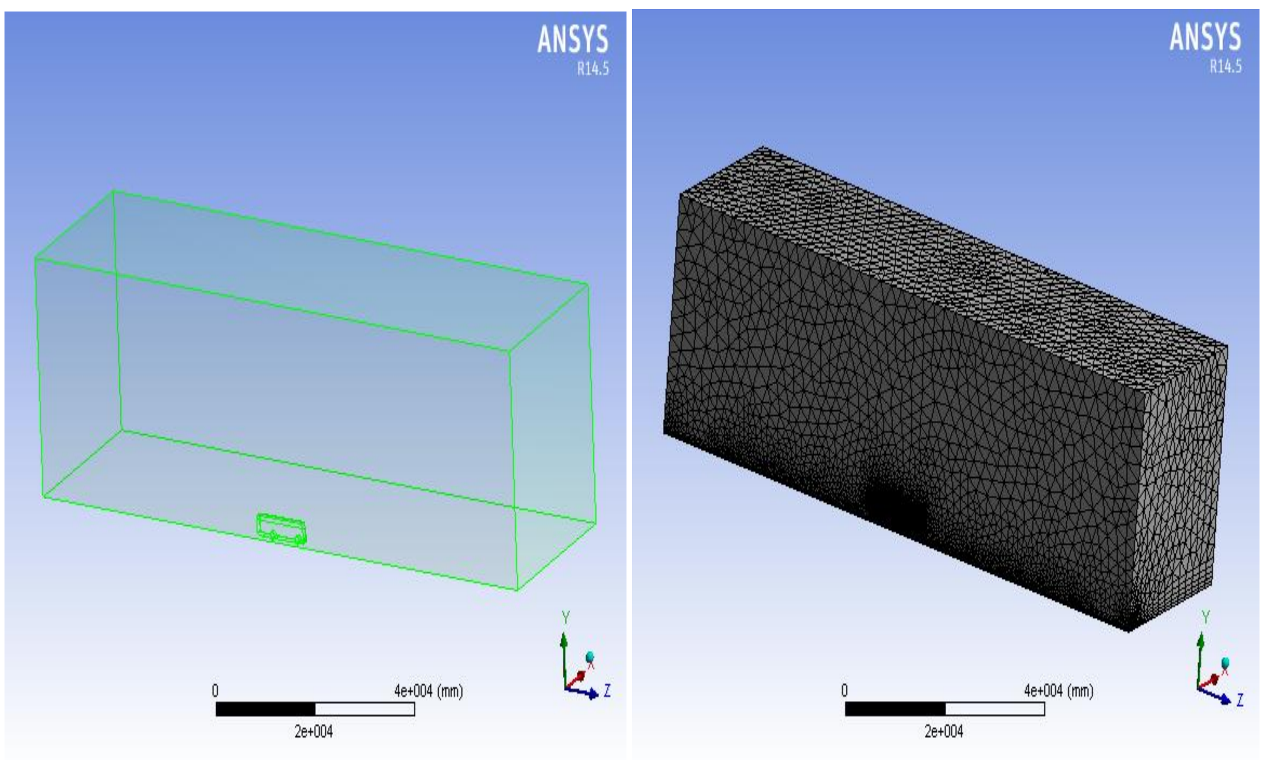

Model 1 Inside Enclosure   Meshed Model 1

Figure 39: Model 1 Inside Enclosure and Meshed Model 1

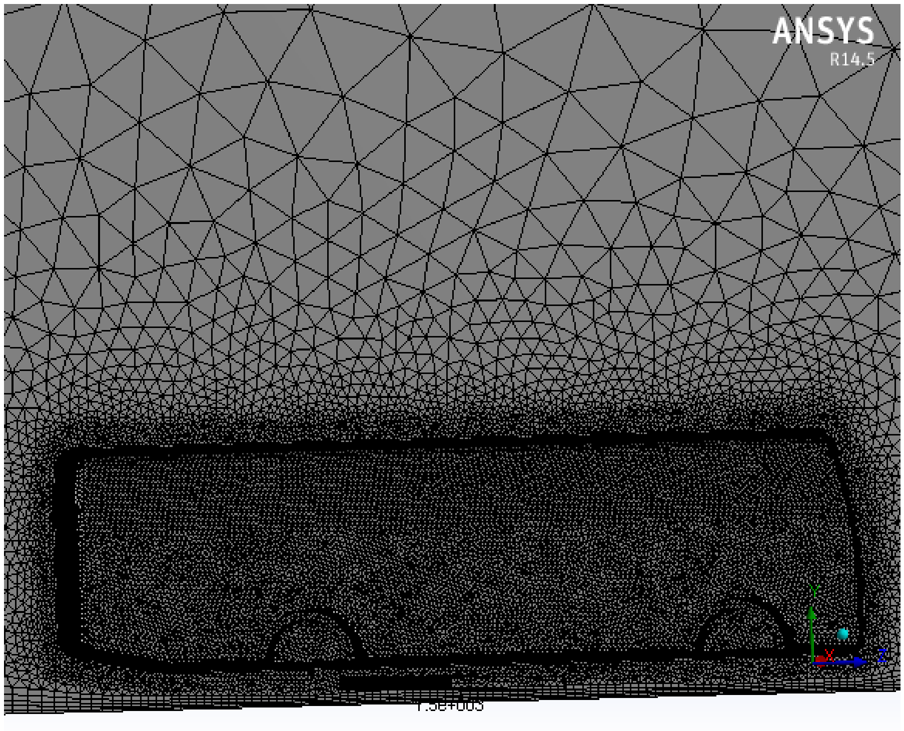

Figure 40: Meshed Model 1

Element Details:

1342263 mixed cells, zone 2, binary.

2780796 mixed interior faces, zone 1, binary.

41075 triangular wall faces, zone 5, binary.

552 mixed velocity-inlet faces, zone 6, binary.

606 mixed pressure-outlet faces, zone 7, binary.

13754 mixed symmetry faces, zone 8, binary.

1140 triangular symmetry faces, zone 9, binary.

1304 mixed symmetry faces, zone 10, binary.

11399 triangular wall faces, zone 11, binary.

330556 nodes, binary.

330556 node flags, binary.

B. Model 2

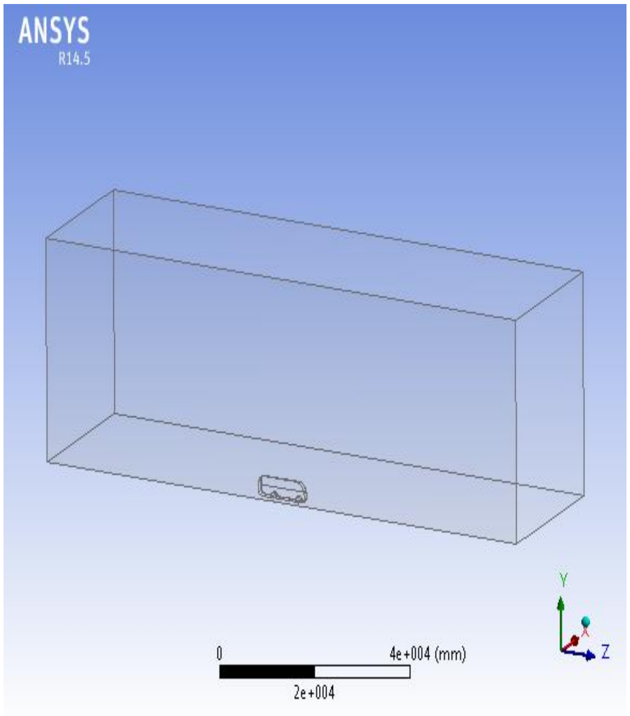

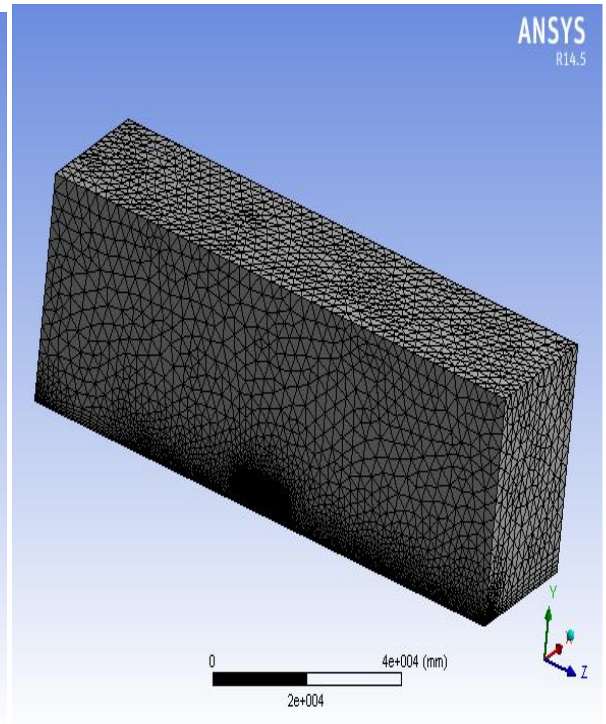

Geometry(Enclosure) Model 2 Meshed Model 2

Figure 41: Model 2 Inside Enclosure and Meshed Model 2

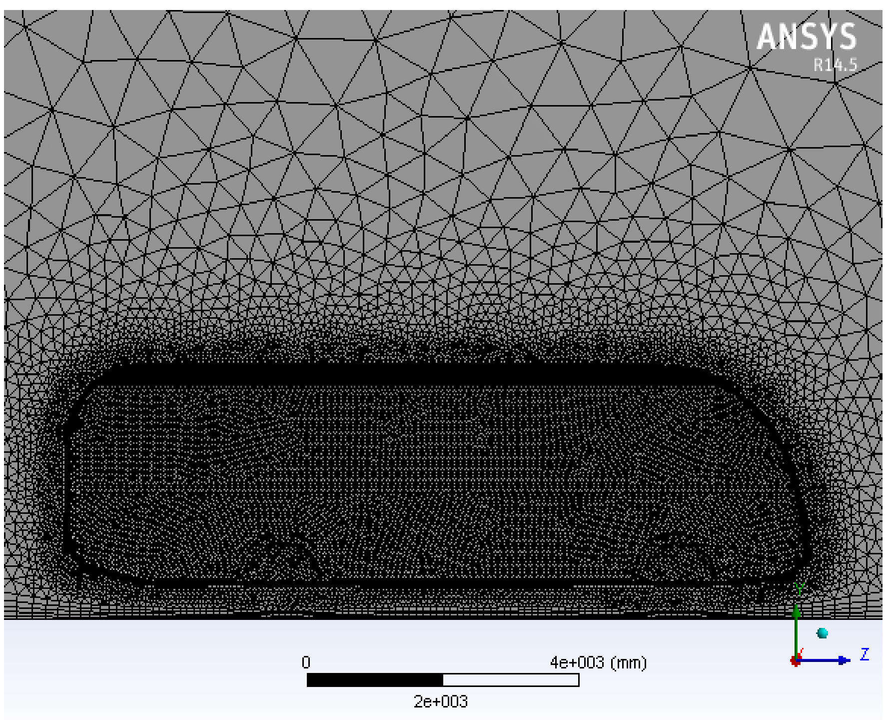

Figure 42: Meshed Model 2

Element Details:

1391681 mixed cells, zone 3, binary.

10381 triangular wall faces, zone 12, binary.

1342 mixed symmetry faces, zone 11, binary.

3864 triangular wall faces, zone 1, binary.

2878769 mixed interior faces, zone 2, binary.

37997 triangular wall faces, zone 6, binary.

568 mixed velocity-inlet faces, zone 7, binary.

586 mixed pressure-outlet faces, zone 8, binary.

14204 mixed symmetry faces, zone 9, binary.

1158 triangular symmetry faces, zone 10, binary.

301236 nodes, binary.

37078 nodes, binary.

C. Model 3

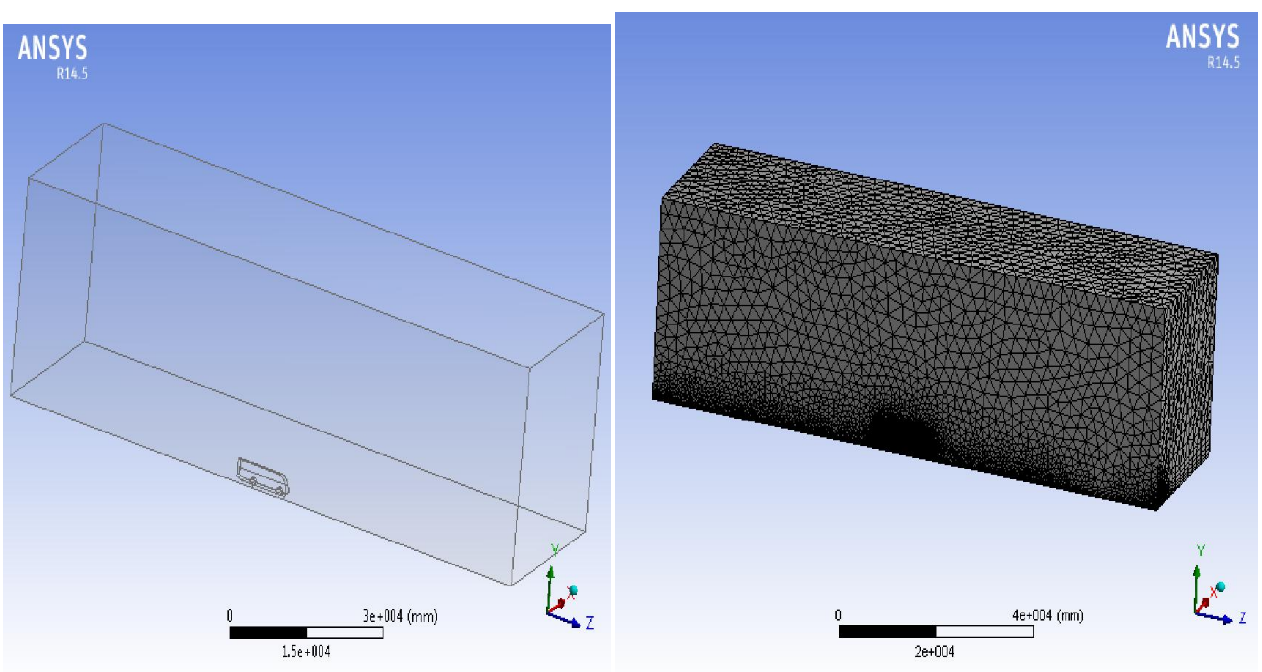

Geometry(Enclosure) Model 3 Meshed Model 3

Figure 43: Model 3 Inside Enclosure and Meshed Model 3

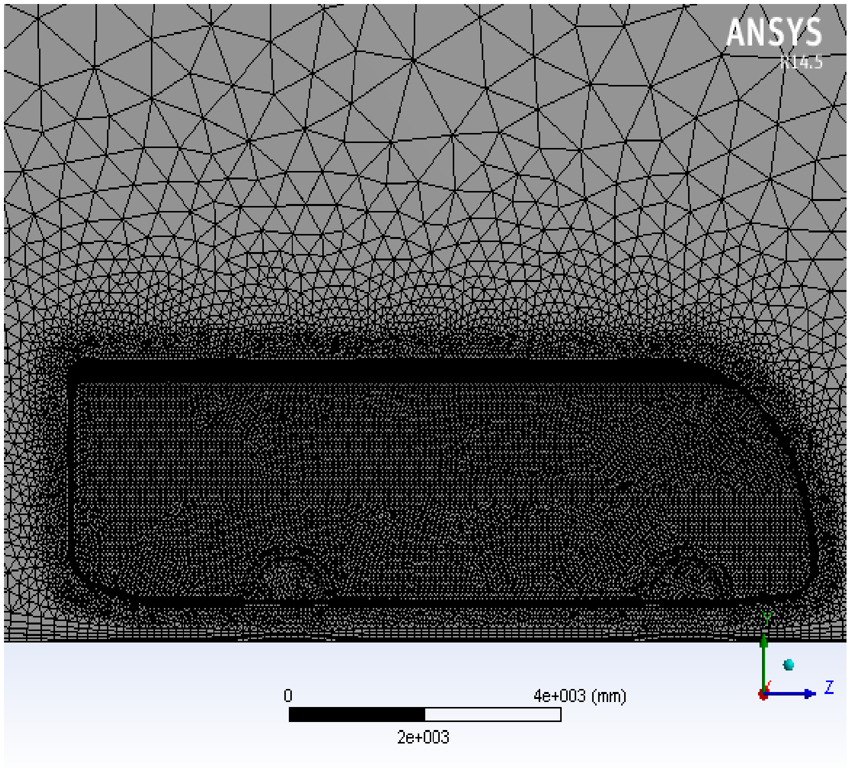

Figure 44: Meshed Model 3

Element Details:

1380386 mixed cells, zone 3, binary.

10448 triangular wall faces, zone 12, binary.

1348 mixed symmetry faces, zone 11, binary.

3768 triangular wall faces, zone 1, binary.

2855644 mixed interior faces, zone 2, binary.

37690 triangular wall faces, zone 6, binary.

554 mixed velocity-inlet faces, zone 7, binary.

580 mixed pressure-outlet faces, zone 8, binary.

14258 mixed symmetry faces, zone 9, binary.

1140 triangular symmetry faces, zone 10, binary.

298950 nodes, binary.

36931 nodes, binary.

4.7 Iterations

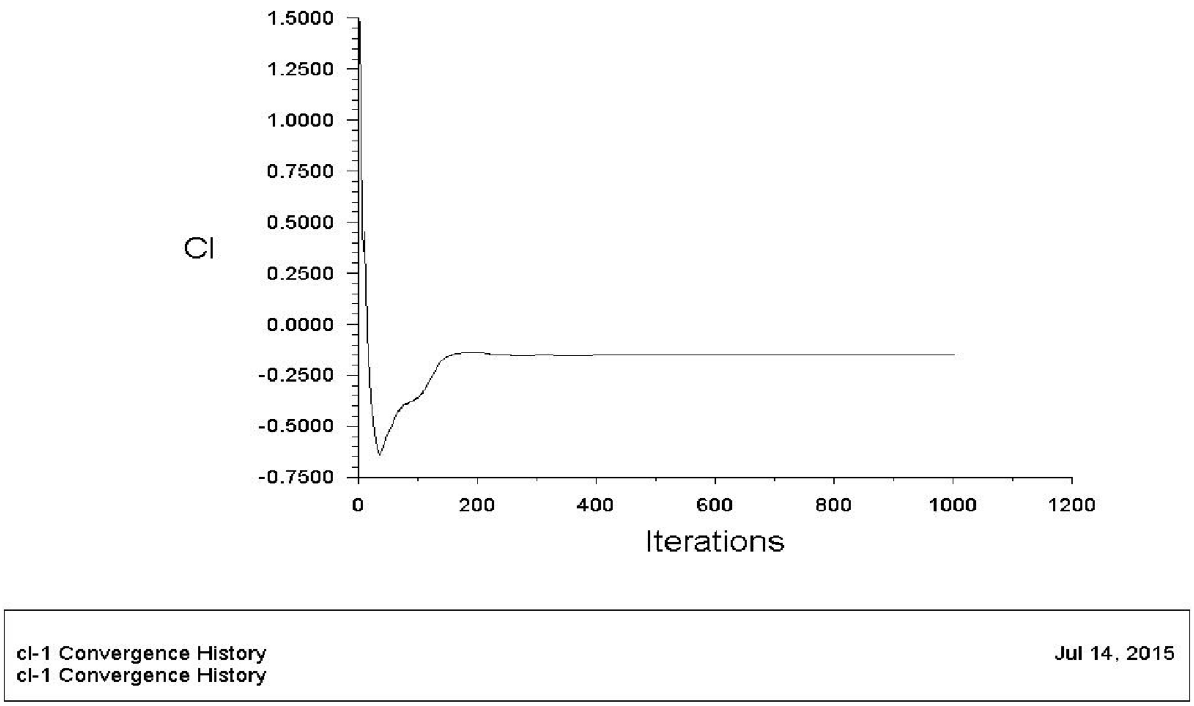

Figure 45: Convergence of Coefficient of Lift(C_l)

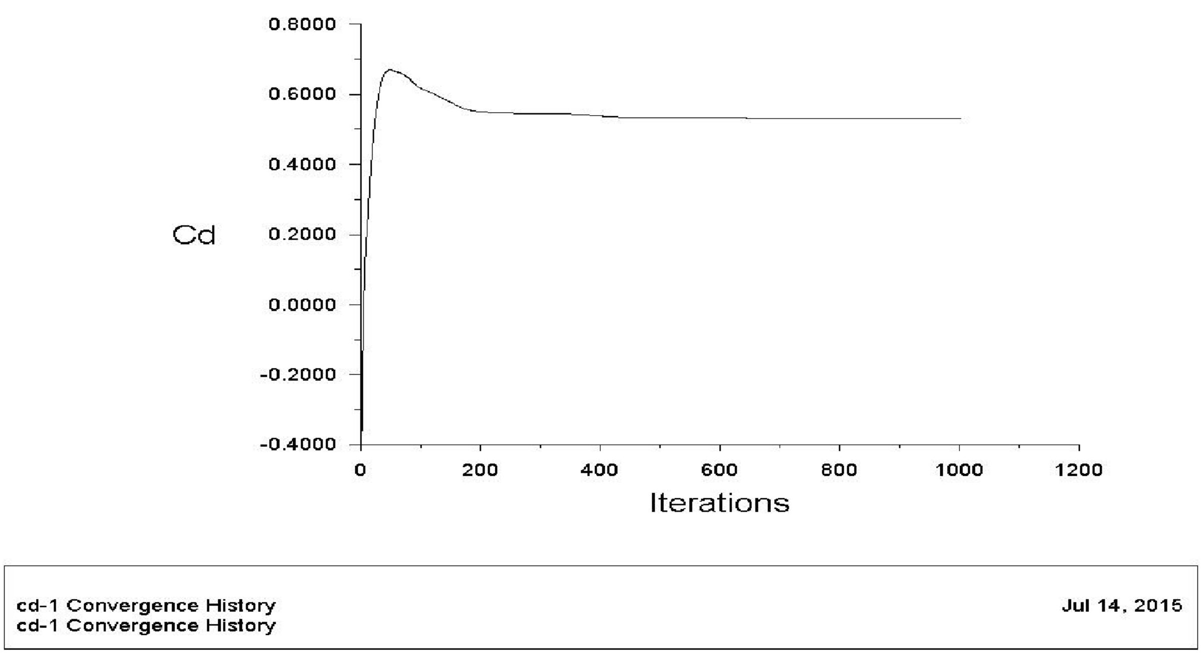

Figure 46: Convergence of Coefficient of Drag(C_d)

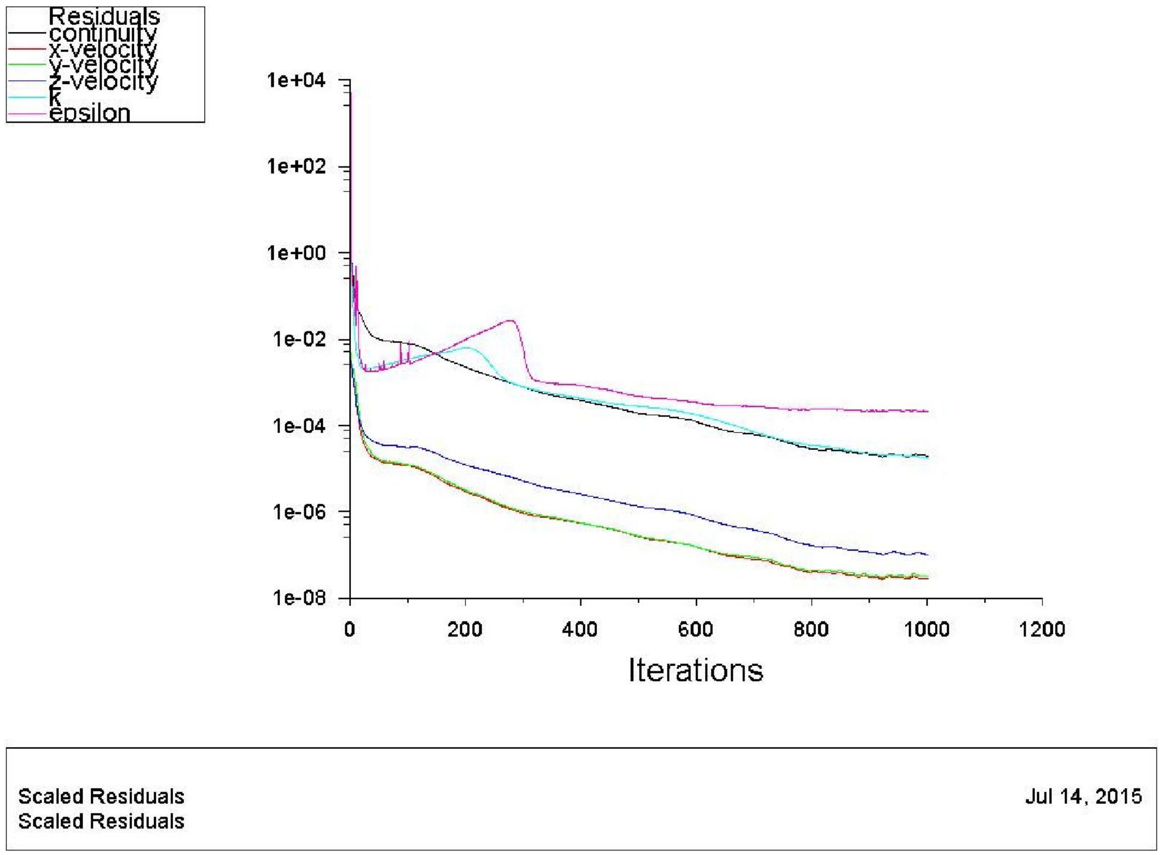

Figure 47: Convergence of Residuals

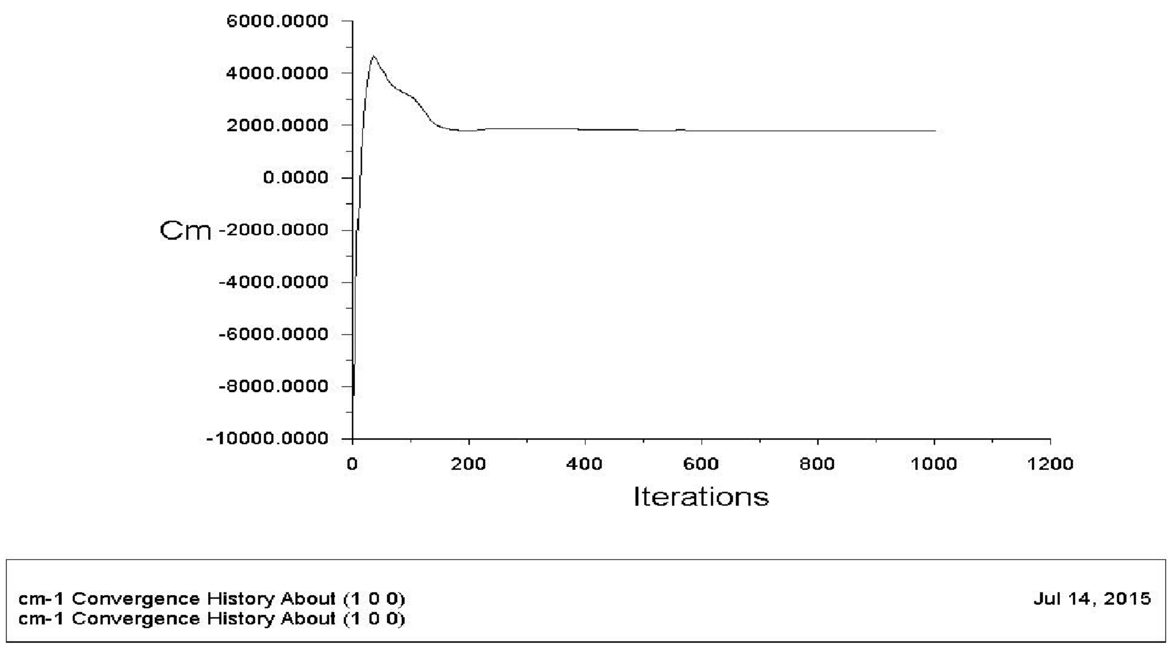

Figure 48: Convergence of Coefficient of Moment(C_m)

CHAPTER FIVE

5. RESULT AND DISCUSSION

5.1 Aerodynamic Pressure and Velocity Distribution of the Models at Various Speeds

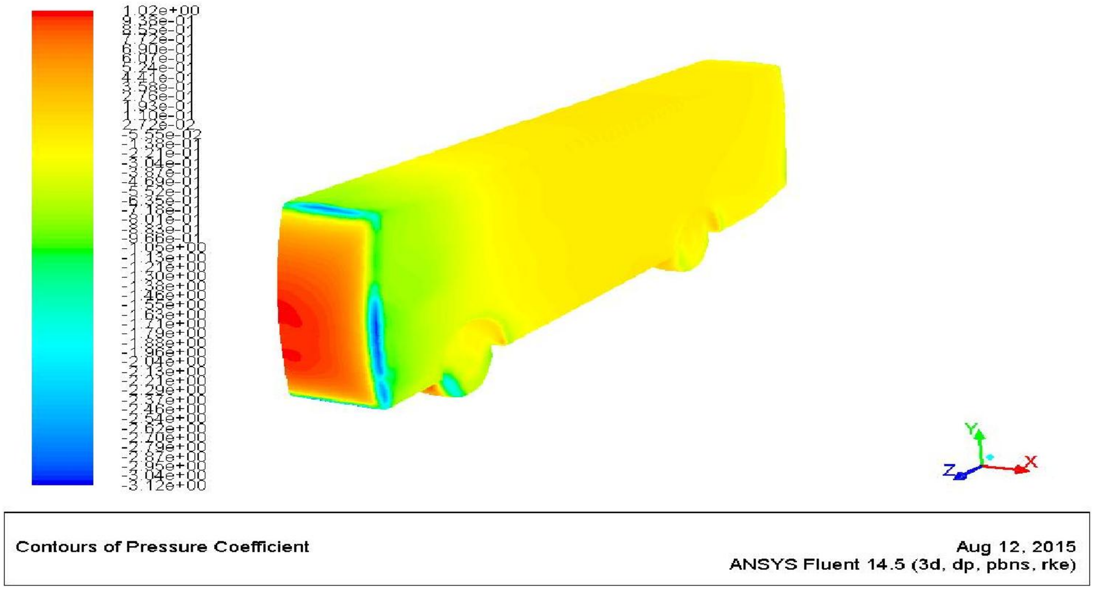

Fig 49(a) : Pressure distribution of Model 1 at 85 Kmph

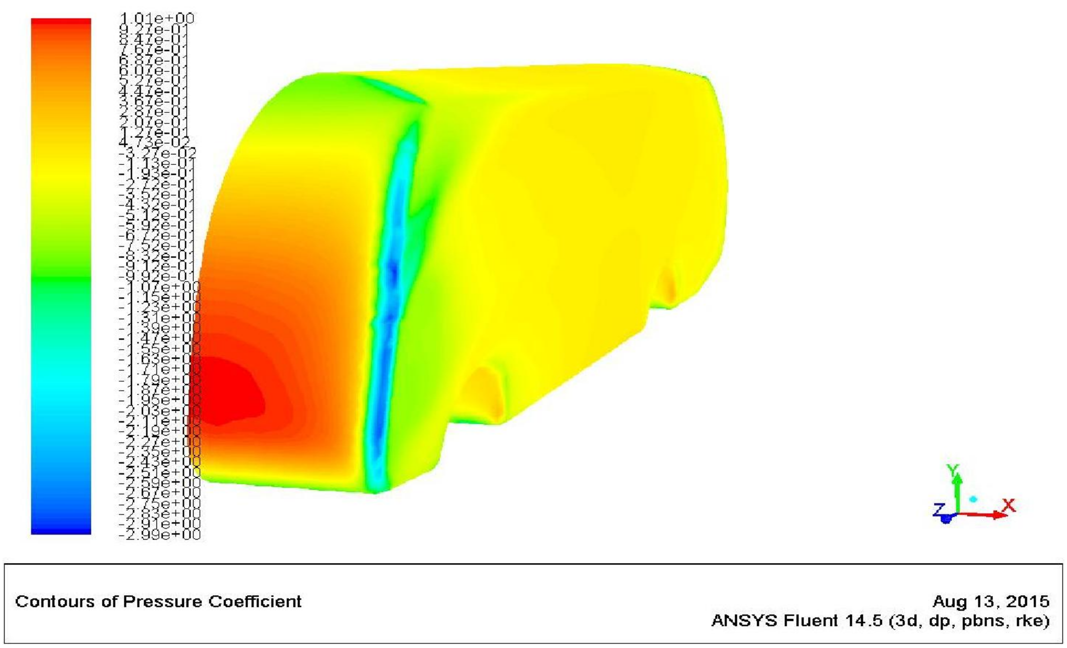

Fig 49(b) : Pressure distribution of Model 2 at 85 Kmph

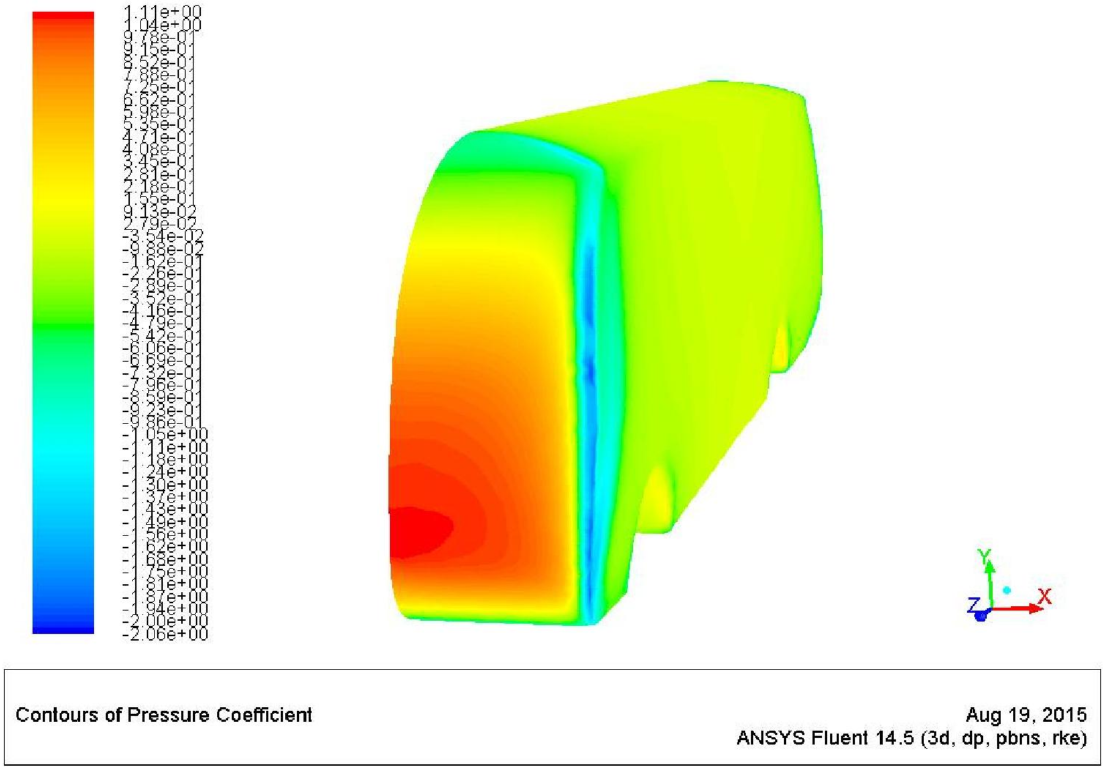

Fig 49(c) : Pressure distribution of Model 3 at 85 Kmph

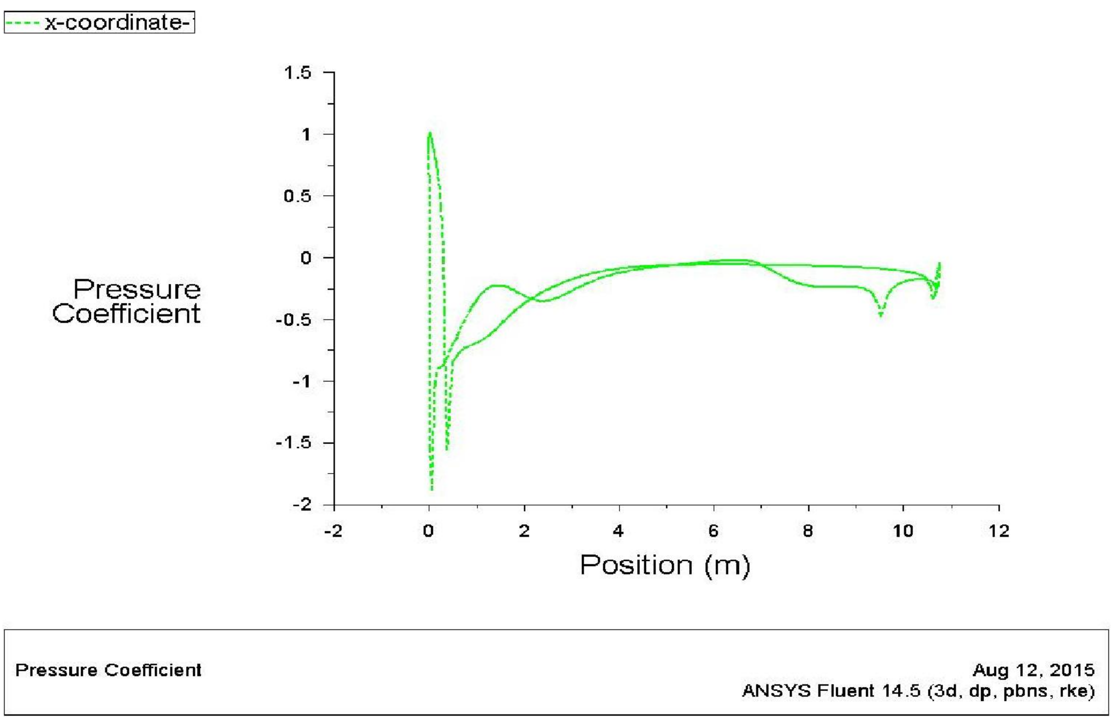

Fig 50(d) : Graph for Pressure distribution of Model 1 at 85 Kmph

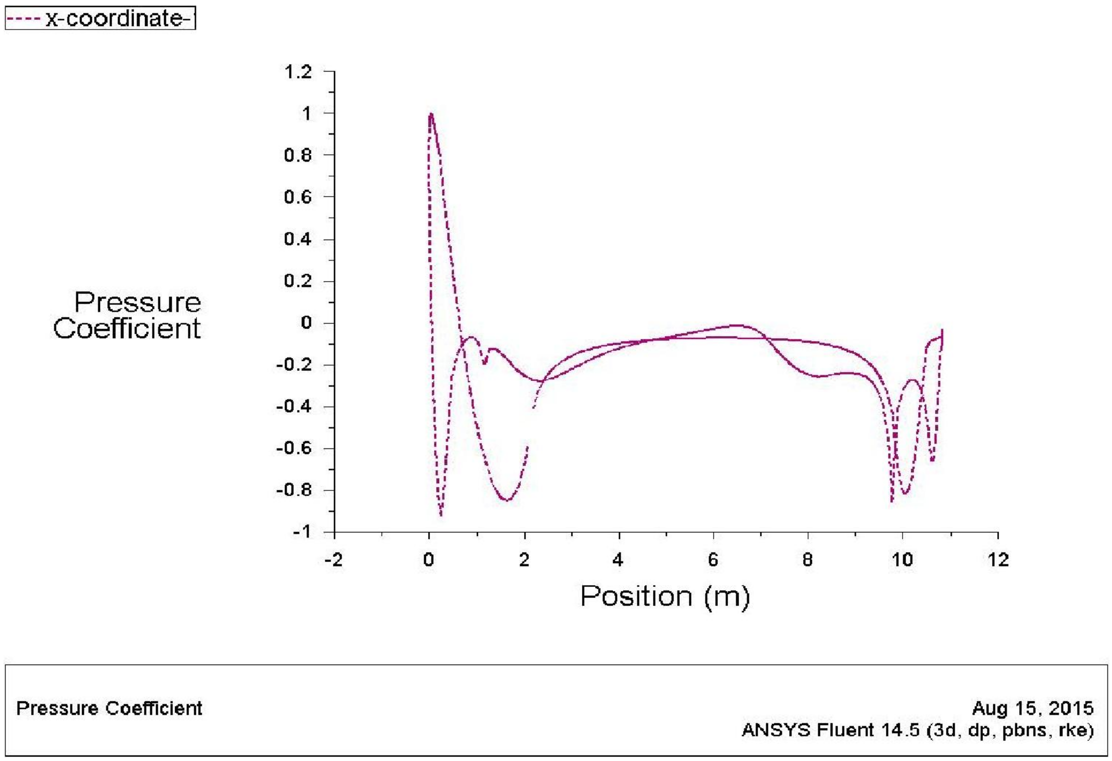

Fig 50(e) : Graph for Pressure distribution of Model 2 at 85 Kmph

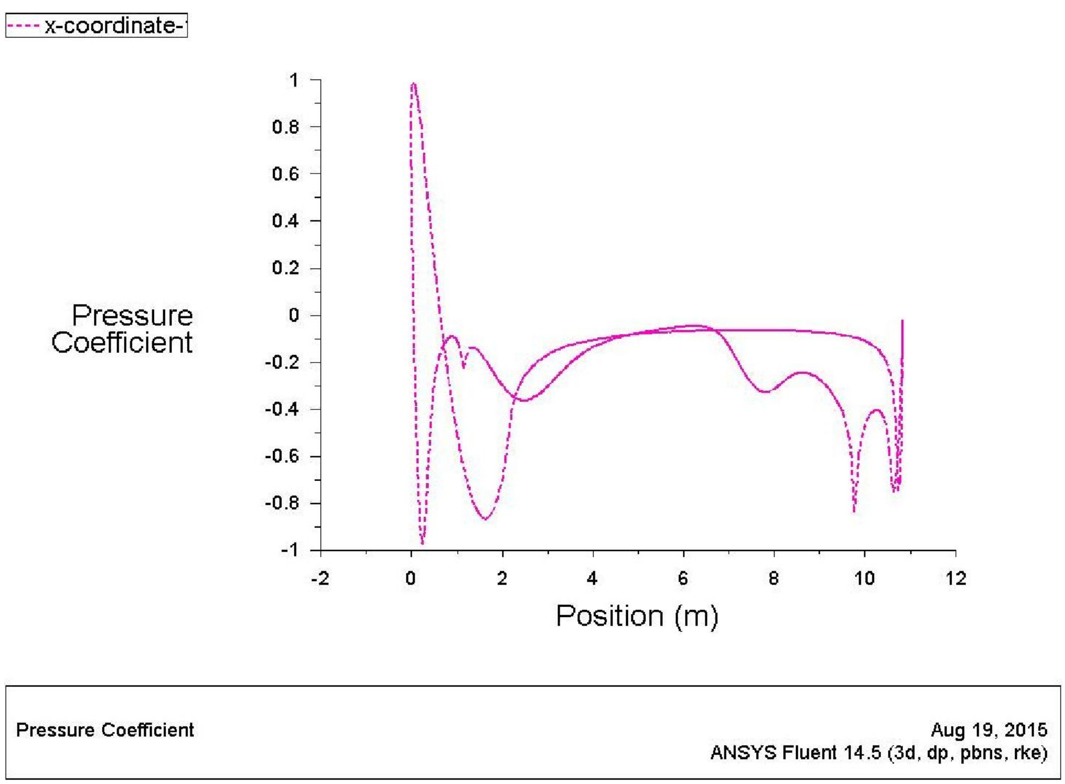

Fig 50(f) : Graph for Pressure distribution of Model 3 at 85 Kmph

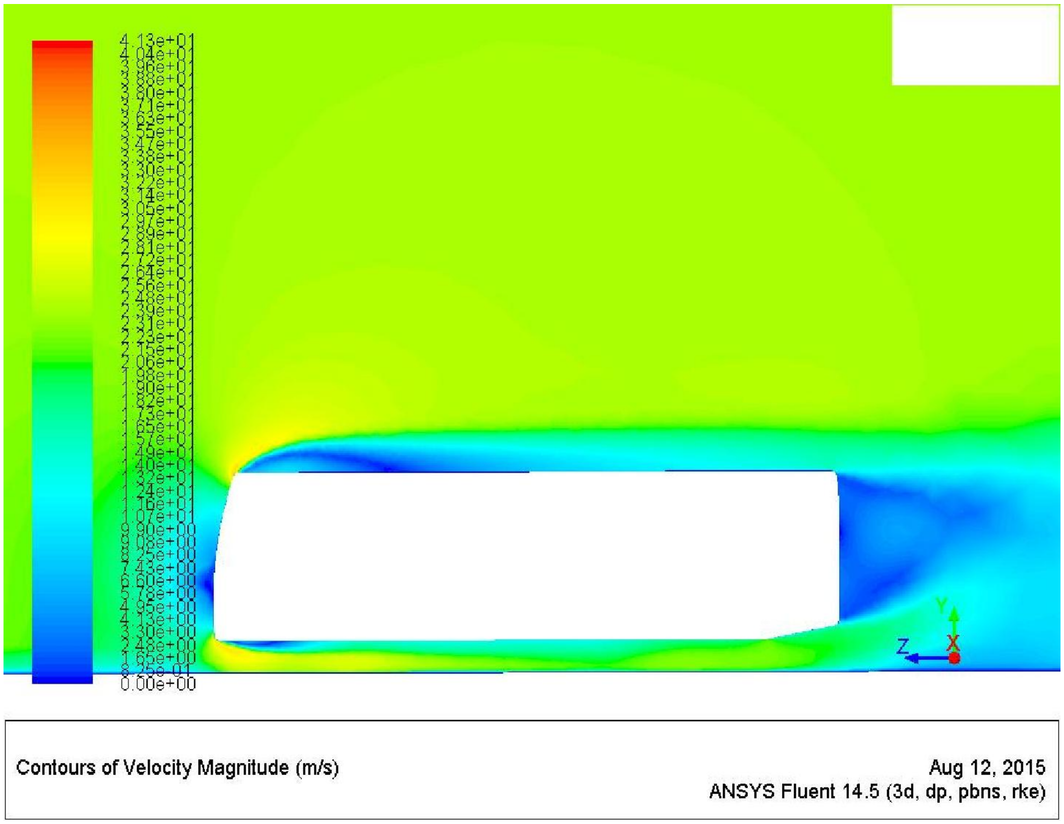

Fig 51(a) : velocity distribution of Model 1 at 85 Kmph

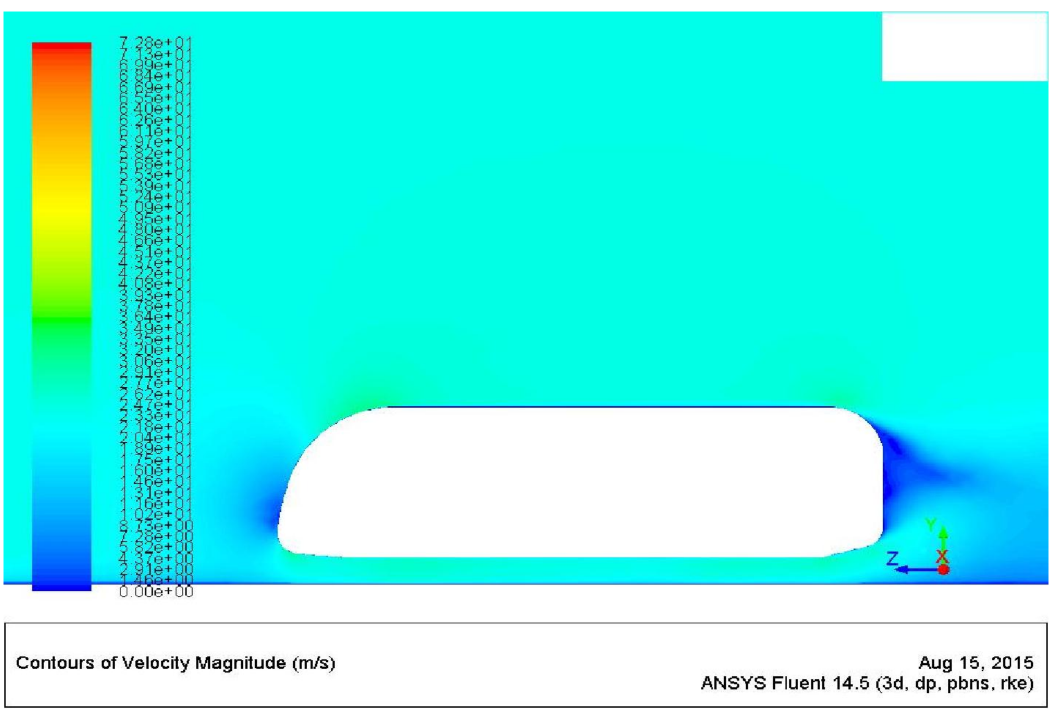

Fig 51(b) : Velocity distribution of Model 2 at 85 Kmph

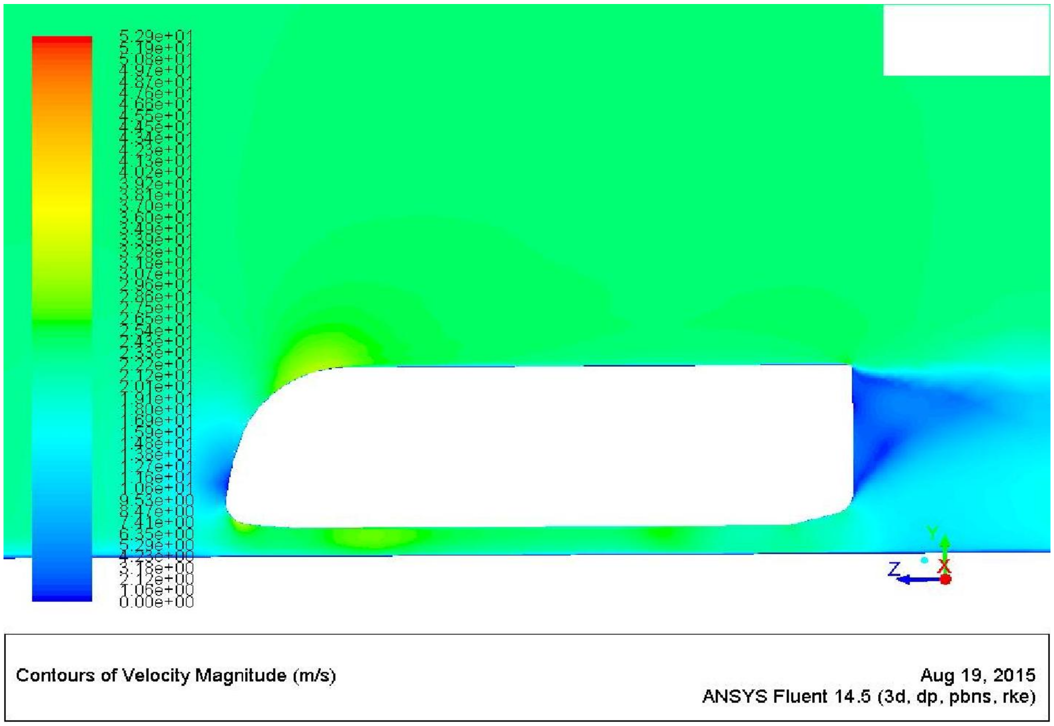

Fig 51(c) : Velocity distribution of Model 3 at 85 Kmph

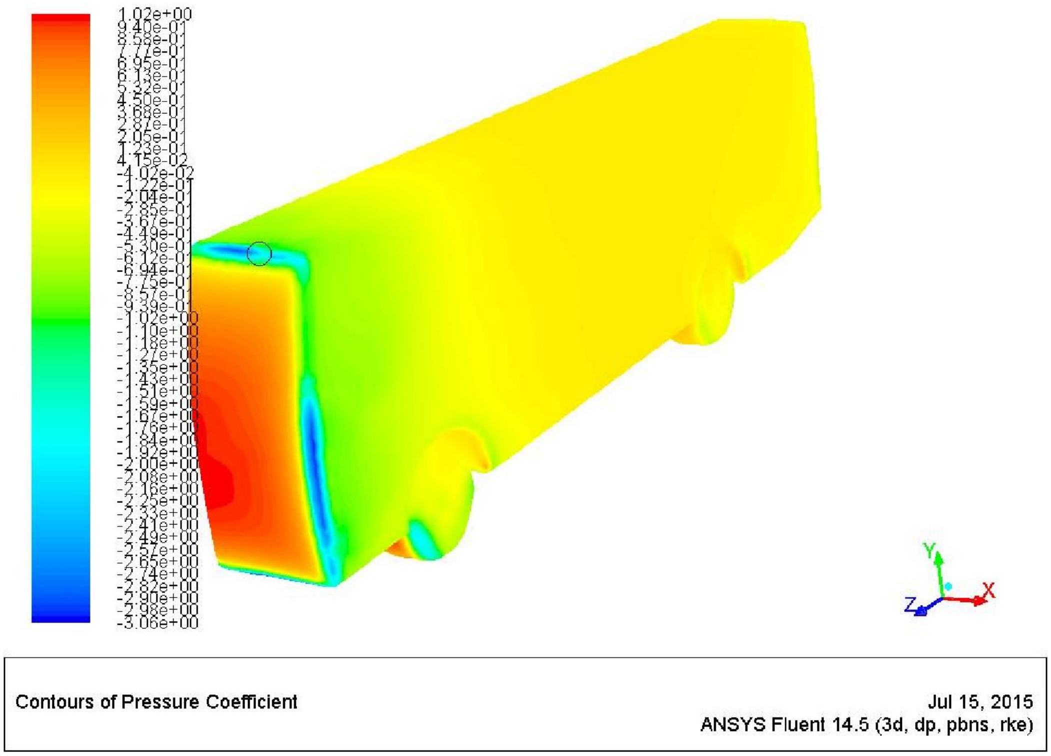

Fig 52(a) : Pressure distribution of Model 1 at 100 Kmph

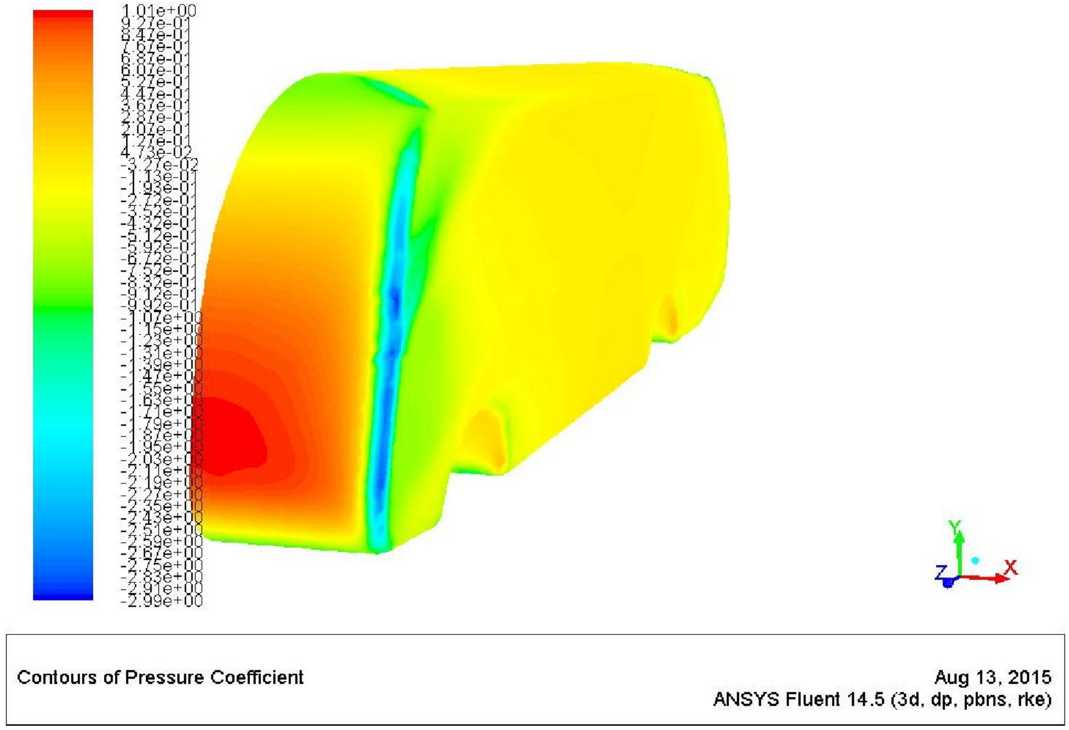

Fig 52(b) : Pressure distribution of Model 2 at 100 Kmph

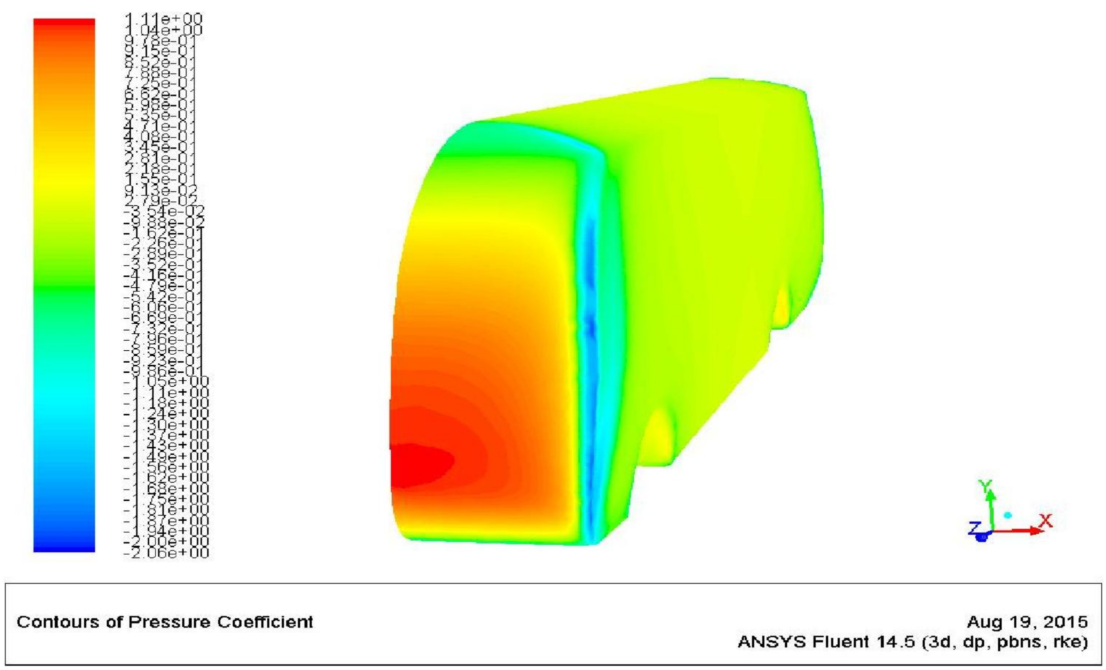

Fig 52(c) : Pressure distribution of Model 3 at 100 Kmph

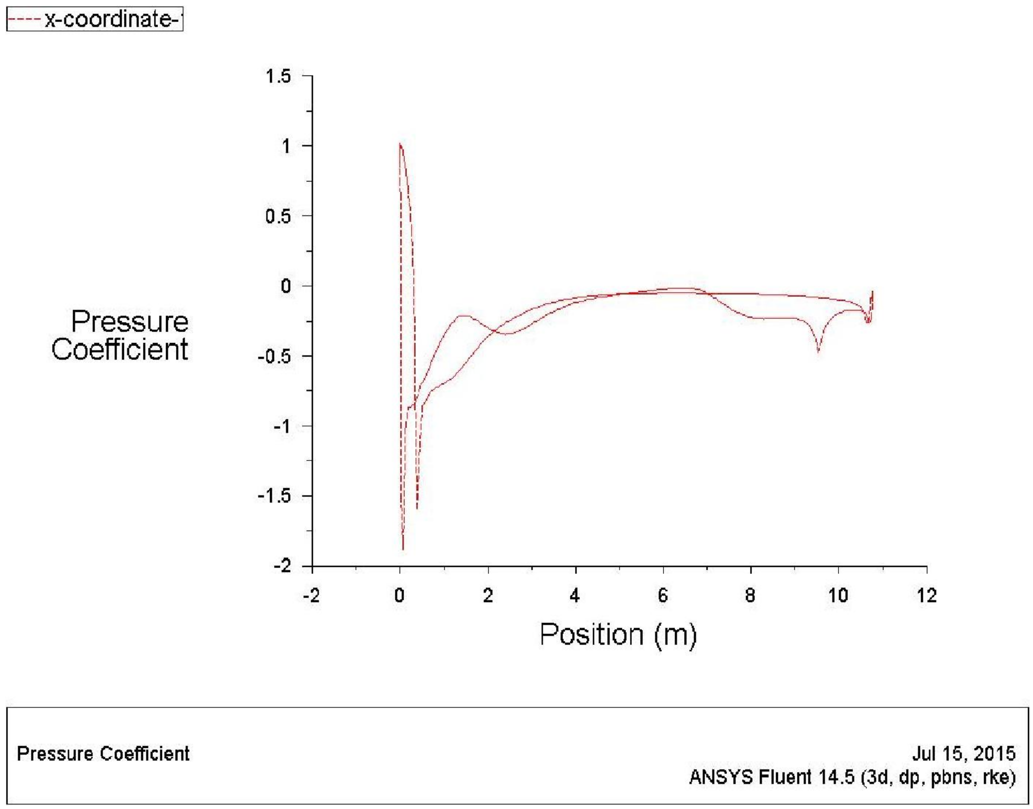

Fig 53(d) : Graph for Pressure coefficient of Model 1 at 100 Kmph

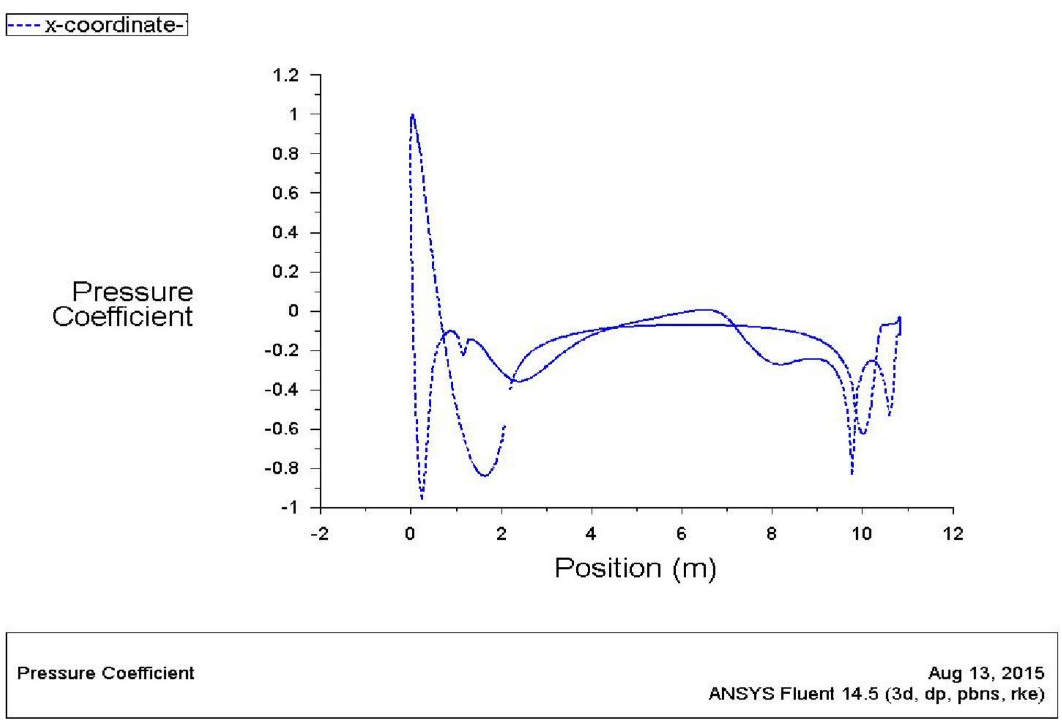

Fig 53(e) : Graph for Pressure coefficient of Model 2 at 100 Kmph

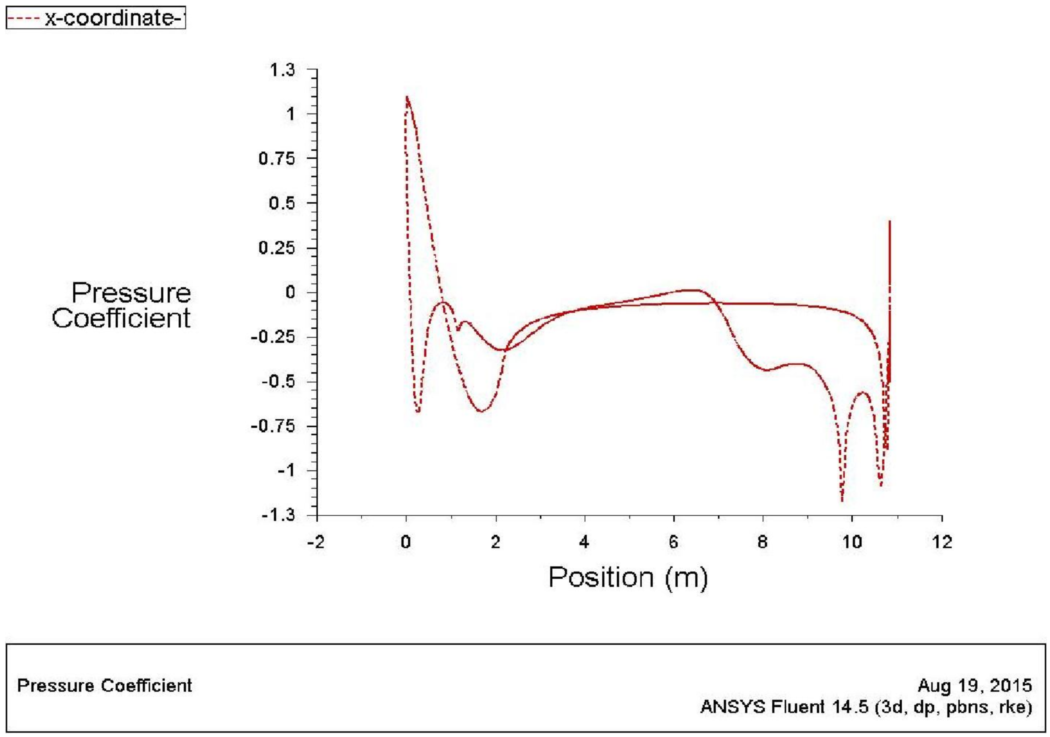

Fig 53(f) : Graph for Pressure distribution of Model 3 at 100 Kmph

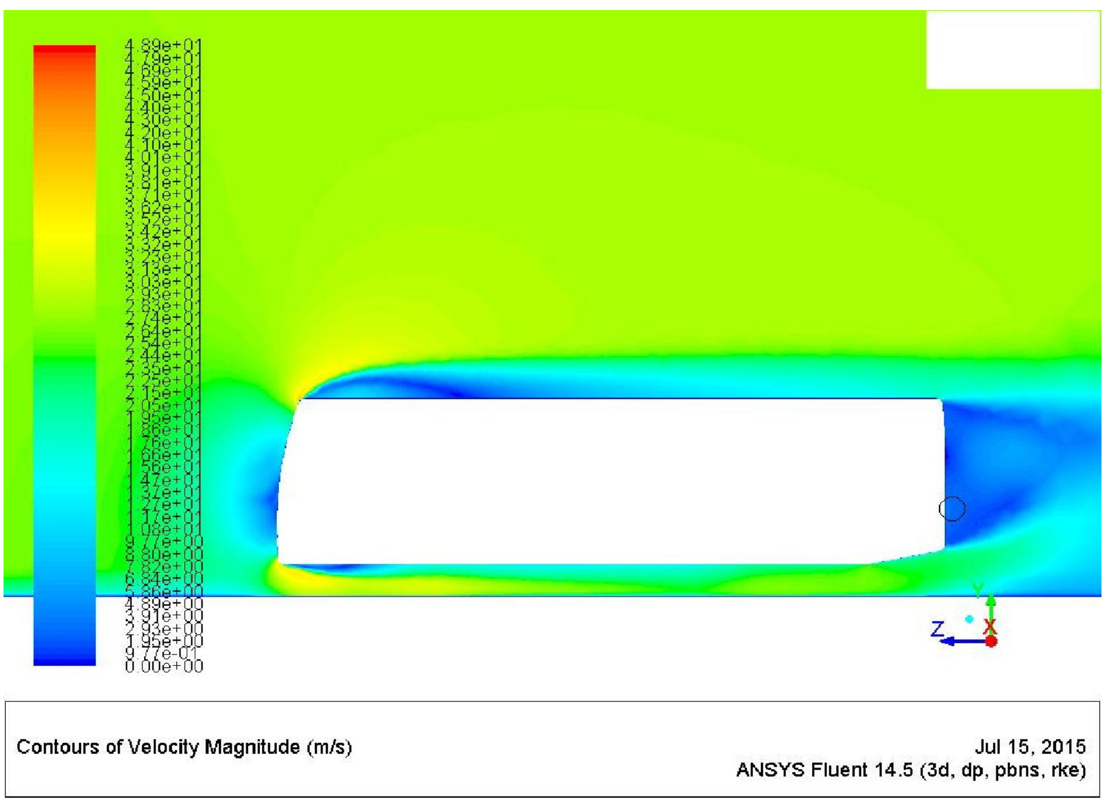

Fig 54(a) : velocity distribution of Model 1 at 100 Kmph

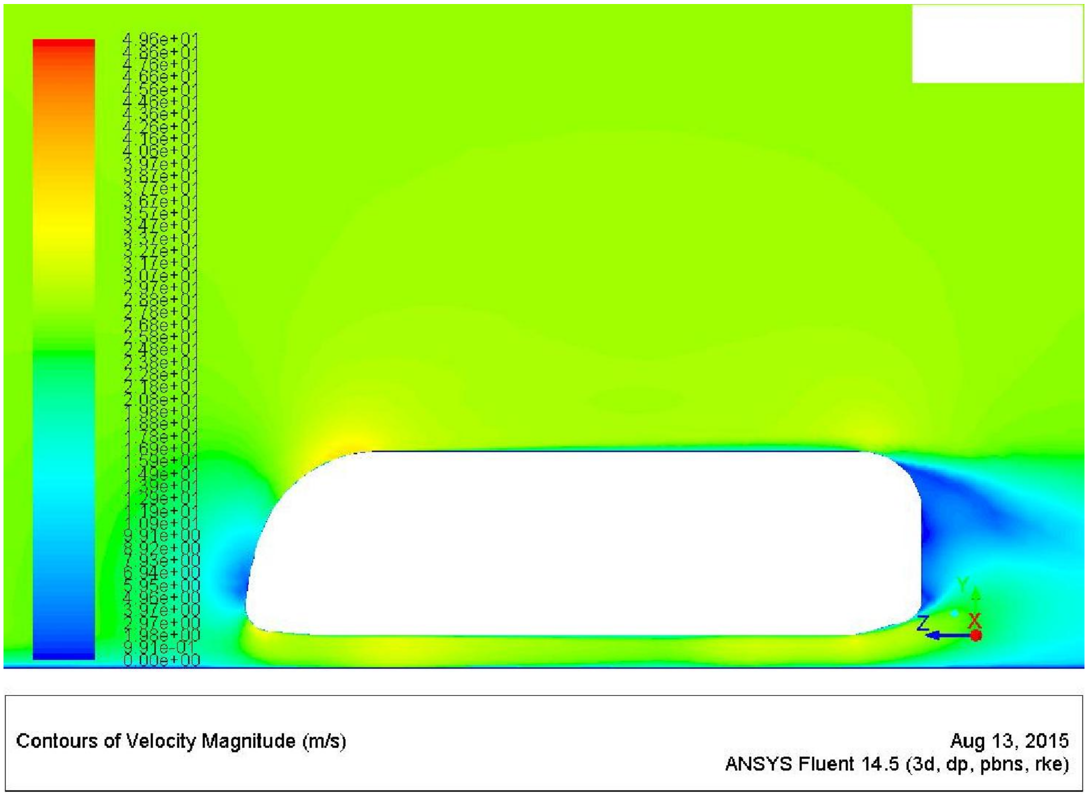

Fig 54(b) : Velocity distribution of Model 2 at 100 Kmph

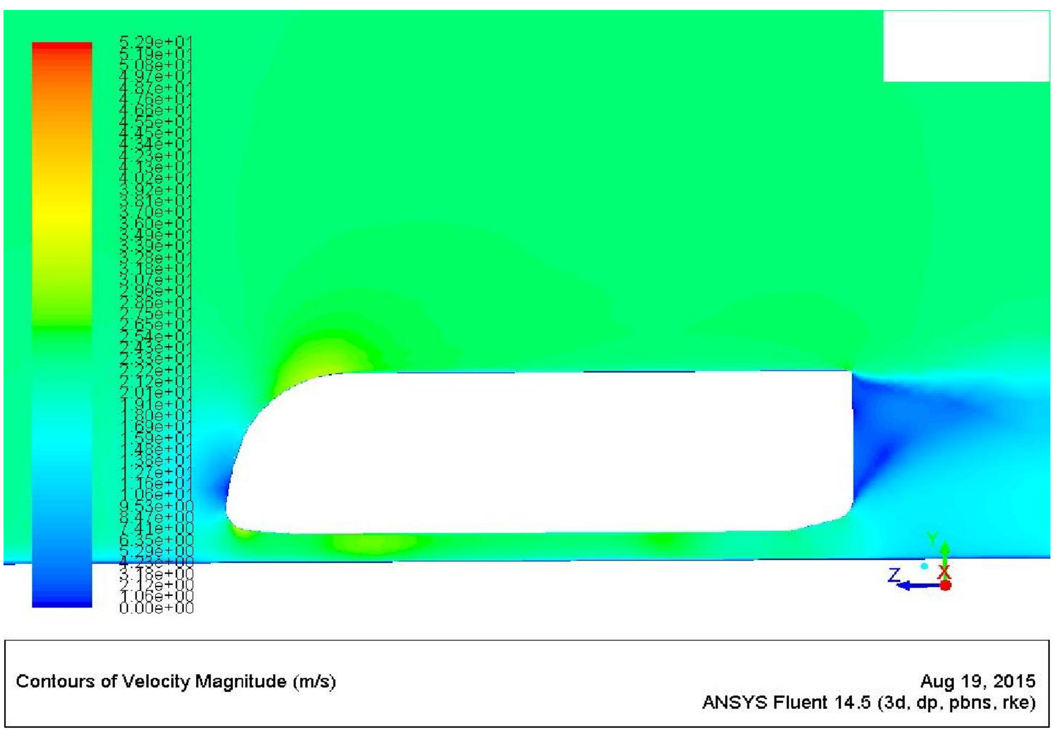

Fig 54(c) : Velocity distribution of Model 3 at 100 Kmph

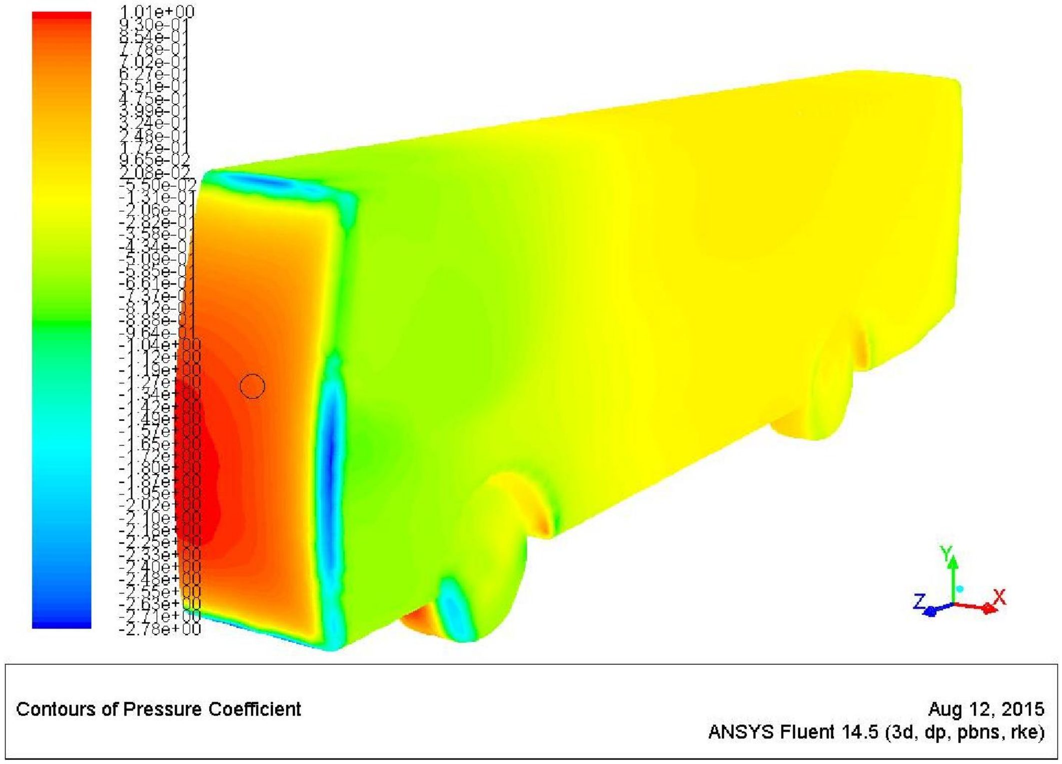

Fig 55(a) : Pressure distribution of Model 1 at 115 Kmph

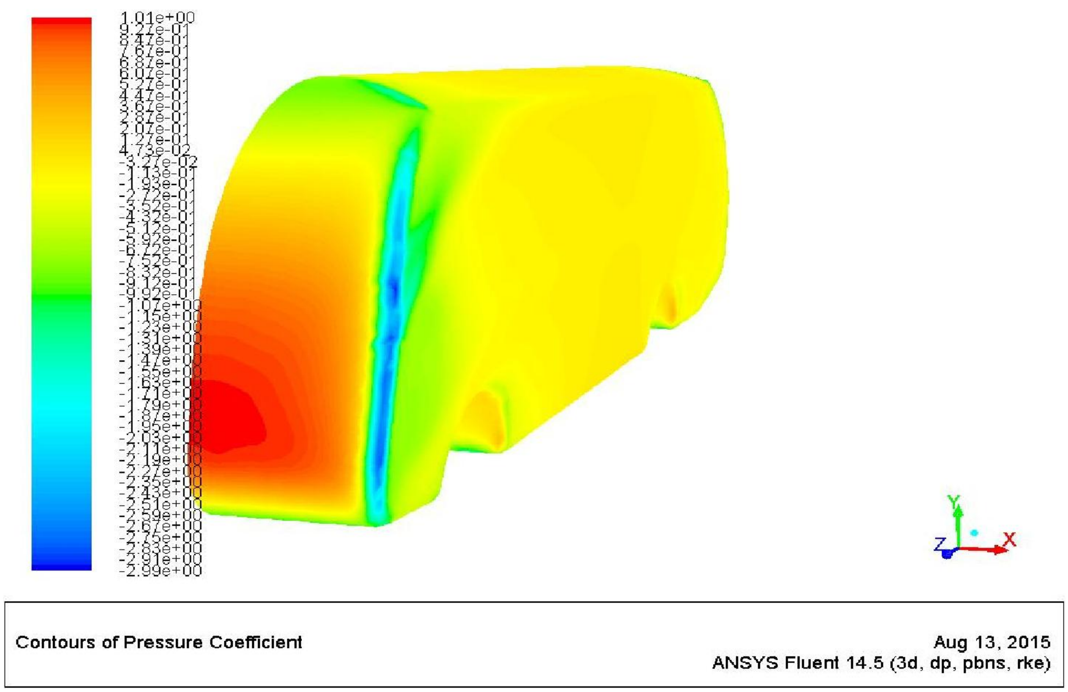

Fig 55(b) : Pressure distribution of Model 2 at 115 Kmph

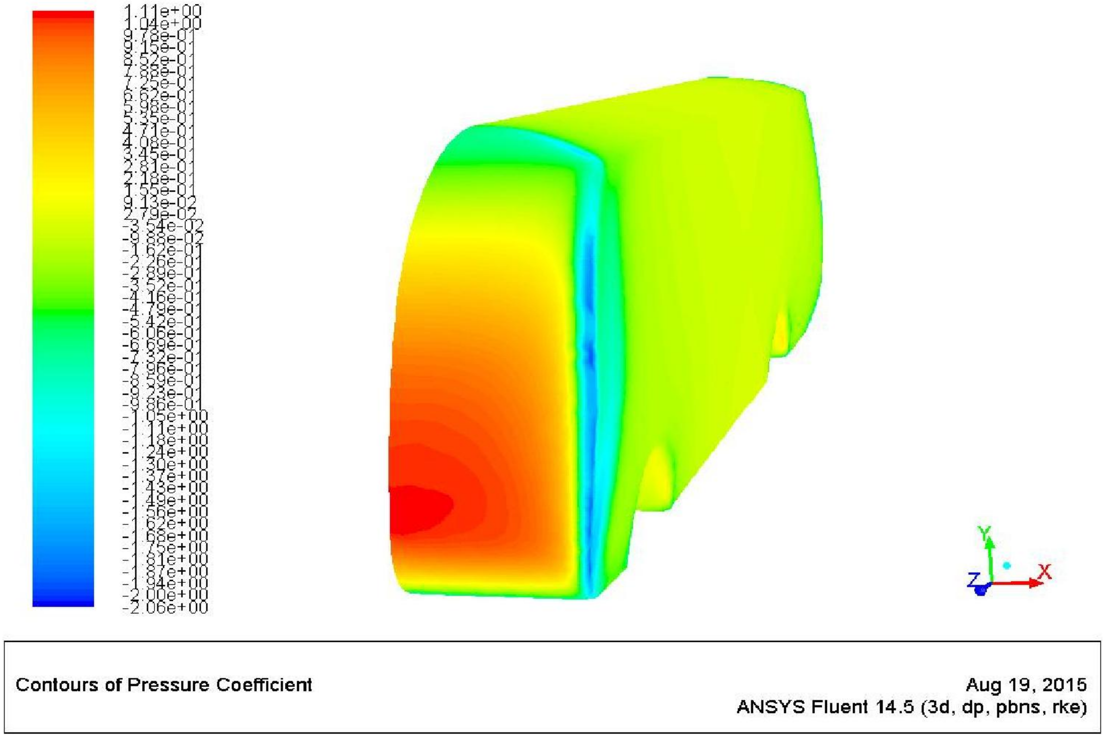

Fig 55(c) : Pressure distribution of Model 3 at 115 Kmph

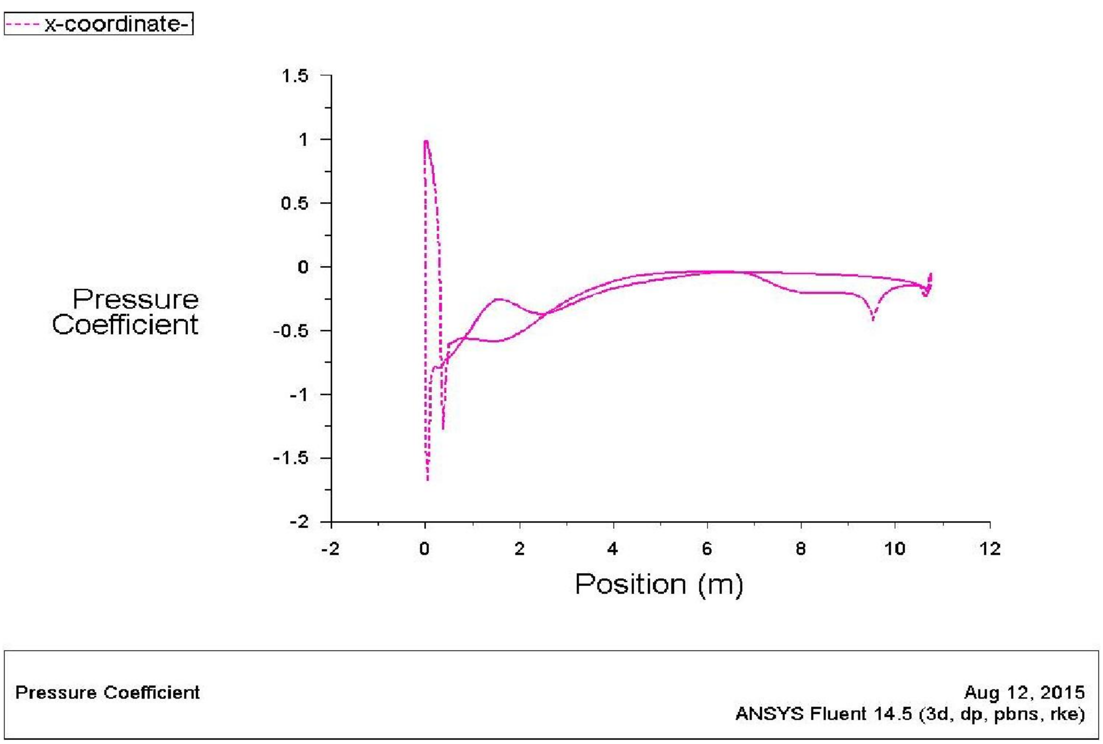

Fig 56(d) : Graph for Pressure distribution of Model 1 at 115 Kmph

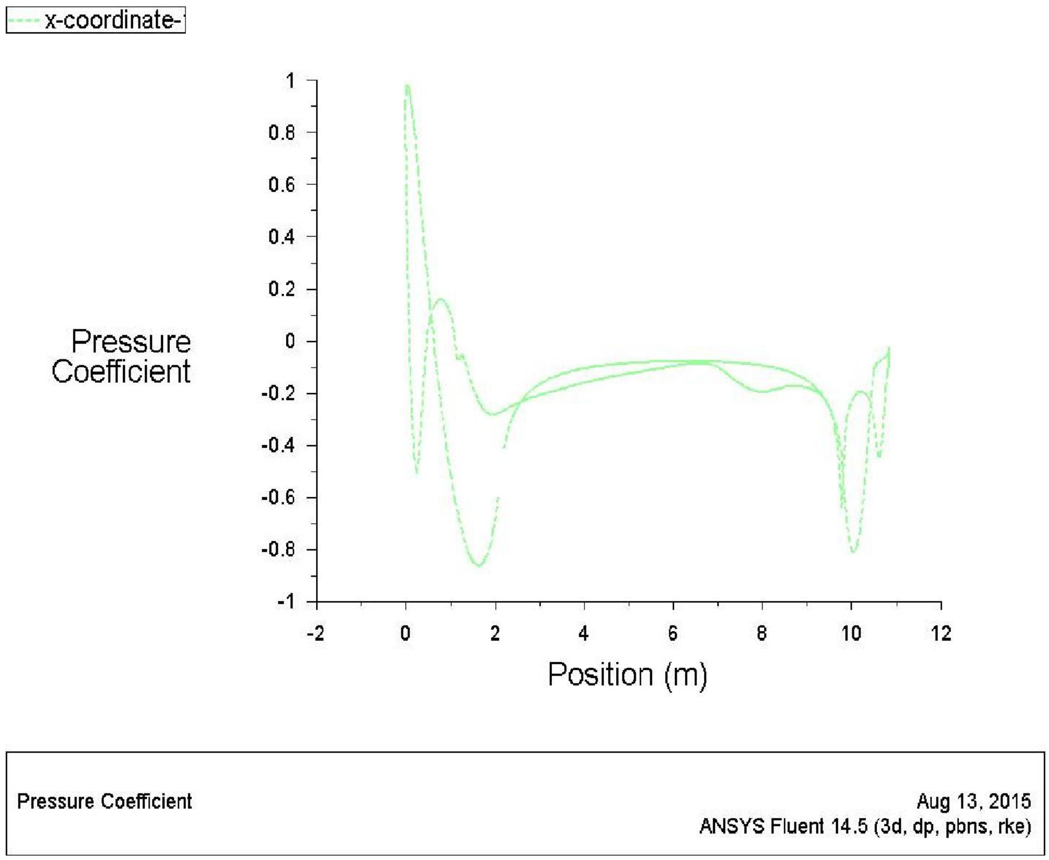

Fig 56(e) : Graph for Pressure distribution of Model 2 at 115 Kmph

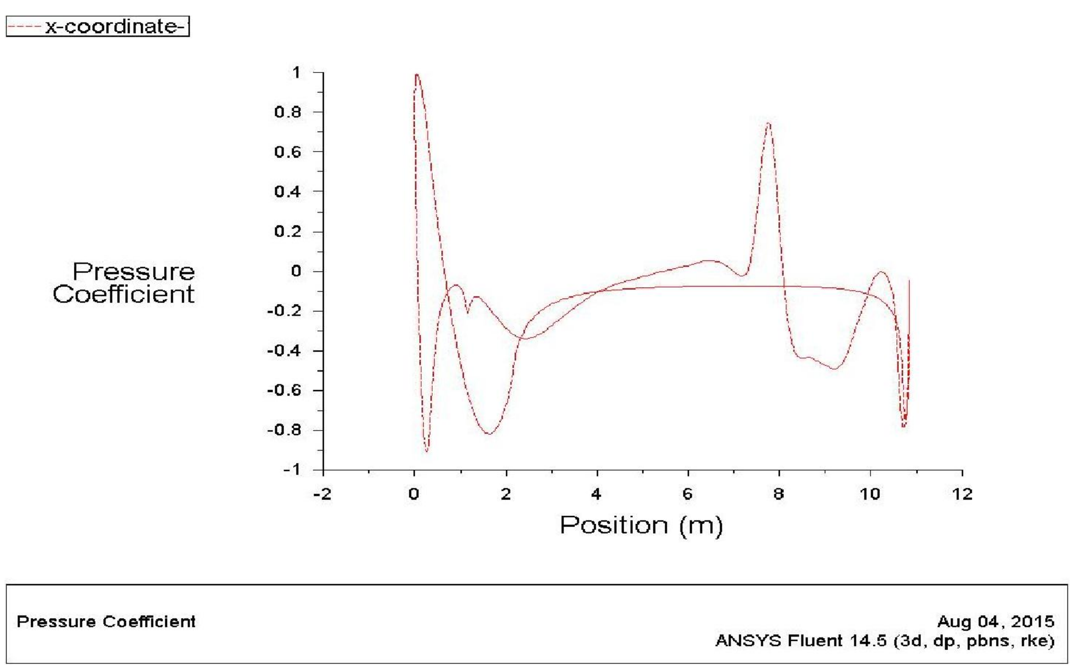

Fig 56(f) : Graph for Pressure distribution of Model 3 at 115 Kmph

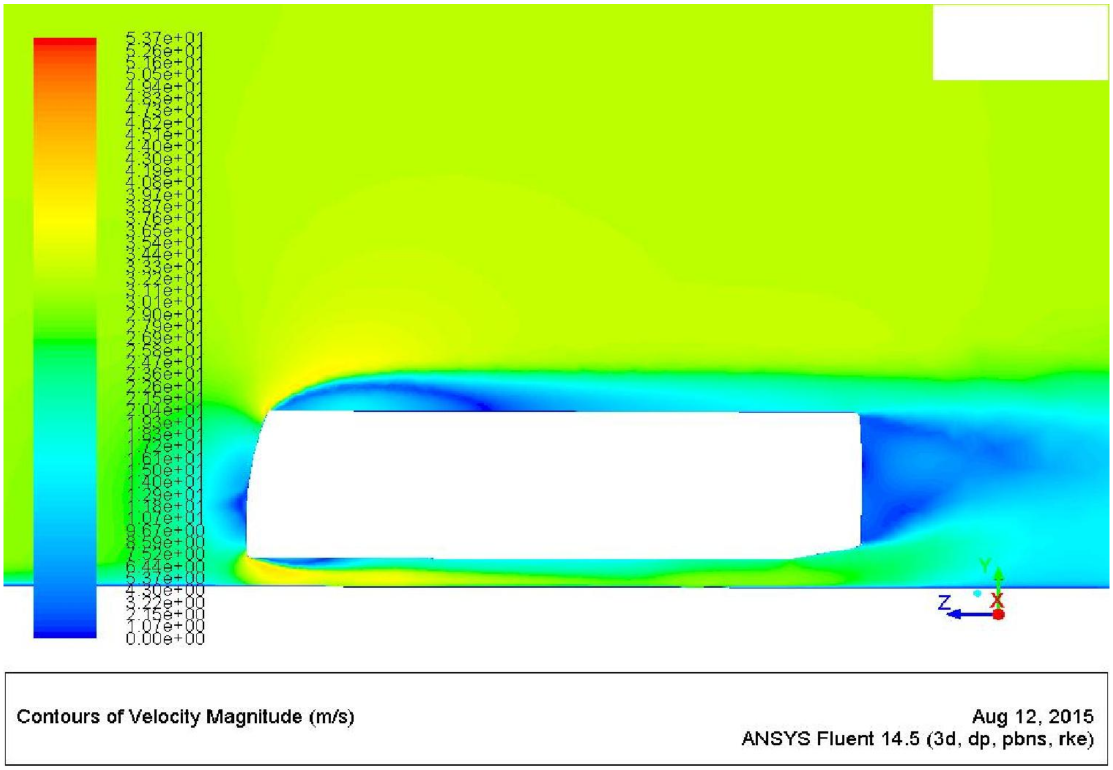

Fig 57(a) : velocity distribution of Model 1 at 115 Kmph

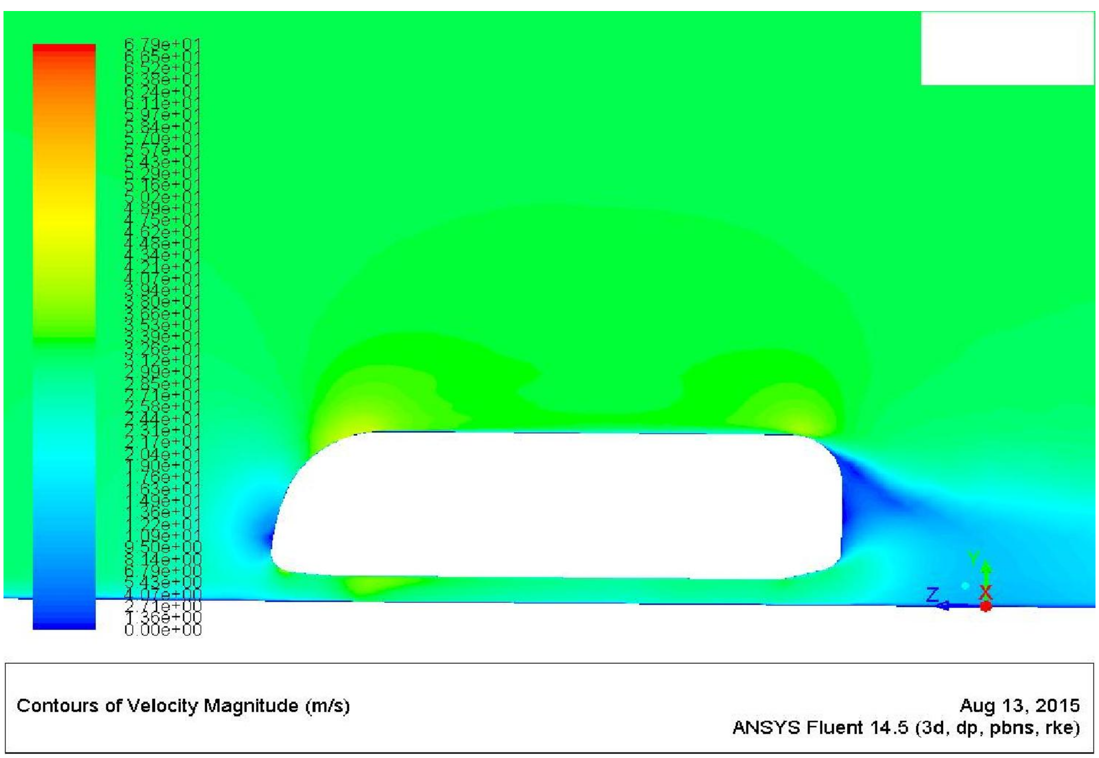

Fig 57(b) : Velocity distribution of Model 2 at 115 Kmph

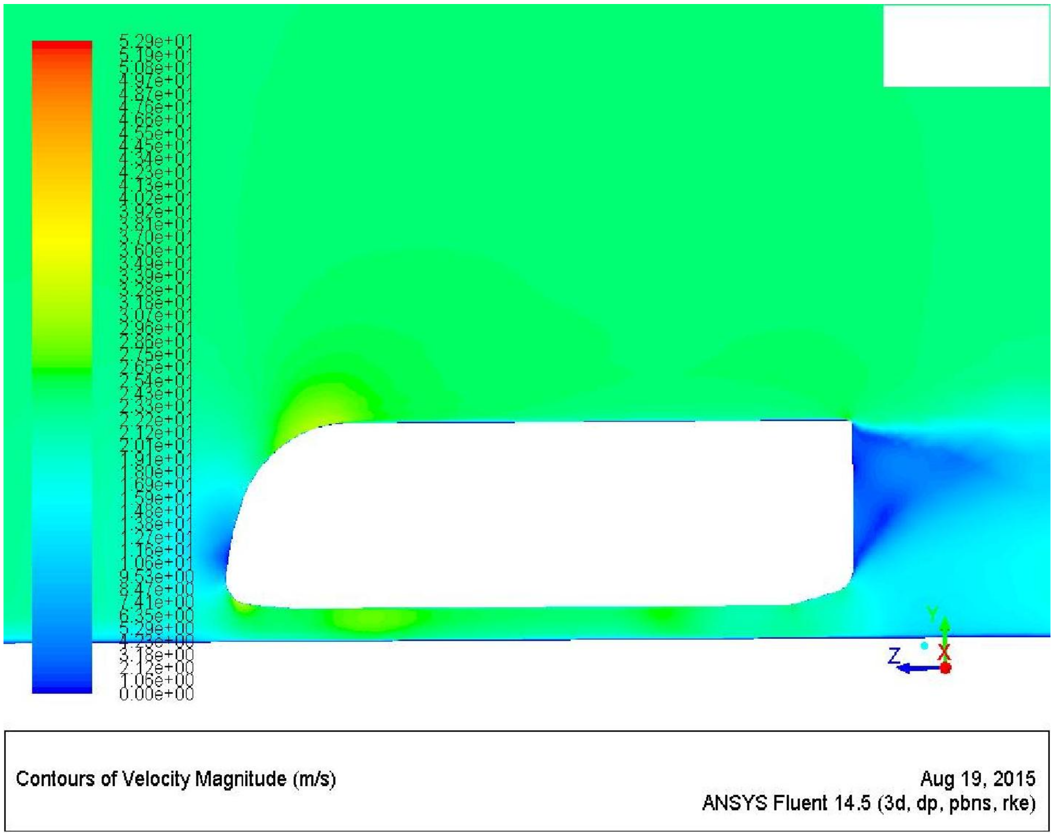

Fig 57(c) : Velocity distribution of Model 3 at 115 Kmph

Discussion

Discussion was made as follows based on the results obtained. That is pressure distribution on the bus, coefficient of pressure and velocity distribution of flow pattern for each case respectively.

Model1 (Existing Bus)

The figures of 49(a), 52(a), 55(a) show the pressure distribution of the existing Yutong bus in various speeds. It shows the pressure act on the body is high at maximum frontal area.

The stagnation points on the front portion is clearly seen in this plot. Rear wall of the bus experiences low pressure compared to the front due to the flow separation and circulation. This pressure difference leads to high pressure drag on the body. Figure 5 shows the path lines of flow around the bus body. The flow gets stagnated at the frontal area and gets accelerated at the front radius area. Flow separation was observed behind the mirrors. Flow remains attached along the sides and roof. Flow eventually gets separated at the rear and forms vortices. Frontal area of the bus experiences maximum pressure due to stagnation. A streamlined front end which allows better air flow will effectively improve the aerodynamic performance of the vehicle.

Incorporating aerodynamic design features as reported in the literature such as roof tapering, roof end lowering, boat tailing, and radius improvements will reduce the drag of bus. Important parameters and their values extracted from the analysis are taken as reference for the new bus design are listed in table 3.

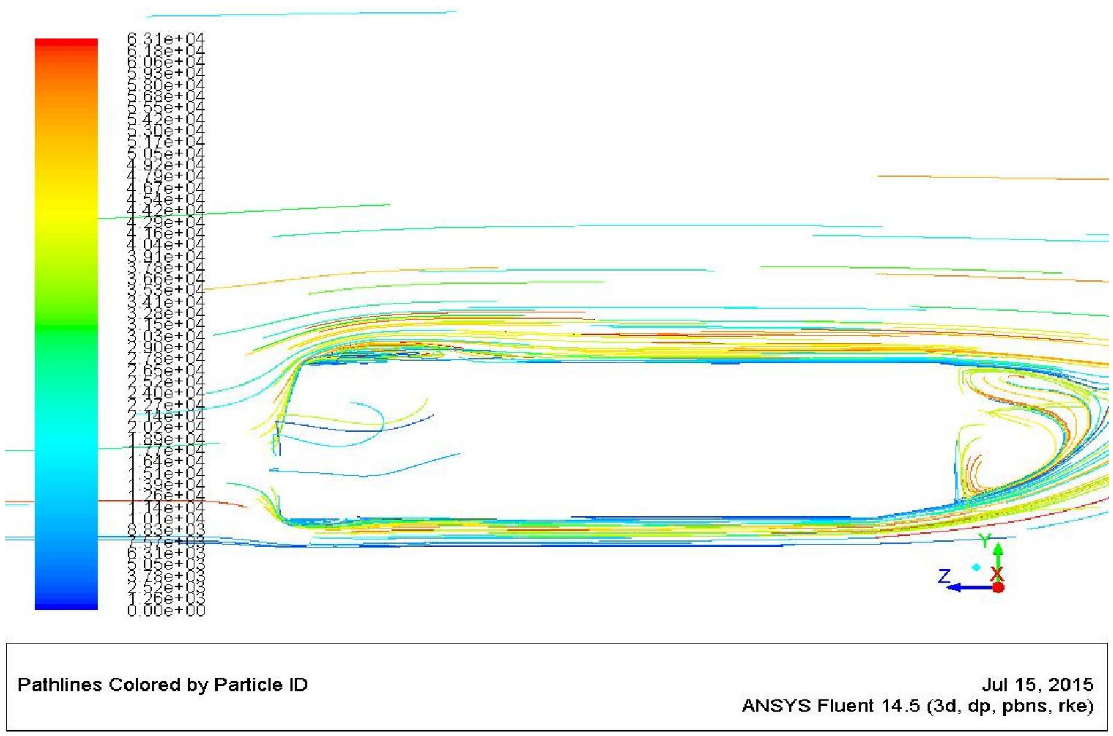

Figure 58: Flow Path line for Model 1

The graphs of 50(d), 53(d), 56(d) show the pressure with respect to distance. It shows the pressure values over the upper and lower parts of the Model

The figures of 51(a), 54(a), 57(a) show the velocity distribution of the Yutong bus in various speeds. It shows the velocity distribution of Model 1 is maximum both at the front end of the roof and at the bottom. The pressure is high than Model 2 and Model 3

Model 2(Modified Bus 1)

The figures of 49(b), 52(b), 55(b) show the pressure distribution of the Modified Bus 1 in various speeds. It shows the pressure act on the body is high at maximum frontal area. Even though it is maximum at the frontal area, it is dramatically reduced while compared to Model1 and Model 3

The graphs of 50(e), 53(e), 57(e) show the pressure with respect to distance. It shows the pressure values over the upper and lower parts of the Model.

The figures of 51(b), 54(b), 57(b) show the velocity distribution of the Modified Bus 1 in various speeds. It shows the velocity distribution over the body. According to the figures, the velocity distribution is still maximum at the front end of the roof and bottom of the bus. But, there is a significant reduction of velocity has been obtained. The velocity is lower than Model 1 and Model 3.

Model 3(Modified Bus 2)

The figures of 49(c), 52(c), 55(c) show the pressure distribution of the Modified Bus 2 in various speeds. It shows the pressure act on the body is high at maximum frontal area. Even though it is maximum at the frontal area, it is reduced while compared to Model 1. But still higher than Model 2.

The graphs of 50(f), 53(f), 56(f) show the pressure with respect to distance. It shows the pressure values over the upper and lower parts of the Model

The figures of 51(c), 54(c), 57(c) show the velocity distribution of the Modified Bus 2 in various speeds. It shows the velocity distribution over the body. According to the figures, the velocity distribution is still maximum at the front end of the roof and bottom of the bus. But, there is a significant reduction of velocity has been obtained. The velocity is lower than Model 1 and larger than Model 2.

NOTE: Pressure distribution plot of the bus body at the speed of 80,100, 115 kmph reveal pressure concentration in front region of the vehicle as the air flow strikes at the front and brought momentarily to rest.
Pressure occupies the frontal region which develops a huge resistance for the vehicle to move forward. Since the pressure occupies a large area vacuum is created on the side of the bus that is the surface which is parallel to the flow. Rear wall of the bus experience low pressure compared to the front due to the flow circulation and separation. This pressure difference leads to high pressure drag on the body.
The velocity of the flow increases while crossing front faces edges respectively. This is because of the front face. Due to the presence of side wings the flow does not expose directly on the road wheels. Flow direction is diverted in the rear portion by the presence of the filleted edge in the rear. Hence the vacuum region created in the rear portion of the vehicle is controlled.

5.2 Vortex Generated at Rear Side(Wake Zone)

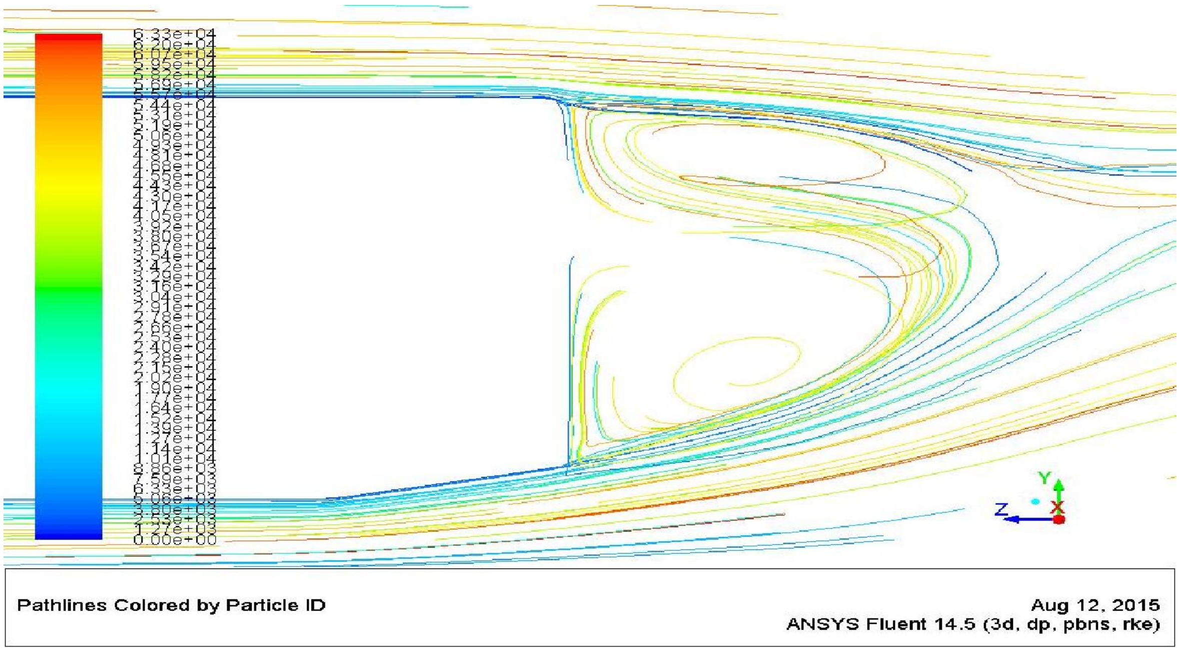

Figure 59: Vortex Generated in Model 1

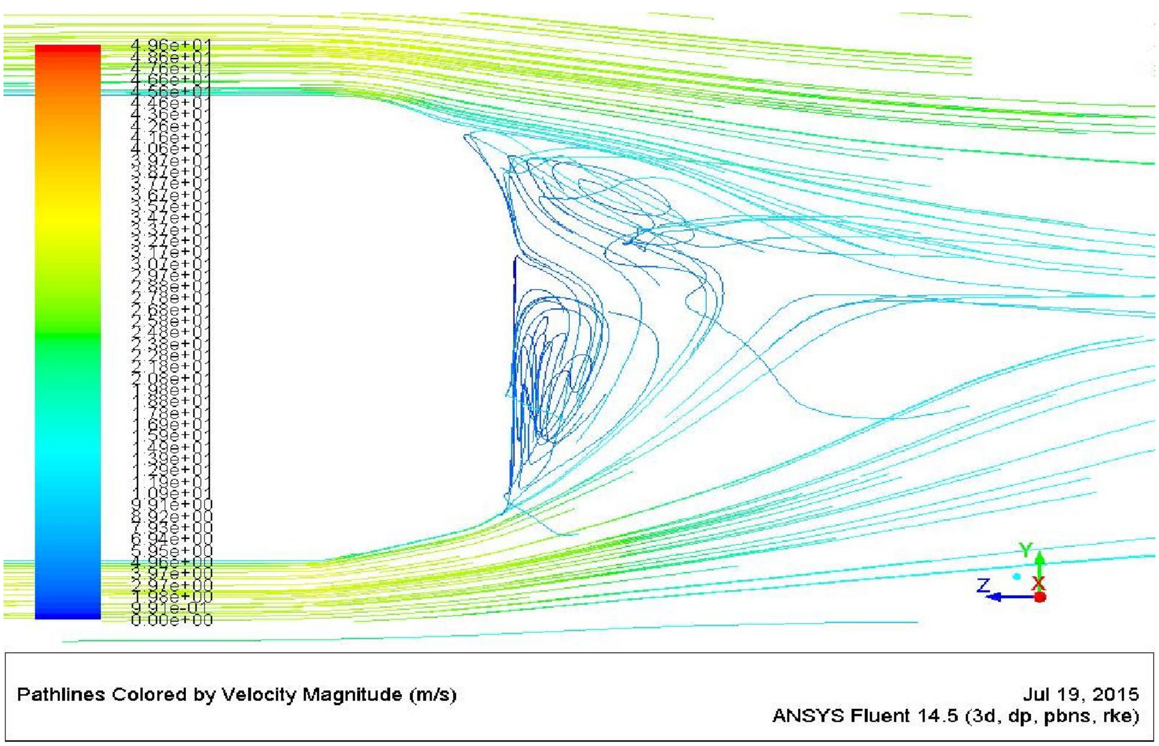

Figure 60: Vortex Generated in Model 2

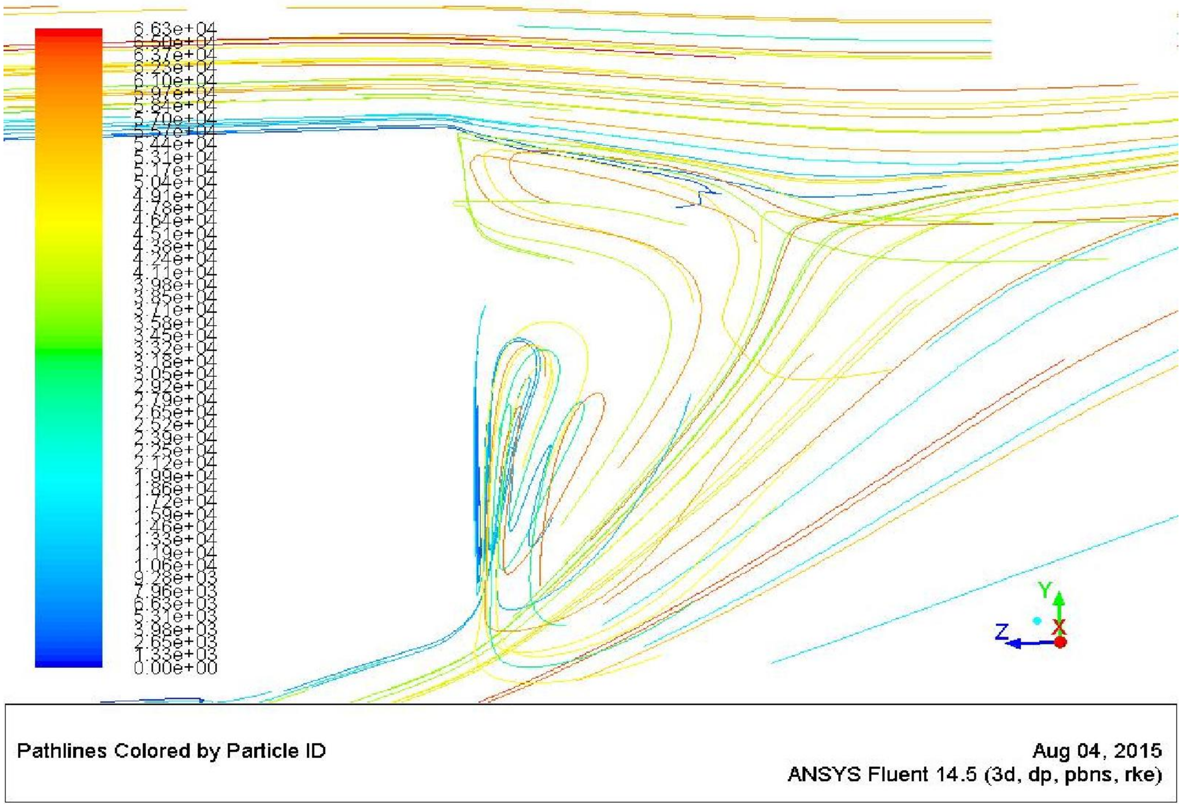

Figure 61: Vortex Generated for Model 3

The low pressure region behind the bus were seen spread across a wider area in the existing bus design(model 1) and a little bit better for model 3 (Fig. 53 and 55). The vortices formed behind the buses(model 1 & model 3) were also spread across the wide region. For model 2 (Fig. 54) the flow is attached leading to suppressed vortices formation at the rear and these vortices were seen moved towards ground. This change in the aerodynamic characteristics is due to the effect of roof tapering, roof lowering, boat tailing and diffuser at the rear. The cornered radii in the front, inclined and rounded wind screen, and elimination of the rear view mirror resulted attached flow right from the front of the vehicle. It was proposed in the current design that new technology of closed circuit TV with cameras placed at the rear and sides and the display screen in the driver cabin would replace the rear view mirror. This arrangement would give wider coverage with minimized blind spots when compared to the rear view mirror. Therefore, the area covered by the wake zone of Model 1 is larger than Model 2 and Model 3. And Model 3 is more than Model 2. This leads us to have significant and reasonable drag reduction with Model 2.

5.3 Drag Coefficient

Table 6: Drag coefficient (C_d) at various speed

Kmph	Speed in m/s (v)	Model 1	Model 2	Model 3
85	23.61	0.525	0.328	0.418
100	27.78	0.533	0.338	0.452
115	31.94	0.557	0.377	0.476

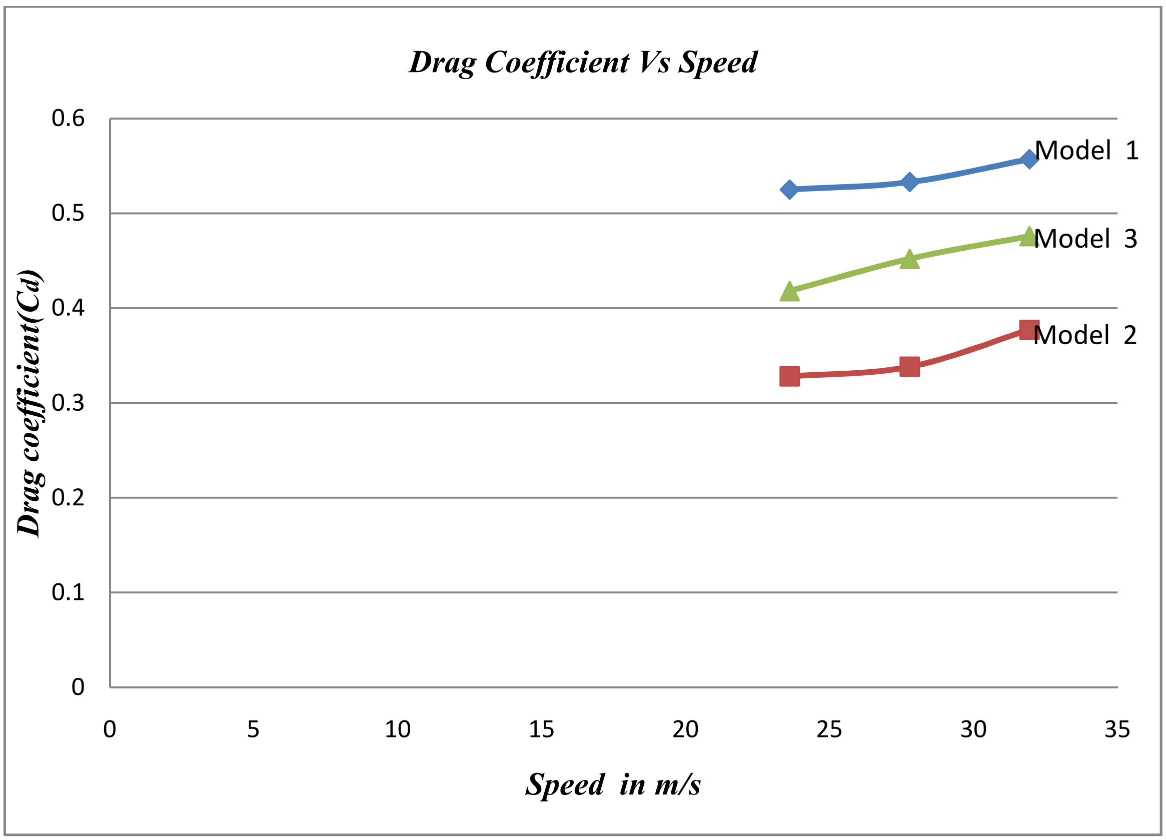

Figure 62: Drag Coefficient Vs Speed

Table 6 and figure 56 show the comparison of drag coefficient acting on the base line model and the new designs at different vehicle speeds. Clear decrease in the drag coefficient is visible in the analysis.

From the above results the percentage of drag coefficient reduction from model1 to model 2 is approximately 38 %, 37%, and 32% at 85, 100 and 115 kmph respectively and on average 35.7%. From model1 to model3 is approximately 20%, 15%, and 15% at 85, 100 and 115 kmph respectively and on average 16.7%. From model 3 to model 2 is approximately 22%, 25%, and

21% at 85, 100 and 115 kmph respectively and on average 22.7%. These reductions are mainly a result of the shape and size of the frontal area of the buses

Thus, the Drag Coefficients are not constant ,but depends on a number of factors, including; Shape of object, the orientation relative to the flow and the fluid's viscosity, mass, density, flow speed and object size.

5.4 Drag Forces

A. Total Drag Force(N) [58]

$$F_d = 1/2\ \rho\ A\ C_d\ V^2$$

Total Drag Force = Pressure Force + Viscous Force

i. Pressure force(Form drag)

Table 7: Pressure force(Form drag) at various speed(N)

Kmph	Speed in m/s (v)	Model 1	Model 2	Model 3
85	23.61	627.49	354.28	479.92
100	27.78	878.89	475.58	609.08
115	31.94	1221.10	738.45	942.70

ii. Viscous force(Skin friction)

Table 8: Viscous force(skin friction) at various speed(N)

Kmph	Speed in m/s (v)	Model 1	Model 2	Model 3
85	23.61	28.90	43.51	47.39
100	27.78	38.96	57.69	64.28
115	31.94	44.60	73.97	85.17

iii. Total Drag Forces (N)

Total Drag Force = Pressure Force + Viscous Force

Table 9: Total Drag Force (N) Total Drag Force = Pressure Force + Viscous Force				
Kmph	Speed in m/s	Model 1	Model 2	Model 3
85	23.61	656.37	397.79	527.30
100	27.78	917.85	533.28	673.36
115	31.94	1265.70	812.42	1027.87

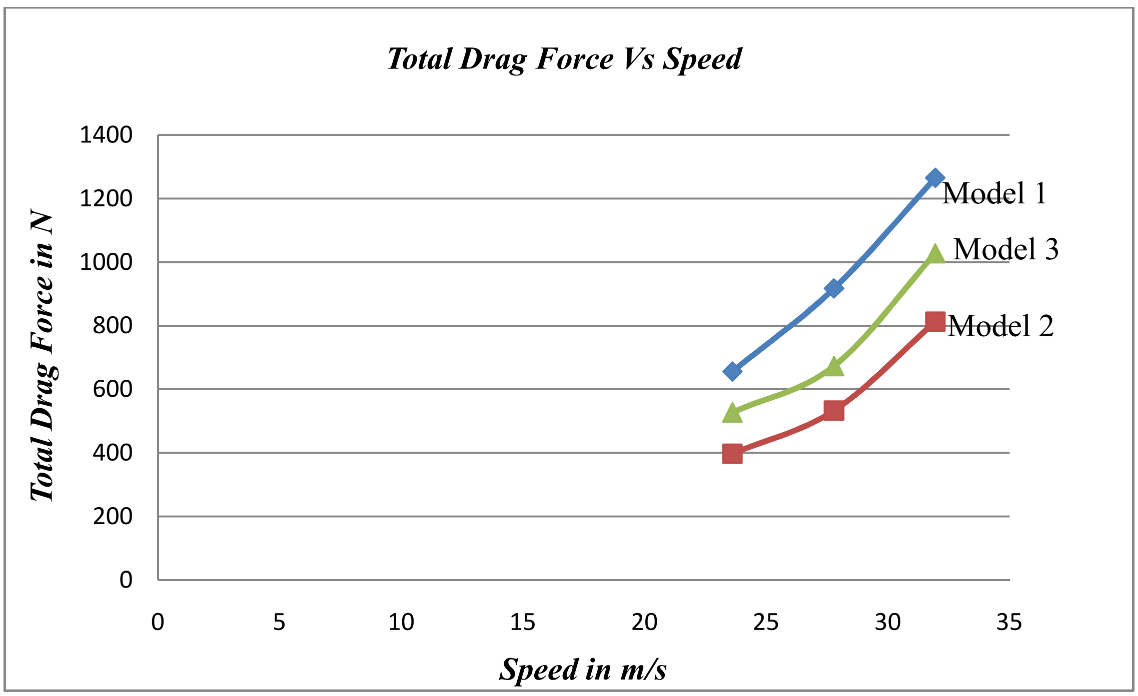

Figure 63: Total Drag Force Vs Speed

Table 9 and figure 57 show the comparison of drag force acting on the base line model and the new designs at different vehicle speeds. Clear decrease in the drag force is visible in the analysis and the total drag force is reduced from 656.37 N to 397.79 N at 85 kmph with model 2 and 656.37 N to 527.30 N at 85 kmph with Model 3. This is an improvement of 39.4% and 19.7%

respectively. The total drag force for model1 decreases quickly for model 2 and it slightly decrease for model 3.

B. Rolling Resistance (N)

Fr = (0.015+0.00016V) W [58]

where, V = bus speed in m/s, W = weight of bus in N

Table 10: Rolling Resistance at Various Speed

Kmph	Speed in m/s	Model 1	Model 2	Model 3
85	23.61	300.442	300.442	300.442
100	27.78	311.117	311.117	311.117
115	31.94	321.766	321.766	321.766

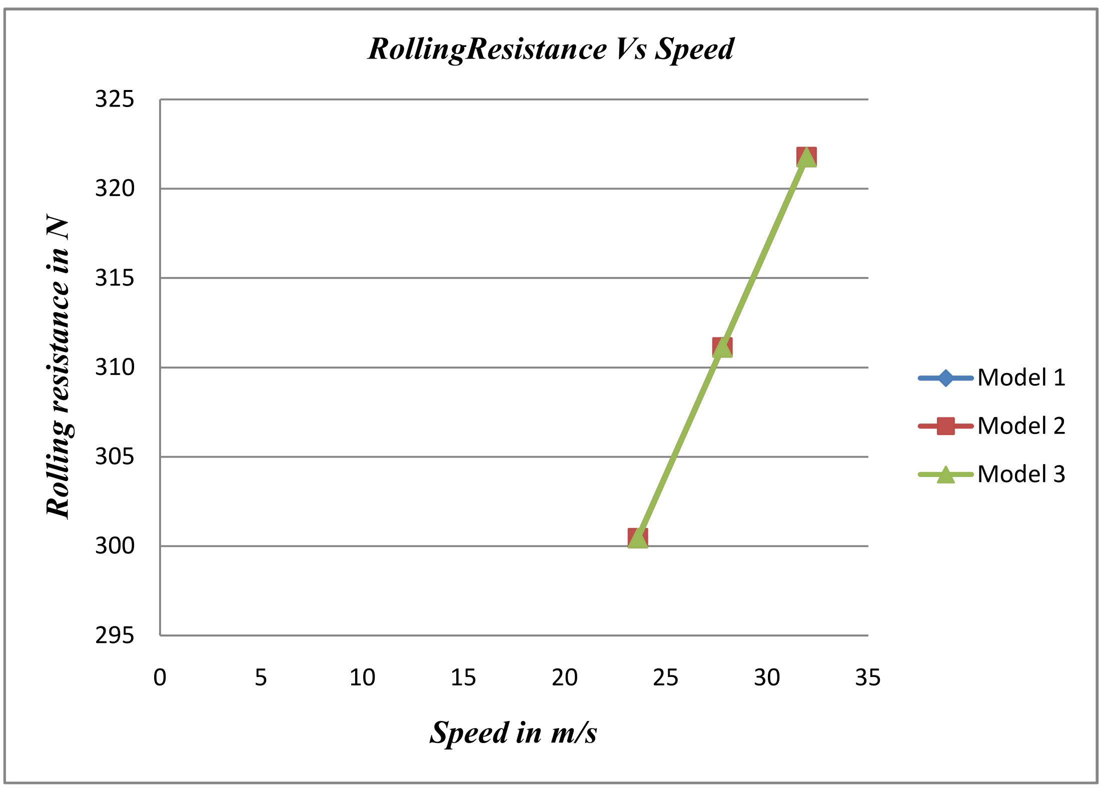

Figure 64: Rolling Resistance Vs Speed

The graph indicates rolling resistances of the models are equal at various speeds. The reason that the speed and weight of the buses are the same.

C. Total Resistance (N) [58]

$$Ft = Fd + Fr + Fg$$

Where, Fd - Drag force, Fr - Rolling resistance, Fg - Gravitational force but, Fg = 0 (leveled surface) = $W\sin\theta$

Table 11: Total Resistance at Various Speeds

Kmph	Speed in m/s	Model 1	Model 2	Model 3
85	23.61	956.812	698.232	827.742
100	27.78	1228.967	844.397	984.477
115	31.94	1587.466	1134.186	1349.636

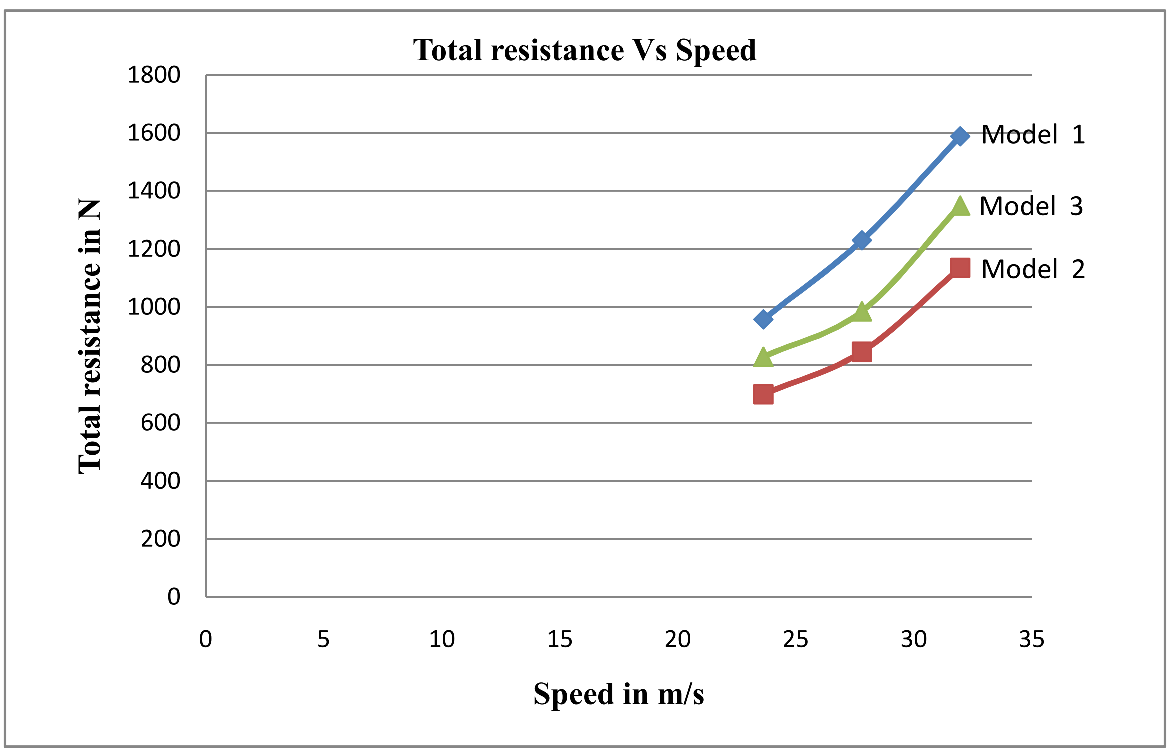

Figure 65: Total Resistance Vs Speed

5.5 Power Requirements

The power required to pull the bus against the resistance in a leveled surface is calculated and their corresponding values for differential speeds were given below.

Table 12: Input Parameters for Power Requirement Calculation			
Parameters	Model1	Model 2	Model 3
Air density in kg/m^3	1.225	1.225	1.225
Frontal area in m^2	3.66	3.45	3.45
Weight in kg (W)	16000	16000	16000
Transmission efficiency (η_t)	0.9	0.9	0.9
Drag coefficient (C_d)	--	--	--

i. Power Required (hp) [58]

$$P = F_t V/\eta_t$$

Where, P = Power

Ft = Total Resistance

V = Vehicle Speed

$\eta_t =$ Transmission efficiency

Table 13: Power Required at Various Speeds				
Kmph	Speed in m/s	Model 1	Model 2	Model 3
85	23.61	25100.368	18316.953	21635.732
100	27.78	37934.115	26063.721	30387.523
115	31.94	56337.404	40251.001	47897.082

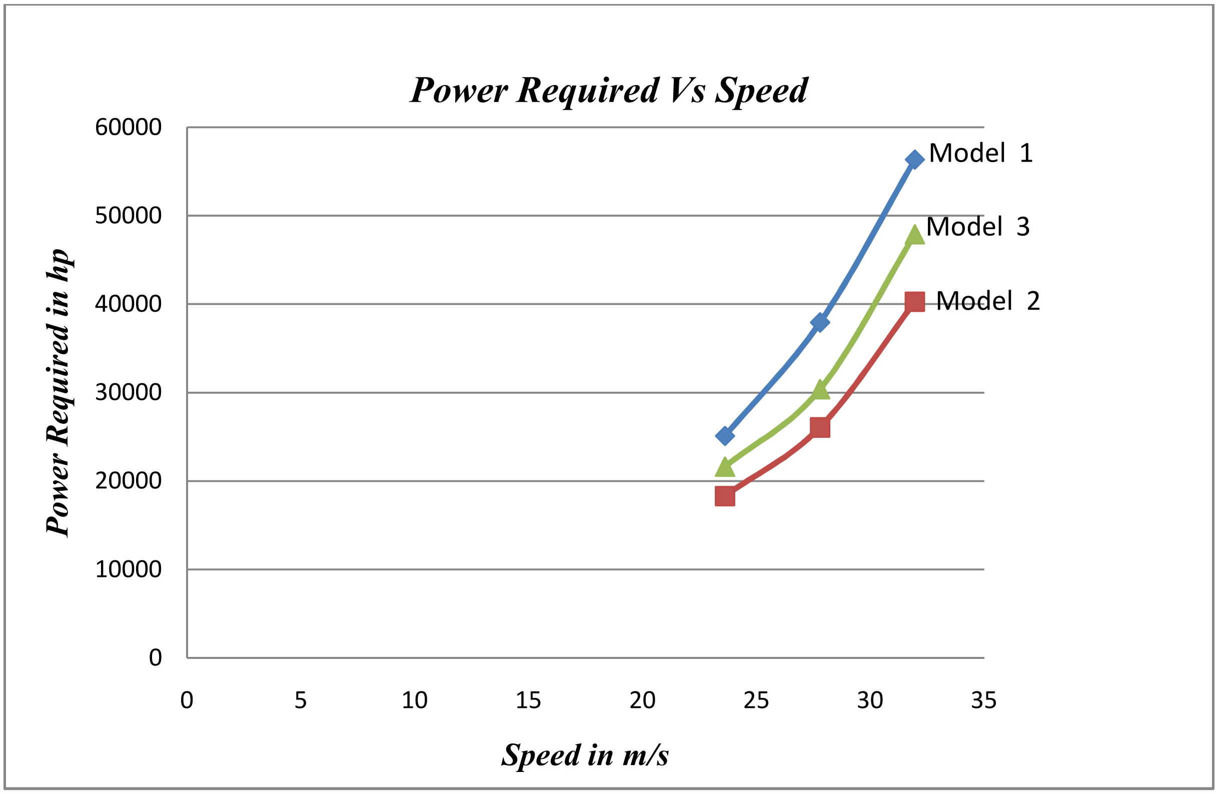

Figure 66: Power Required Vs Speed

The graph indicates power requirements at various speeds for model 1, model 3 and model 2 respectively.

- The power required by model 1 is greater than both model 2 and model 3 and model 3 is greater than model 2. Which means model 1 consumes more fuel than the two models and similarly model 3 consumes more than model 2. Therefore model 1 needs major improvements.

5.6 Calculation of Fuel Consumption[24]

Percentage fuel reduction = 3/5[percentage total drag reduction]

Table 14: Fuel saving in(%)

Models	Speed(kmph)	Drag coefficient(C_d)	C_d percentage reduction(%) from baseline	Fuel saving(%)
Modell 1	85	0.525	---	---
	100	0.533	----	---
	115	0.557	---	---
Model 2	85	0.328	38	22.8
	100	0.338	37	22.2
	115	0.377	32	19.2

Model 3	85	0.418	20	12
	100	0.452	15	9
	115	0.476	14.5	8.7

Table 14 shows a maximum of 22.8% fuel can be saved in Model 2 at 85 kmph from Model 1 at the same speed. Which means 22.8% of the total fuel consumed by Model 1 can be saved. The average fuel consumed by Model 1 per 100 km is 23L(Table 14). From this the bus Model 2 can save 22.8% of 23 L, which is 5.24 L. Therefore, Bus Model 2 consumes 17.8 L per 100 km.

5.7 Lift Coefficient

Table 15: Lift Coefficient at various Speed

Kmph	Speed in m/s (v)	Model 1	Model 2	Model 3
85	23.61	-0.143	-0.020	-0.202
100	27.78	-0.147	-0.029	-0.347
115	31.94	-0.177	-0.109	-0.767

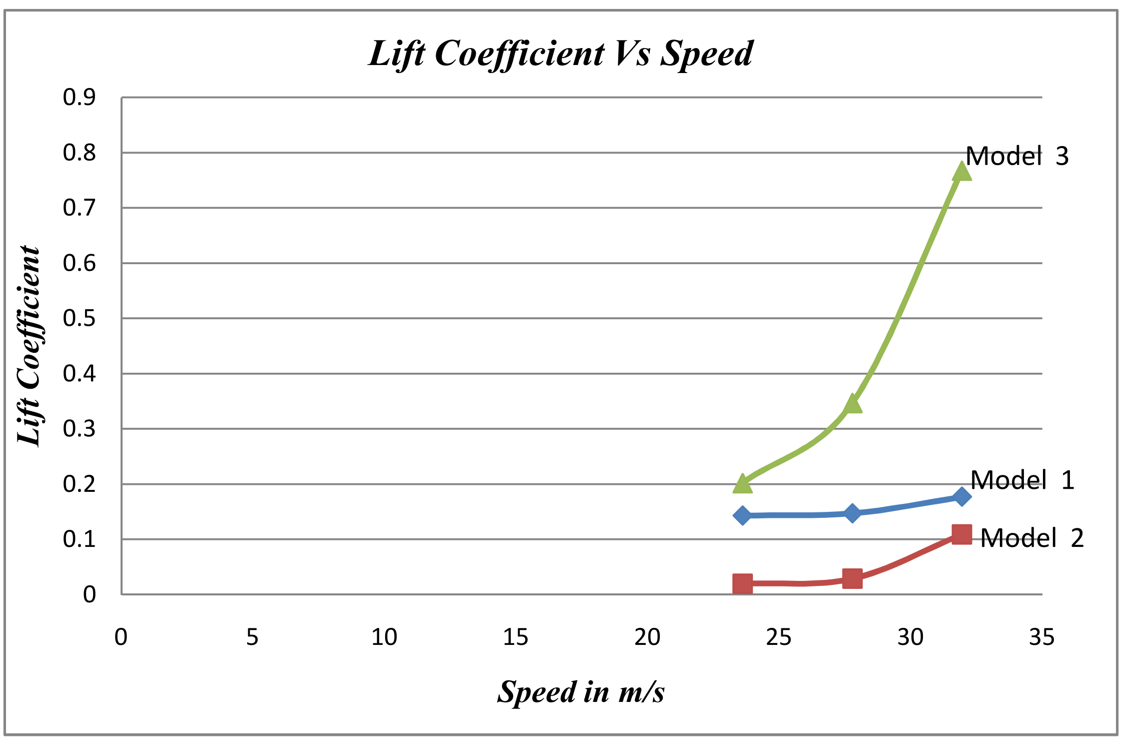

Figure 67: Lift Coefficient Vs Speed

5.8 Lift Force

Table16: Lift Force at Various Speed				
Kmph	Speed in m/s	Model 1	Model 2	Model 3
85	23.61	-178.976	-23.282	-238.234
100	27.78	-254.339	-47.840	-749.117
115	31.94	-405.630	-234.890	-1251.682

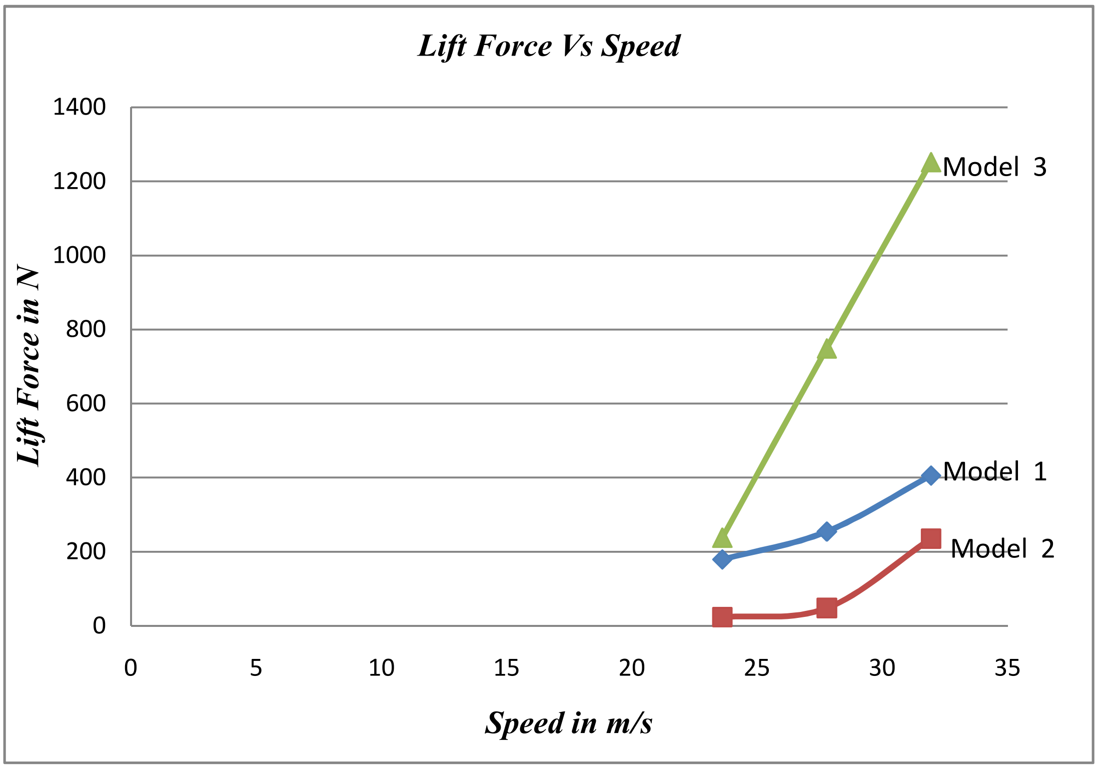

Figure 68: Lift Force Vs Speed

Table 16 shows the values of lift forces are negative, this indicates the lift forces are downward lift and which is very useful to improve the vehicle's road holding capacity and reduce steering instability of the bus. But, even though there are adequate reductions of drag coefficient, drag forces and power while using Model 2, its downward lift force is very less compared to Model 1 and Model 3. This needs to modify the under body profile(shape) and add additional downward force improvement methods like, under body dam, negative rear spoiler, etc. Figure 14 shows the comparison of lift force acting on the base line model and the new designs at different vehicle speeds. Clear increase in the lift force is visible in Model 3. Therefore, an additional underbody designs(mentioned above) are required for Model 1 and especially in Model 2. The lift force is reduced from -178.976 N to-23.282 N at 85 kmph in Model 2(Table 14). Which is 87% reduction of lift force and the lift force is increased from -178.976 N to -238.234 N in Model 3. This is an improvement of 33%.

5.9 Pressure Coefficient

The Pressure Coefficient is a dimensionless characteristic variable which can represent the relative pressure field in the domain.

$$C_p = \frac{p - p_\infty}{\frac{1}{2}\rho_\infty v_\infty^2}$$

Equation 5.1[123]

Where, p_∞ = Free stream pressure

v_∞ = Free stream velocity

In the front section, high pressure arise since the flow is stopped by the car then the velocity decreases and pressure increases based on the Bernoulli Equation (3.7). Depression evolve in the front underbody section because the accelerating flow captured under the car. On the windshield close to the roof the velocity is increasing and high value is reached at the roof edge. Along the roof the velocity damps into the free stream and pressure is normalizing until the back where separation occurs due to the geometry.

$$\frac{1}{2}\rho v^2 + \rho g H + p = const$$

Equation 5.2 [13]

Table 17: Pressure Coefficient at Various Speed

Kmph	Speed in m/s	Model 1	Model 2	Model 3
85	23.61	0.502	0.292	0.407
100	27.78	0.508	0.301	0.413
115	31.94	0.534	0.343	0.437

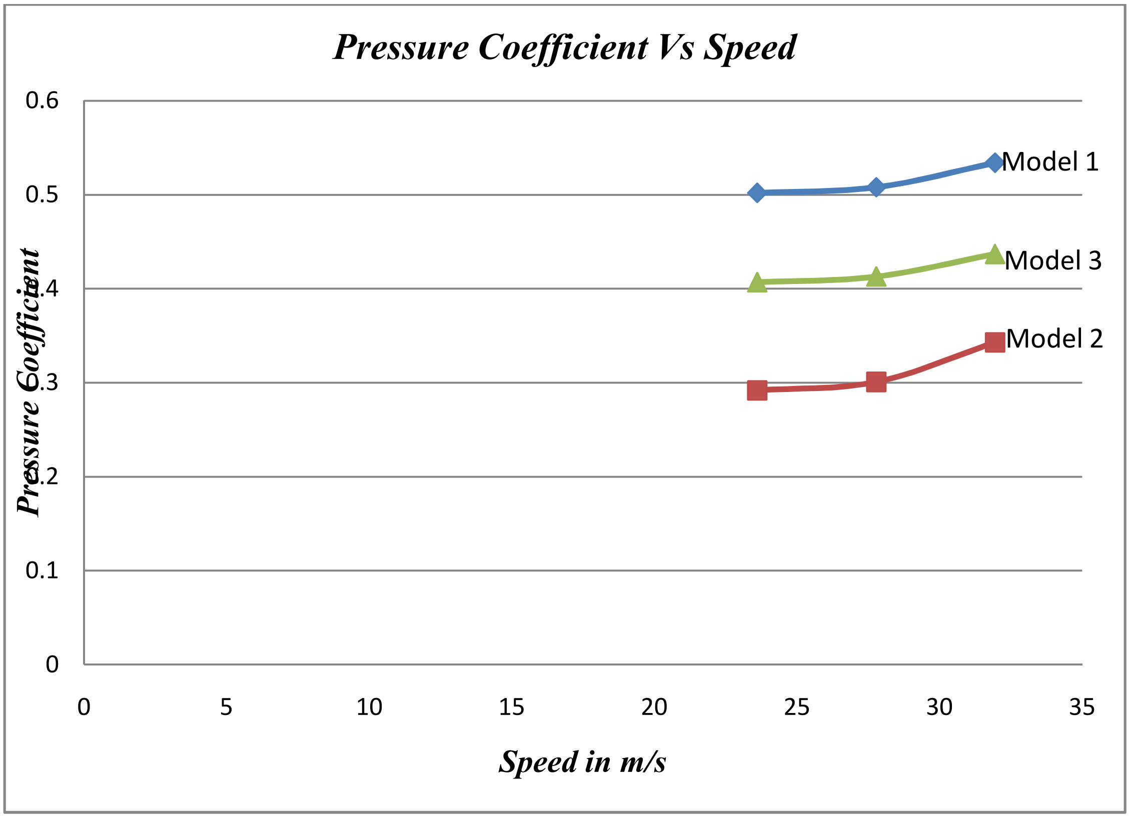

Figure 69: Pressure Coefficient Vs Speed

Table 17 and figure 63 shows the comparison of pressure coefficient in the base line model and the new designs at different vehicle speeds. Clear decrease in the drag force is visible in the analysis and the total drag force is reduced from 2411 N to 955 N at 100 kmph (Fig. 14). This is an improvement of 60.39 %.

The coefficient of pressure value of Model 2 is found to be 0.292 at 85 kmph, which is 41.8 % and 28.26% improvement compared to the baseline model 1(0.502) and Model 3(0.407) respectively. And I got 0.407 in Model 3 at 85 kmph, this is an improvement of 18.9% compared to Model 1. The pressure coefficient for model 2 decreases quickly than Model 3 while compared to Model 1 for the predetermined speeds.

5.10 Summery of drag, lift and pressure Forces of all studied

Table 18: Drag, lift and pressure forces of all studied

Models	kmph	Pressure force(**F_p**) in N	Shear(viscous)force(**F_v**) in N	Total drag force(**F_d**) in N	Lift force in N	Percentage reduction in **F_p**(%) from baseline	Percentage reduction in **F_v**(%) from baseline	Percentage reduction in **F_d**(%) from baseline	Percentage reduction in **F_l**(%) from baseline
Model 1	85	627.49	28.90	656.37	-178.98	0	0	0	0
	100	878.89	38.96	917.85	-254.34	0	0	0	0
	115	1221.10	44.60	1265.70	-405.63	0	0	0	0
Model 2	85	354.28	43.51	397.79	-23.28	44	-51	39	87
	100	475.58	57.69	533.28	-47.84	46	-48	42	81
	115	738.45	73.97	812.42	-234.89	40	-66	36	42
Model 3	85	479.92	47.39	527.30	-238.23	24	-64	20	-33
	100	609.08	64.28	673.36	-749.12	31	-65	27	-195
	115	942.70	85.17	1027.87	-1251.68	23	-91	19	-209

5.11 Summery of Drag, lift and pressure coefficient of all studied

Table 19: Drag, lift and pressure coefficient of all studied

Models	kmph	Drag Coefficient (C_d)	Lift Coefficient(C_l)	Pressure Coefficient(C_p)	Percentage reduction in C_d(%) from baseline	Percentage reduction in C_l(%) from baseline	Percentage reduction in C_p(%) from baseline
Model 1	85	0.525	-0.143	0.502	0	0	0
	100	0.533	-0.147	0.508	0	0	0
	115	0.557	-0.177	0.534	0	0	0
Model 2	85	0.328	-0.020	0.292	38	86	42
	100	0.338	-0.029	0.301	37	80	41
	115	0.377	-0.109	0.343	32	38	36
Model 3	85	0.418	-0.202	0.407	20	-41	19
	100	0.452	-0.347	0.413	15	-136	19
	115	0.476	-0.767	0.437	14.5	-333	18

CHAPTER SIX

6. CONCLUSION AND RECOMMENDATION

6.1 Conclusion

The aerodynamic design of bus is an area where a lot of improvements will appear in the near future, in concern of drag reduction. The guidelines pointed out in the text are of a general nature that can be implemented in most modern road going vehicles; Smooth bus shape, rounded corners, High rake angle for the windscreen, Tapered rear end. The aerodynamics of buses have been described in order to get notions about how to reduce drag resistance, and sometimes even theoretically ideal techniques have been recommended. However, design has to deal with a whole lot of other performance, functionality and styling issues which sometimes, and not so few, still tend to rule when meeting incompatibilities with aerodynamic ones. Analysis was completed successfully in 3-D by using CFD software. By taking in account the boundary conditions; velocity, pressure, density of air and the frontal area of the bus, new shape can be designed by the help of drag reduction techniques like rear spoiler, roof deflector in future. Thus it is possible to produce the bus's body shape with optimum frontal area that will offer less resistance to the air moving in the opposite direction.

In the process of redesigning, exterior styling with improved aerodynamics of existing cross country bus(Yutong bus) plying on Ethiopian roads, a detailed computational analysis has been done. This computational analysis shows that there is possibility of improving the aerodynamic performance of bus by modifications in exterior design of bus body. These modifications are helpful in reducing the coefficient of drag i.e. Cd which effects the fuel consumption. A three dimensional flow analysis has been performed on the models at various speeds to predict the airflow characteristics around bus. The results provide the flow pattern and associated drag of the bus body.

The three buses body have been modeled for performing numerical analysis using CFD software. The Bus No.1 is the existing model, Bus No.2 is the existing model with the front and rear end modified, Bus No.3 is the existing bus with modification at front end and partially rear end. The three models have been separately tested for optimizing how each modification is contributing towards the drag force.

Velocity given to the fluent analysis are 85 kmph, 100 kmph, and 115 kmph. It was found that the least drag force was acting on Bus No.2. Bus No.3 gave an intermediate result as expected. The percentage reduction in drag force of Bus No.2 from Bus No.1 is found to be 39.4%. The average drag coefficient of the baseline model is 0.54, model 2 is 0.35 and model 3 I got is 0.45. By these modifications the coefficient of drag is reduced by model 2 and model 3 are approximately 35.7% and 16.7% respectively. Fuel consumption of about 22.8% can be reduced from 85 kmph to 115 kmph. This improvement in fuel efficiency will have a high impact on the reduction of annual fuel consumption. Hence the aim has been achieved.

6.2 Recommendation

- There are a lot of drag reduction possibility that can be applied to change the geometry of the bus to a more stream lined shape that will also have a great effect on turbulence reduction. But, more experienced mechanical designer is required to analyze the stability, strength and efficiency of the new model.
- More powerful computer is required, at least 3.0GHz CPU and 16GB of RAM memory to create a better geometry and to increase meshed cells, which makes better analysis and good result.
- Due to shortage of time, grid independency test and validation of the simulation result are not done(included).
- Genuine CFD tool(ANSYS Fluent) software is required for better aerodynamic analysis of the bus. Therefore, the department should purchase ANSYS Fluent software.
- The department should review MSc. course delivery system. A semester is not sufficient to carry out remarkable MSc. thesis work as expected, unless it is not a project. So, the three semester course should be reduced to two semester and the last one year should be free for thesis.

7. BIBLIOGRAPHY

[1] A. A. Abdel Aziz, and A. F. Abdel Gawad, "Aerodynamic and Heat Transfer Characteristics around Vehicles with Different Front Shapes in Driving Tunnels", Eighth International Congress of Fluid Dynamics & Propulsion (ICFDP 8), December 14-17, 2006, Sharm El-Shiekh, Sinai, Egypt, ICFDP8-EG-128.

[2] Adrien Becot. Aerodynamic force modification via base roughness. Master's thesis, Cranfield University, 2012.

[3] Ahmad Kamal Matamin, "Aerodynamic Study of a Coach Using Computational Fluid Dynamic(CFD) Technique", August 2006

[4]. Ahmad Kamal Matamin, "Aerodynamic Study of a Coach Using Computational Fluid Dynamic(CFD) Technique", August 2006

[5] A. Huminic and G Huminic. Numerical Flow Simulation for a Generic Vehicle Body on Wheels with Variable Underbody Diffuser. SAE Technical Paper 2012-01-0172,2012, 2012.

[6]. AIS – 052 - (2008), "Automotive industry standards code of practicefor bus body design and approval (First Revision)", The automotive research association of India on behalf of automotive industry standards committee.

[7] Alexander Diehl, Jose Nuno Lopes, Rui Miranda, Christoffer Mursu Simu and John Viji, autumn 2002, "Reducing Drag Forces in Future Vehicles", Department of Thermo and Fluid Dynamics, Chalmers, University of Technology.

[8] . A. Muthuvel, M. K. Murthi, N. P. Sachin, Vinay M. Koshy, S. Sakthi, and E. Selvakumar, "Aerodynamic Exterior Body Design of Bus", International Journal of Scientific & Engineering Research, ISSN2229-5518, Vol. 4, Issue 7, pp. 2453-2457, July-2013.

[9] Arun Raveendran, D. Rakesh, S. N. Sridhara (2009), "Exterior Styling of an Intercity

[10] Asproulis N. Thornber B., Konozsy L. and Moulitsas I. Lecture Notes. Cranfield University, 2013. [40] Wilcox D. Turbulence modelling for CFD. 1993.

[11] A Tewari. Atmospheric and Space Flight Dynamics. Lecture Notes in Mathematics. Chapter 10 Elements of Aerodynamics p233-267, Springer, 2007.

[12] Barnard, R.H., "Road Vehicle Aerodynamic Design-An Introduction", 2nd Edition, Longman ISBN 0-582-24522-2, 1996.

[13] Barnard, R.H., "Road Vehicle Aerodynamic Design-An Introduction", 2nd Edition, Longman ISBN 0-582-24522-2, 1996.

[14] Basara et. al.(2001) "The Calculation of External Aerodynamics: Industrial Benchmarks", SAE 2001-01-0701

[15] Bus drag reduction by trapped vortex concept for a single bus and two buses in tandem by C.A.J. Fletcher and G.D.H. Stewart.

[16]. Bus drag reduction by trapped vortex concept for a single bus and two buses in tandem by C.A.J. Fletcher and G.D.H. Stewart.

[17]. Bus drag reduction by trapped vortex concept for a single bus and two buses in tandem by C.A.J. Fletcher and G.D.H. Stewart.
[18] Carr.G.W., (1982), “The aerodynamics of basic shapes of road vehicles, part 1, Simple rectangular bodies”, MIRA report No.1982/2
[19]. Carr.G.W., (1982), “The aerodynamics of basic shapes of road vehicles, part 1, Simple rectangular bodies”, MIRA report No.1982/2.
[20] CD-Adapco. STARCCM+ Manual, version 4.06.011 edition.
[21] Chauhan Rajsinh B. and Thundil Karuppa. Numerical Investigation of External Flow around the Ahmed Reference Body Using Computational Fluid Dynamics. Research Journal of Recent Sciences, 2012.
[22] Costelli A. F. Onorato, M. and A Garonne. Drag Measurement Through Wake Analysis.
[23] Creuse-E Depeyras D. Gillireon P. Bruneau, C.H. and I. Mortazavi. Active Procedures to Control the Flow Past the Ahmed Body with a 25 rear window. Universite de Bordeaux, 2009.
[24] D Bitchtas. Aerodynamic evaluation of hgv trailer upper surface curvature. Master’s thesis, Cranfield University, 2012.
[25] D. B. Ivady. Assignments. Cranfield University, 2013.
[26] Depardon S. Pujals, G. and C Cossu. Drag Reduction of a 3D Bluff Body Using Coherent Stream wise Streaks. Experiments in Fluids, 49:1085-195,2010, 2010.
[27]. D. G. François, J. S. Delnero, J. Colman, J. Marañón Di Leo, and M. E. Camocardi, "Experimental Determination of Stationary Aerodynamics Loads on a Double Deck Bus", 11thAmerican Conference on Wind Engineering, San Juan, Puerto Rico, Jan. 22-26, 2009.
[28] Doe’s effort to reduce aerodynamic drag through joint experiments and computations. SAE, 2005-01-3511, 2005.
[29] Don Bur’s homepage. www.donbur.co.uk/index.shtml, accessed 16 Mars 2010.
[30]. Drag Reduction of an Ahmed car model by means of active separation control at the rear vehicle slant by A. Brunn and W. Nitsche.
[31] 314. Edwin. J. Asltzman and Robert. R. Meyer., (1999), “*A reassessment of heavy duty truck aerodynamic design features and priorities*”, NASA/tp-1999-206574.
[32] . Edwin J Saltzman, Robert R Meyer, Mc Callen and K Salari (200723), “International
[33] Edwin. J. Asltzman and Robert. R. Meyer., (1999), “A reassessment of heavy duty truck aerodynamic design features and priorities”, NASA/tp-1999-206574
[34] E. Konstantinidis and E Bouris. Bluff Body Aerodynamics and Wake Control. In Tech-Applied Aerodynamics, Chapter 4, 2012.
[35] E Selvakumar, M K Murthi and A Muthuvel (2013), “Conducted Research on Aerodynamic Exterior Body Design of Bus”.
[36] F. Alam, H. Chowdhury, H. Moria, and S. Watkins, "Effects of Vehicle Add-ons on Aerodynamic Performance", Proceedings of the 13thAsian Congress of Fluid Mechanics, Dhaka, Bangladesh, 17-21 December 2010.
[37]. Frank M. White.Fluid Mechanics. McGraw-Hill, 5th edition, 2005.

[38] F. R Menter. Two-Equation Eddy-Viscosity Turbulence Models for Engineering Applications. AIAA Journal, vol. 32, no 8. pp. 1598-1605, 1994.
[39] Frederque Muyl, Laurent Dumas and Vincent Herbert, [October 2001], “Hybrid method for Automotive Shape Optimization in Automotive Industry, PSA Peugeot Citroen, Centre technique, Veliz Villacoublay, France
[40] FLUENT. User Manual 14.1. Ansys FLUENT, 2013.
[41]. Fluid mechanics Fundamentals and applications 2006.
[42]. Fred Browand., (2005), “*Reducing the drag and fuel consumption”,* Advanced transportation workshop. October, 10 -11.
[43] G Buresti, G V Lungo and G Lombardi (2007), “Carried out a Research on Methods for the Drag Reduction of Bluff Bodies and Their Application to Heavy Road”.
[44] G. Faltin S.R. Ahmed, G. Ramm. Some salient features of the time-averaged ground vehicle wake. SAE Paper 840300, 1984, 1984.
[45] Gilhaus A., (1998) “Main parameters determining the aerodynamic drag of buses, colloque construire avec le vent, vol 2.

[46] Gilhaus A., “*Main parameters determining the aerodynamic drag of buses*, colloque construire avec le vent, vol 2.
[47] Gillireon P. Bruneau, C.H. and I Mortazavi. Passive Control Around the Two Dimensional Square back Ahmed Body Using Porous Devices. University de Bordeaux, 2011.
[48] Gilieron P. Roumeas, M. and A Kourta. Drag Reduction by Flow Separation Control on a Car After Body. Lecture Notes in Mathematics. International Journal for Numerical Methods in Fluids, vol.60, no. 11, pp. 1222-1240, 2009. SAE Technical Paper 840302, 1984, 1984.
[49]. H K Versteeg and W Malalasekera.An Introduction to Computational Fluid Dynamics The Finite Volume Method. Pearson Education Limited, 2nd edition, 2007.
[50] H. Lien hart and S. Becker. Flow and Turbulence Structure in the Wake of a Simplified Car Model. SAE Paper 2003-01-0656 , 2003, 2003.
[51] Hucho,W.H., “Aerodynamics of Road Vehicles”, , SAE International, Warrendale, PA, 1998.
[52] Hucho, W. H. and Sovran, G. (1993) Aerodynamics of road vehicles, Annual Review of Fluid Mechanics, Vol. 25(1), pp485-537.
[53] Hucho, W. H. and Sovran, G. (1993) Aerodynamics of road vehicles, Annual Review of Fluid Mechanics, Vol. 25(1), pp485-537.
[54] Hucko,W.H Emmelmann. H.J (1977) “*Aerodynamiche Formoptimierung,ein weg zur steigerung der wirtschsftlichkeit von nutzfahrzeugen,”* Series.12, NO.31 1977.
[55 Iain Robertson. Aerodynamic force modification via base roughness. Master’s thesis, Cranfield University, 2012.
[56] Inchul Kim and Xin Geng, [2002], “Optimization of Body Shape through Computation of Aerodynamic Forces on Low Mass Vehicle (LMV)”, Department Of Mechanical Engineering, University Of Michigan-Dearborn, Dearborn, Mi 4

[57] I. S. Dr Ali and A. A Mahmood. Improvement of Aerodynamics Characteristics of Heavy Trucks", 3rd International Conference on Trends in Mechanical and Industrial Engineering. 3rd International Conference on Trends in Mechanical and Industrial Engineering, 2013.
[58] J. Abinesh and J. Arunkumer "CFD Analysisn of Aerodynamic Reduction and Improve Fuel Economy", ISSN 2278-0149, Vol, No. 4, October, 2014.
[59] J. B. Freund and M. G Mungal. Drag and Wake Modification of Axisymmetric Bluff Bodies Usinf Coanda Blowing. Journal of Aircraft, May-June 1994, Volume 31, No.3 pp572-578, 1994.
[60] J Katz. Aerodynamics of Race Cars. Annual Review of Fluid Mechanics, 2006.38:27-63, 2006.
[61] J. Leuschen and K.R. Cooper. Full-scale wind tunnel tests of production and prototype, second generation aerodynamic drag-reducing devices for tractor-trailers.SAE, 2006-01-3456, 2006.
[62] John P, Nisha K, Neha Mittal, Neenu Ittyerah, (2005),"Urban transport crisis in India", Transport Policy 12 185–198.
[63] Ketan G. Pranami. el. al(2014), "Improvement of Bus Body Aerodynamic Shape by CFD Analysis"
[64] Knowles K. Strachan, R. and Lawson N. Comparison Between CFD and Experimental Results for a Simplified Car Model in Wall Proximity. Cranfield University, 2012.
[65] Krajnovic. S and Davidson. L., (2002) "Exploring the flow around a simplified bus with large eddy simulation and topological tools"IMECE2002-32833.
[66] L. Davidson. An introduction to turbulence models. 2003.
[67] Lietz et, al. (2000) "A CFD Validation Study for Automotive Aerodynamics", SAE Technical Paper 2000-01-0129, 2000, doi: 10.4271/2000-01-0129
[68] L. Lofdahl L. Sterken, S. Sebben. Alternative Approach in Ground Vehicle Wake Analysis. World Academy of Science, Engineering and Technology 68, 2012.
[69] Ludovico Consano and Davide Lucarelli., (2007), "Fuel Reduction on a Tractor-Trailer Truck at IVECO IVECO S.p.A",3rdEuropean automotive CFD conference, EACC 2
[70] Mason, W.T., Jr., Beebe, P.S., (1999), "The drag related flow field of characteristics of trucks and buses"plenum press, PP 253-286.
[71911] Mayer, W., and Wickern, G. (2011) The new audi A6/A7 family-aerodynamic development of different body types on one platform, SAE International Journal of Passenger Cars-Mechanical Systems, Vol. 4(1), pp197-206
[72] Mayer, W., and Wickern, G. (2011) The new audi A6/A7 family-aerodynamic development of different body types on one platform, SAE International Journal of Passenger Cars-Mechanical Systems, Vol. 4(1), pp197-206
[73] Mc Callen (2004), "Investigated on a Reduction in Drag Value Until the Front Leading Edge".
[74] Meshing Research Corner. http://www.andrew.cmu.edu/user/sowen/survey/tetsurv.html, accessed11 May 2010.

[75] Mitschke, M., Wallentowitz, H., Dynamik der Kraftfahrzeuge 4. Auflage, ISBN: 3-540-42011-8, 2004.
[76]. M. M. Yelmule, and S. R. Kale, "Aerodynamics of a Bus with Open Windows", Int. J. Heavy Vehicle Systems, Vol. 16, No. 4, 2009.
[77] Mond Fadhlan Bin Zahari, " Aerodynamic Investigation of a Commercial Vehicle Using CFD", May 2008
[78] Mr. Ludovico Consano and Davide Lucarelli., (2007), *"Fuel Reduction on a Tractor-Trailer Truck at IVECO IVECO S.p.A",* 3 rd European automotive CFD conference, EACC 2007.
[79] Murad, N.M., J. Naser F. Alam and S. Watkins(2004). Simulation of a Vehicle A-Pillar aerodynamics Using Various Turbulence Models", SAE 2004-01-0231
[80] Nordström, P-E., Nyström, N. E., Scania bus parade 1911-1991, 1991.
[81]. Panu Sainio, Kimmo Killstrom and Matti Juhala (2003), "From Aalto University Conducted a Research on Aerodynamics Possibilities for Heavy Vehicles".
[82] Passmore M. Little wood, R. and D. Wood. An Investigation into the Wake Structure of Square Back Vehicles and the Effect of Structure Modification on Resultant Vehicle Forces. SAE Technical Papers 2011-37-0015, 2011.
[83] Passmore M. Littlewood, R. Aerodynamic Drag Reduction of a Simplified Square back Vehicle Using Steady Blowing. Experiments in Fluids, Vol 53, pp 519-529,2011.
[84] Passmore M. Littlewood, R. The Optimization of Roof Trailing Edge Geometry of Simple Square-Back. SAE Technical Papers 2010-01-0510, 2011.
[85] Paul Schreier. Modelling: Aerodynamics, turbulent times. Scientific computing world, June/July 2010.
[861418] P Bearman. Bluff Body Flow Research with Applications to Road Vehicles. The Aerodynamics of Heavy Vehicles II: Trucks, Buses and Trains, Springer, Volume 41, 2009, pp 3-13, 2009.
[87] Petel, P. and Vijayakumar, S., "External Flow Analysis Over a Car to Study The Influence of Different Body Profiles Using CFD", SAE Technical Paper 2001-01-3085, 2001, doi: 10.4271/2001-01-3085
[88]. P. Gopal, and T. Senthilkumar, "Aerodynamic Drag Reduction in a Passenger Vehicle Using Vortex Generator with Varying Yaw Angles", ARPN Journal of Engineering and Applied Sciences, ISSN 1819-6608, Vol. 7, No. 9, September 2012.
[89] P.N Krishnani. Study of Drag Reduction of a Generic Sport Utility Vehicle. PhD thesis, Mumbai University, 2006.
[90] R. Mc. Callen, K. Salari, J. Ortega, F. Browand, M. Hammache, T. Hsu., (2004), "Effort to Reduce Truck Aerodynamic Drag – Joint Experiments and Computations Lead to Smart Design", AIAA Fluid Dynamics Conference.
[91] R.. Mc. Callen, K. Salari, J. Ortega, F. Browand, M. Hammache, T. Hsu., (2004), "*Effort to Reduce Truck Aerodynamic Drag – Joint Experiments and Computations Lead to Smart Design*", AIAA Fluid Dynamics Conference, June 28 – July 1. 007

[92] R.M. Wood. Impact of advanced aerodynamic technology on transportation energy consumption. SAE, 2004-01-1306, 2004.
[93]. R. M. Wood, "Impact of Advanced Aerodynamic Technology on Transportation Energy Consumption", SOLUS-Solutions and Technologies, 2004 SAE International.

[94] Roy and Srinizasen (2000) " External Flow Analysis of a Truck for Drag Reduction", -2000-01-3500
[95]. R. Schoon and F.P. Pan. Practical devices for heavy truck aerodynamic drag reduction.SAE, 2007-01-1781, 2007.
[96]. Sachin Thorat and G Amba Prasad Rao (1999), "Conducted an Research on Computational Analysis of Intercity Bus with Improved Asthetics and Aerodynamic Performance on Indian Roads".
[97] Sims-Williams D. Sprot A. Howell, J. and F Hamlin. Bluff Body Drag Reduction with Ventilated Base Cavities. SAE Int J. Passenger Cars-Mech-Syst152-160,2012, 2012.
[98] Siniˇsa Krajnovi ´c and Lars Davidson, (2001), "Large-Eddy Simulation of the Flow around a Ground Vehicle Body",SAE 2001-01-0702.
[99] S. Jakirlic B. Basara. Flow round a Simplified Car Body.
[100] Sofu T. Chang J. Pointer, D. and D Weber. Applicability of Commercial CFD Tools for Assessment of Heavy Vehicle Aerodynamic Characteristics. The Aerodynamics of Heavy Vehicles II: Trucks, Buses and Trains, Springer, Volume 41, 2009, pp 349-361, 2009.
[101] S. Mansor and M. A Passmore. Estimation of Bluff Body Transient Aerodynamics Using an Oscillating Model Rig. Southborough University , LE11 3TU, UK.
[102]. S. Roy, and P. Srinivasan, "External Flow Analysis of a Truck for Drag Reduction", 2000 01-3500, 2000 Society of Automotive Engineers, Inc., 2000
[103]. S. Thorat, and G. Amba Prasad Rao, "Computational Analysis of Intercity Bus with Improved Aesthetics and Aerodynamic Performance on Indian Roads", International Journal of Advanced Engineering Technology, E-ISSN 0976-3945, July-Sep 2011.
[104] T. Cebeci and P. Bradshaw. Momentum Transfer in Boundary Layers. Hemisphere Publishing Corporation, New York,, 1977.
[105]. The effect of vehicle spacing on the aerodynamics of a representative car shape by Simon Watkins and Gioacchino Vino.
[106]. The International Energy Outlook 2009 report
[107] T Lajos. Az Aramlastan Alapjai, 4. kiadas. Budapest, Hungary, 2008.
[108] Versteeg and Malalasekera (1995). "An Introduction to Computational Fluid Dynamics The Finite Volume Method" -ISBNO-582-21884-5
[109] Verzicco R. Fatica M. Iaccarino G. Khalighi, B. and P Moins. Large Eddy Simulation of a Road Vehicle with Drag-Reduction Devices. AIAA Journal, Vol40, No. 12 ,2002, 2002.
[110] Volvo 3P/CVL. Optifuel lab - demotruck: Fuel economy results. Technical report, Volvo 3P, 2009.

[111] Volvo Trucks global homepage. www.volvo/trucks/global/en-gb/home.htm, accessed 23 February 2010.
[112] Wassen E Sperber D. Nitsche W. Brunn, A. and F Thiele. Active Drag Control for a Generic Car Model. NNFM, Vol 95, 2007, pp247-259, Springer, 2007.
[113] Way A. Hunt, J. C. R. and P Moin. Eddies Stream and Convergence Zones in Turbulent Flows. Center for turbulence research proceedings of the summer program 1988, pp. 193-208, 1988.

[115] W. H. Hucho. Aerodynamics of Road Vehicles, 4th Edition. SAE International,1998.
[116] W. H. Hucho. Aerodynamics of Road Vehicles, 4th Edition. SAE International, 1998.
[117] W. H. Hucho and G Sovran. Aerodynamics of Road Vehicles. Annual Review of Fluid Mechanics, 1993.25:485-537, 1993.
[118] Windsor S. W. Irving-Brown, Y. A. and A Gaylard. The E ect of Base Bleed and Rear Cavities on the Drag of an SUV. SAE Technical Paper, 2010-01-0512, 2010.
[119]. Wolf Heinrich Hucho., (2001), "*Aerodynamics of road vehicles",* 4 th edition, SAE International, vol.1, pp. 11-88.
[120] W Seay J.Bledsoe, D. Landman and R Wood. Understanding practical limits to heavy truck drag reduction. SAE, 2009-01-2890, 2009.
[121] Yang, Z., and Khalighi, B., "CFD Simulation for Flow Over Pickup Trucks", SAE Paper No. 2005-01-0547, 2005.
[122] Zenitha Chronéer., (2007),"The CFD Process for Aerodynamics at Volvo Cars using HARPOONFLUENTE"., 3rdEuropean automotive CFD conference, EACC.
[123] Wahba et.al "Aerodynamic Drag Reduction for Ground Vehicles using Lateral Guide Vanes" Vol.4(2) 2012.

APPENDIX

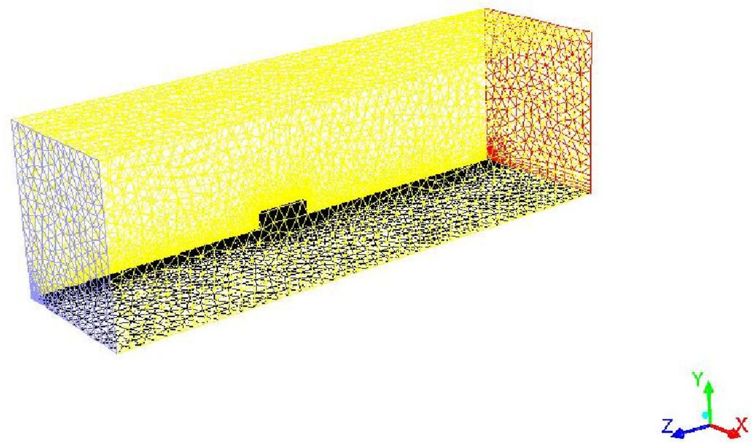

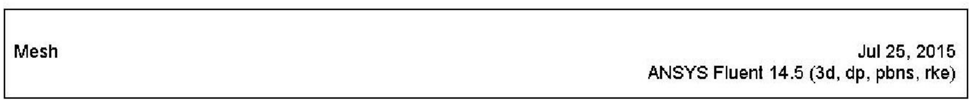

Appendix A: Meshed Model 1 Inside an Enclosure at 100 kmph

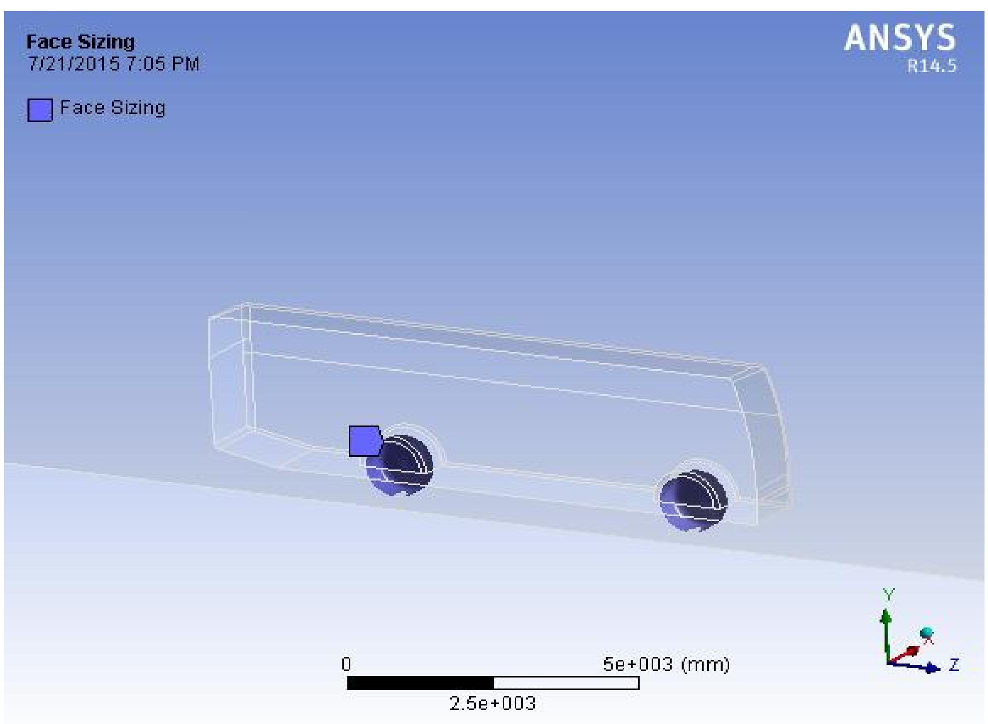

Appendix B: Face Sizing(Meshing)

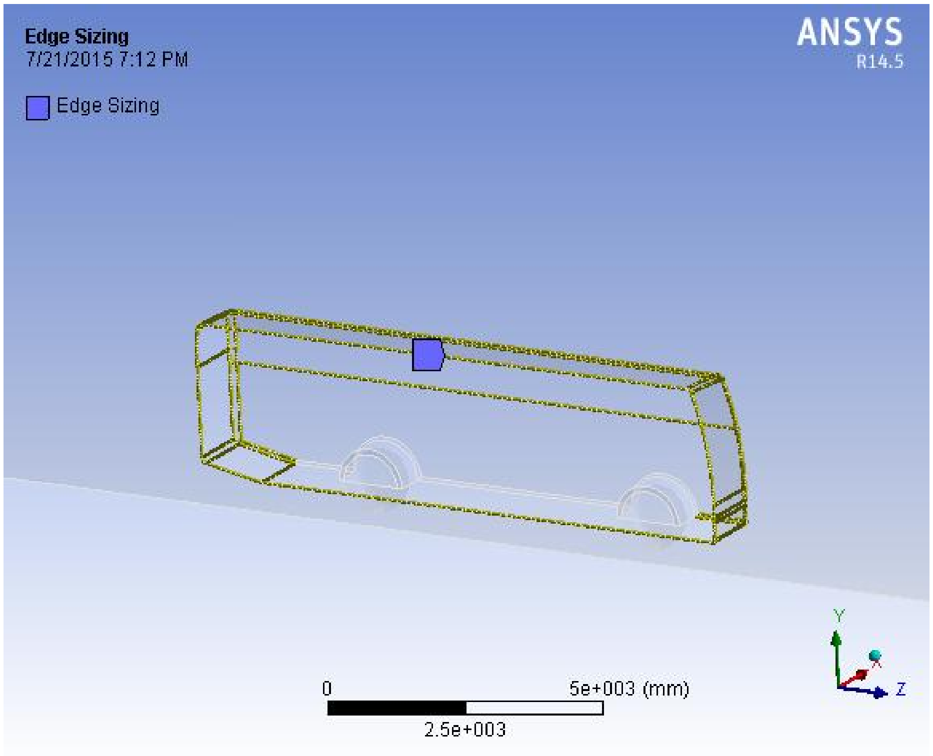

Appendix C: Edge Sizing(Meshing)

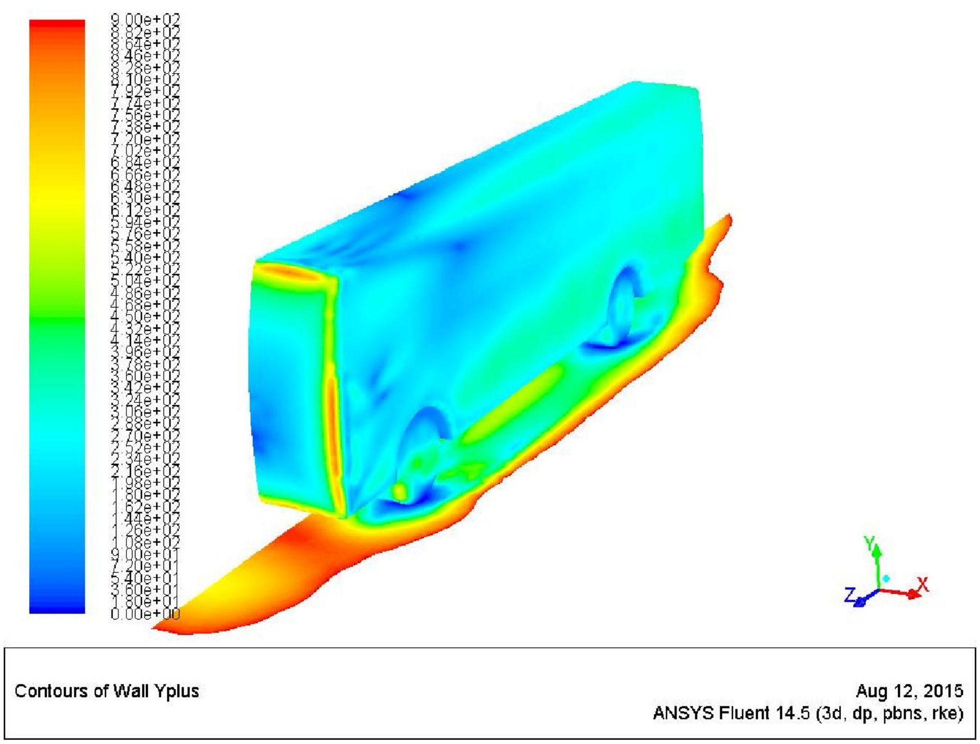

Appendix D: Contours of Wall Y plus of Model 1 at 85 kmph

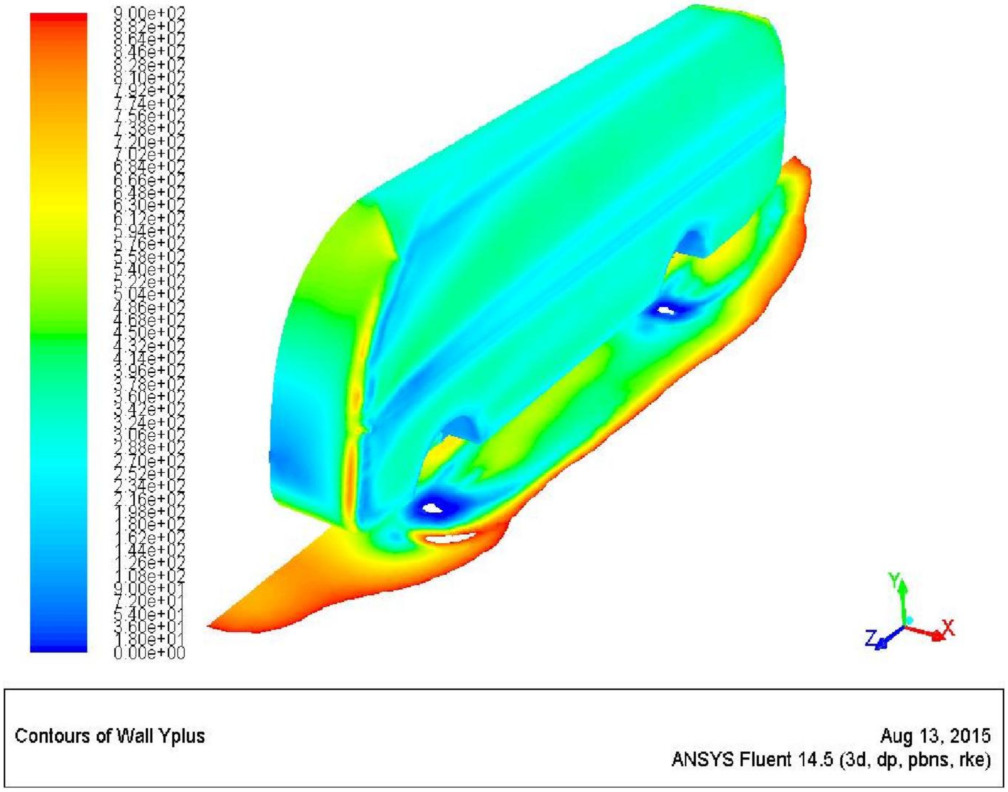

Appendix E: Contours of Wall Y plus of Model 2 at 85 kmph

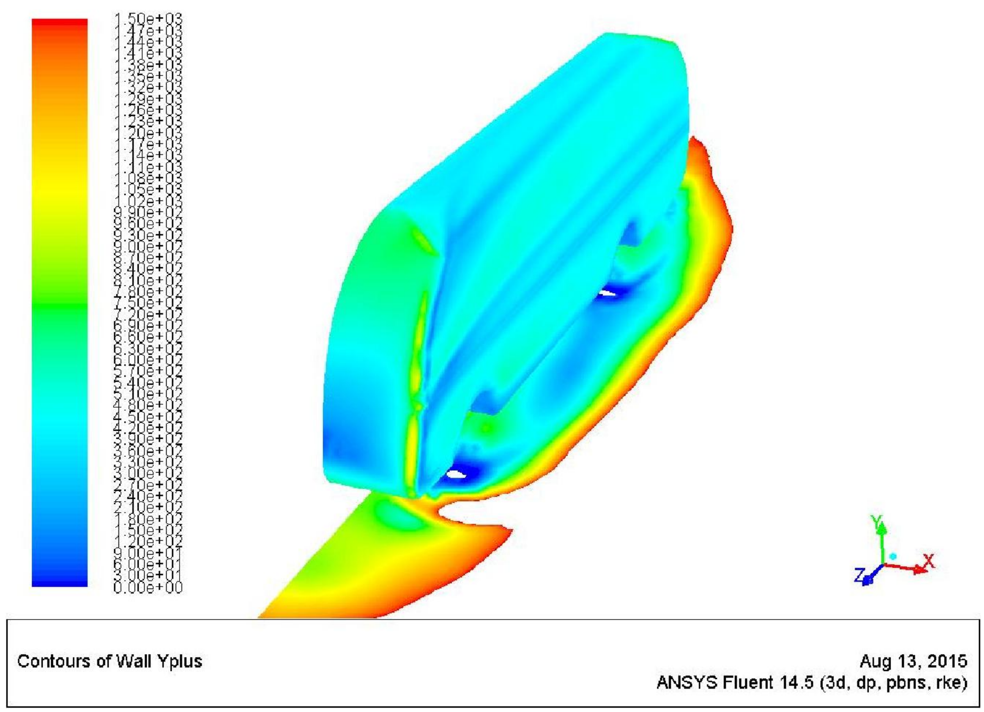

Appendix F: Contours of Wall Y plus of Model 2 at 100 kmph

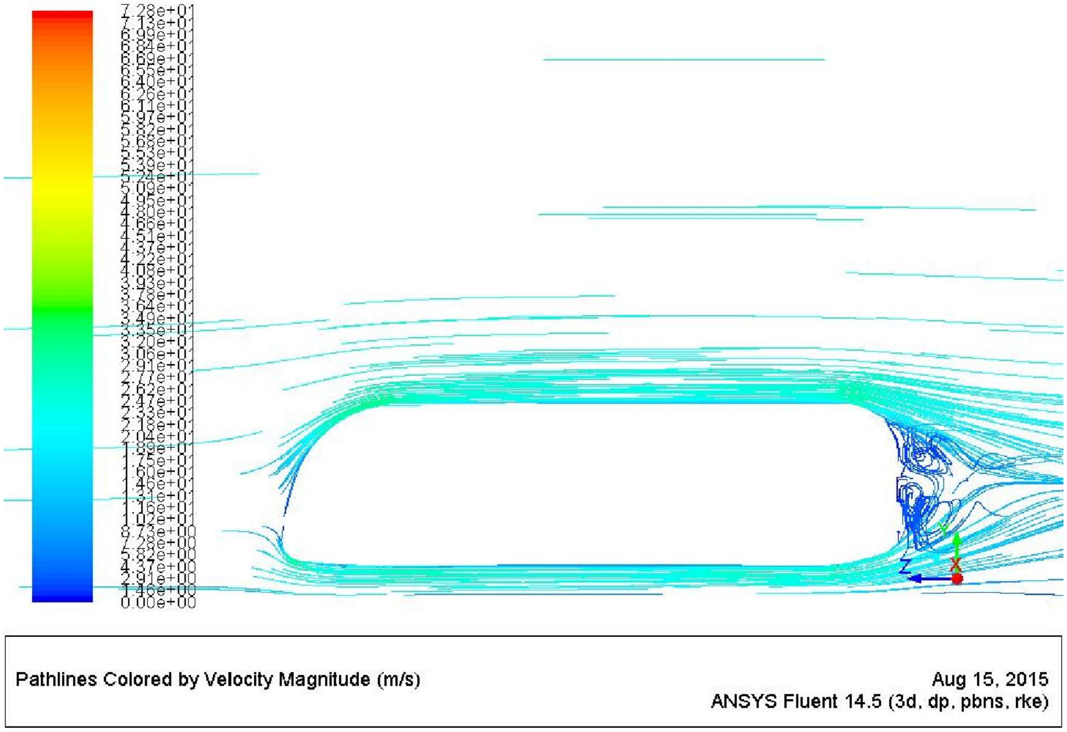

Appendix G: Contours of Velocity Magnitude of Model 2 at 85 kmph

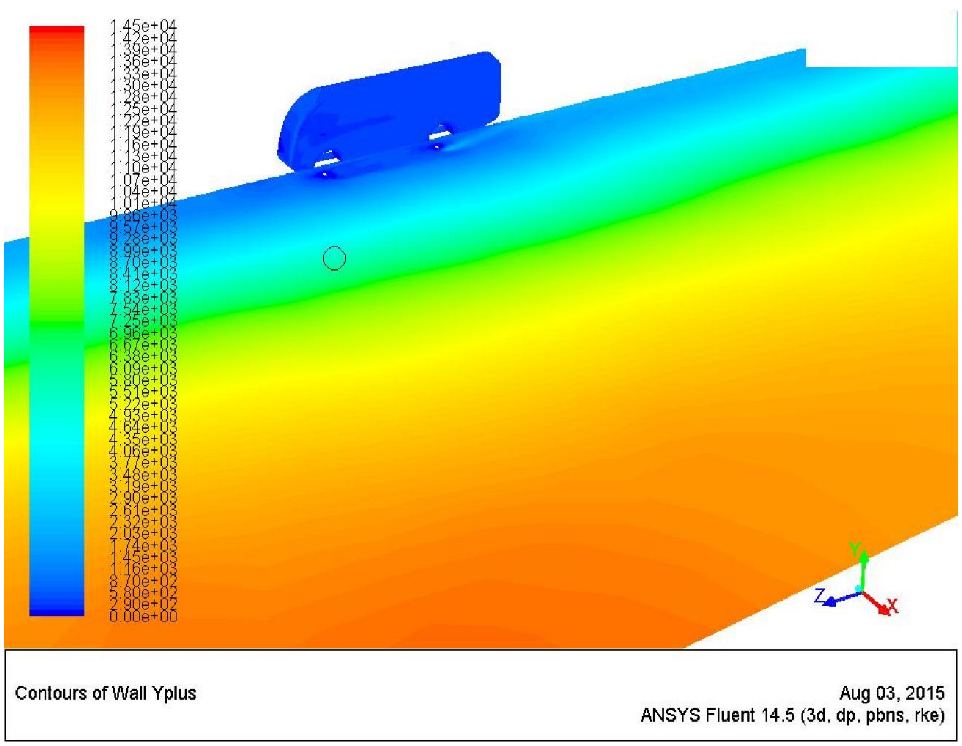

Appendix H: Contours of Wall Y plus of Model 3 at 85 kmph

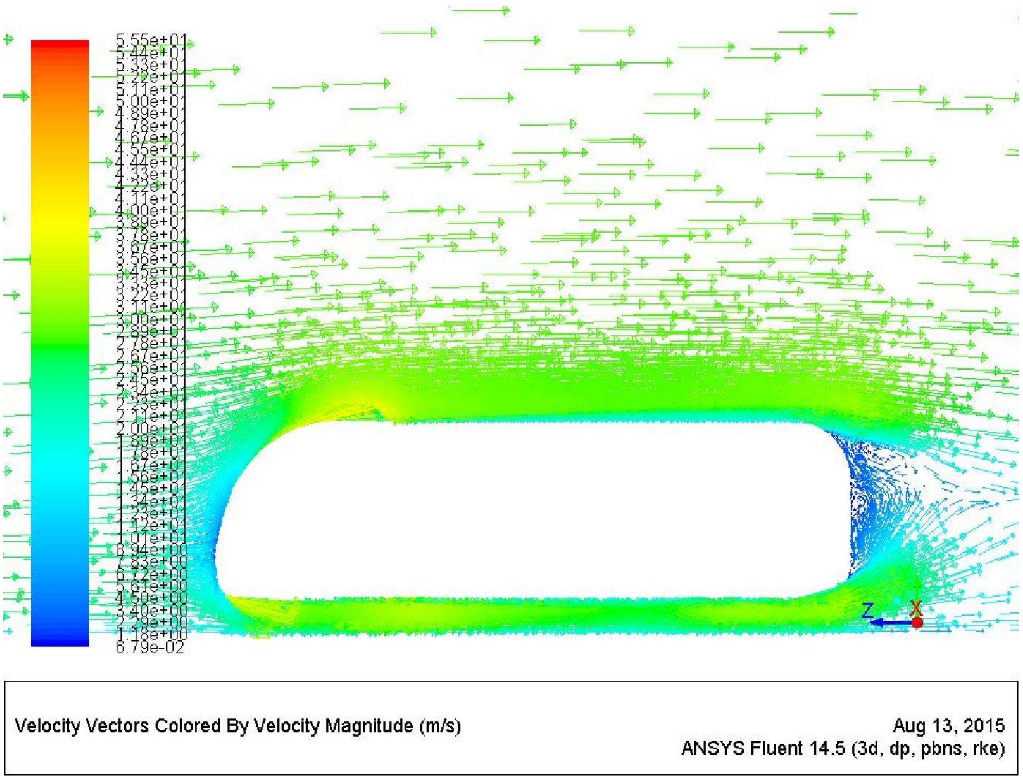

Appendix I: Velocity Vectors of Model 2 at 100 kmph

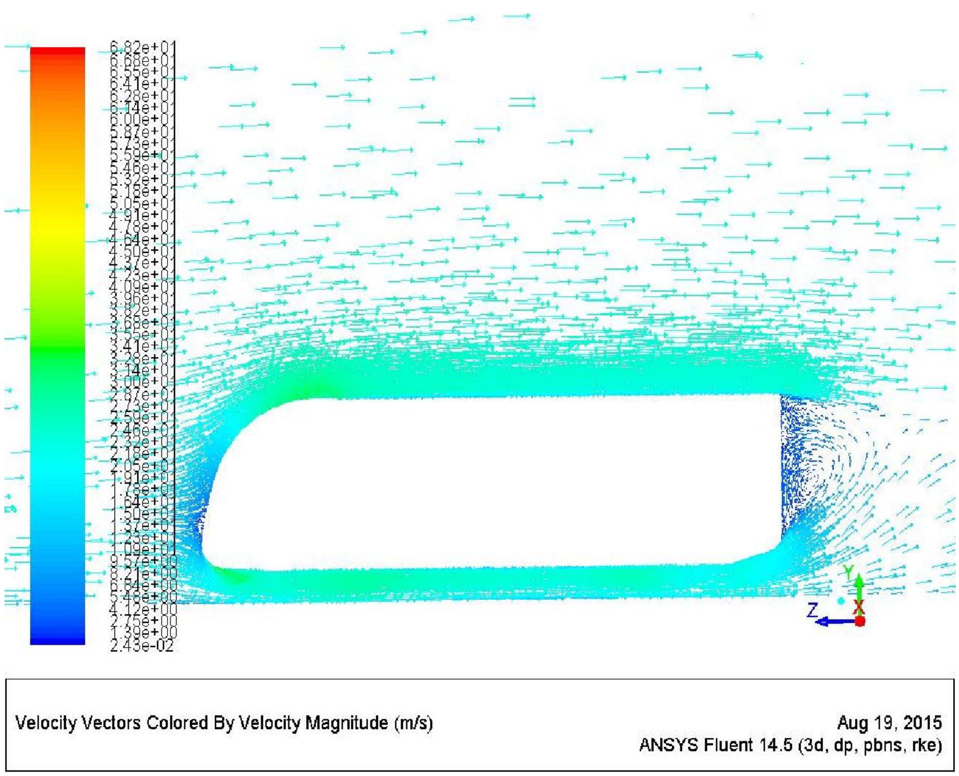

Appendix J: Velocity Vectors of Model 3 at 85 kmph